Weighted-Power-Mean Mixture Model for the Gibbs Energy of Fluid Mixtures: Composite Document

Desireé Strauss

Weighted-Power-Mean Mixture Model for the Gibbs Energy of Fluid Mixtures

by

Desireé Strauss

Department of Chemical Engineering
University of Pretoria

Contents

Introduction

Nomenclature

α Polarizability of a pure substance $[\alpha] = \dfrac{\mathrm{C}^2\mathrm{m}^2}{\mathrm{J}}$

$\bar{\Gamma}_{ij}$ Average potential energy $\left[\bar{\Gamma}_{ij}\right] = \mathrm{J}$

$\bar{G}_i^{ideal}$ Partial molar Gibbs energy of pure component i in an ideal mixture $\left[\bar{G}_i^{ideal}\right] = \dfrac{\mathrm{J}}{\mathrm{mol}}$

$\bar{H}_i^{ideal}$ Partial molar enthalpy of pure component i in an ideal mixture $\left[\bar{H}_i^{ideal}\right] = \dfrac{\mathrm{J}}{\mathrm{mol}}$

$\bar{M}_i$ Partial molar property of component i in a mixture

$\bar{S}_i^{ideal}$ Partial molar entropy of pure component i in an ideal mixture $\left[\bar{S}_i^{ideal}\right] = \dfrac{\mathrm{J}}{\mathrm{molK}}$

$\bar{V}_i^{ideal}$ Partial molar volume of pure component i in an ideal mixture $\left[\bar{V}_i^{ideal}\right] = \dfrac{\mathrm{cm}^3}{\mathrm{mol}}$

ΔG Change in Gibbs energy on mixing $[\Delta G] = \dfrac{\mathrm{J}}{\mathrm{mol}}$

ΔH Change in enthalpy on mixing $[\Delta H] = \dfrac{\mathrm{J}}{\mathrm{mol}}$

ΔS Change in entropy on mixing $[\Delta S] = \dfrac{\mathrm{J}}{\mathrm{molK}}$

ΔT_{int} Size of temperature intervals for the calculation of m in the modified van der Waals equation of state

ΔV Change in molar volume on mixing $[\Delta V] = \dfrac{\mathrm{cm}^3}{\mathrm{mol}}$

ϵ Energy parameter in Mie's potential energy function $[\epsilon] = \mathrm{J}$

Γ Potential energy between two molecules $[\Gamma] = \mathrm{J}$

Γ_{ij} Potential energy between two charged particles, molecules or dipoles $[\Gamma_{ij}] = \mathrm{J}$

Γ_T Total potential energy of a system of N molecules $[\Gamma_T] = \mathrm{J}$

Λ_{ij} Parameter used in the Wilson model

e Unit charge 1.60218 $\times 10^{-19}$ C

μ Magnitude of a dipole moment $[\mu] = \mathrm{D}$

μ^i Magnitude of induced dipole moment $[\mu^i] = \mathrm{D}$

μ_i Chemical potential of species i $[\mu_i] = \dfrac{\mathrm{J}}{\mathrm{mol}}$

μ_i Magnitude of a dipole moment i $[\mu] = \mathrm{D}$

ν_{0i} Characteristic electronic frequency of molecule i in unexcited state $[\nu_{0i}] = \dfrac{1}{\mathrm{s}}$

Φ Characteristic constant of the cubic equation of state

ϕ_i Parameter used to describe orientation of dipole moment i relative to another $[\phi_i] = \mathrm{rad}$

π Number of phases in a heterogeneous system

σ Distance parameter in Mie's potential energy function $[\sigma] = \mathrm{m}$

θ_i Parameter used to describe orientation of dipole moment i relative to another $[\theta_i] = \mathrm{rad}$

ε Absolute permittivity of a medium $[\varepsilon] = \dfrac{\mathrm{C}^2}{\mathrm{Jm}}$

ε_0 Dielectric permittivity of a vacuum 8.85419 $\times 10^{-12}$ $\dfrac{\mathrm{C}^2}{\mathrm{Jm}}$

ε_{ij} Energy parameter used in the derivation of the Wilson model

ε_r Dielectric constant of a medium $[\varepsilon_r] = \dfrac{\mathrm{C}^2}{\mathrm{Jm}}$

A Total Helmholtz free energy of a system $[A] = \dfrac{\mathrm{J}}{\mathrm{mol}}$

a Adjustable parameter in the van der Waals equation for correction of attractive forces between molecules

A^E Excess Helmholtz energy of a real mixture $\left[A^E\right] = \dfrac{\mathrm{J}}{\mathrm{mol}}$

A^E Excess Helmholtz free energy of a real mixture $\left[A^E\right] = \dfrac{\mathrm{J}}{\mathrm{mol}}$

A^{ideal} Helmholtz free energy of an ideal mixture $\left[A^{ideal}\right] = \dfrac{\mathrm{J}}{\mathrm{mol}}$

A^E_∞ Helmholtz free energy of an Equation of State at infinite pressure

a_c Adjustable parameter in the van der Waals equation evaluated at critical temperature

A^E_{EOS} Helmholtz free energy of an Equation of State

A_i Helmholtz free energy of pure component i in a mixture $\left[A^E\right] = \dfrac{\mathrm{J}}{\mathrm{mol}}$

A_{vp} Constant used for the calculation of the vapour pressure of a pure compound as a function of temperature

b Adjustable parameter in the van der Waals equation for correction of repulsive forces between molecules

B_{vp} Constant used for the calculation of the vapour pressure of a pure compound as a function of temperature

c_1 Characteristic variable to establish the form of a cubic equation of state

c_2 Characteristic variable to establish the form of a cubic equation of state

c_i Proportionality constant for component i in the ideal solution relation

C_{vp} Constant used for the calculation of the vapour pressure of a pure compound as a function of temperature

d Distance between two opposite charges of a dipole $[d] = \mathrm{m}$

d_i Distance between two opposite charges of a dipole i or distance from arbitrary origin of a linear quadrupole $[d_i] = \mathrm{m}$

D_{vp} Constant used for the calculation of the vapour pressure of a pure compound as a function of temperature

E Strength of electric field $[E] = \dfrac{\mathrm{V}}{\mathrm{m}}$

F Electrostatic force between two point charges $[F] = \mathrm{N}$

f_i Fugacity of component i in a mixture

f_i^0 Fugacity of component i in a mixture at an arbitrary reference standard state

f_i^{ideal} Fugacity of component i in an ideal mixture

f_i^{pure} Fugacity of pure component i

G Total Gibbs energy of a system $[G] = \dfrac{\mathrm{J}}{\mathrm{mol}}$

g Reduced total Gibbs energy of a system, $g = \dfrac{G}{RT}$

G^E Excess Gibbs energy of a real mixture $\left[G^E\right] = \dfrac{\text{J}}{\text{mol}}$

G^{ideal} Gibbs energy of an ideal mixture $[G_{ideal}] = \dfrac{\text{J}}{\text{mol}}$

G_i Gibbs energy of pure component i in a mixture $[G_i] = \dfrac{\text{J}}{\text{mol}}$

H Total enthalpy of a system $[H] = \dfrac{\text{J}}{\text{mol}}$

h Planck's constant 6.62606 $\times 10^{-34}$ Js

$H\left(\overline{x}\right)$ Hessian matrix of the Gibbs energy of a mixture, as a function of composition

H^E Excess enthalpy of a real mixture $\left[H^E\right] = \dfrac{\text{J}}{\text{mol}}$

H^{ideal} Enthalpy of an ideal mixture $[H_{ideal}] = \dfrac{\text{J}}{\text{mol}}$

H_i Enthalpy of pure component i in a mixture $[H_i] = \dfrac{\text{J}}{\text{mol}}$

k Boltzmann constant 1.38 $\times 10^{-23}$ $\dfrac{\text{J}}{\text{K}}$

M Extensive property of a mixture

m Adjustable parameter for the repulsive term from the Adachi-Lu relation

m Number of components in a heterogeneous system

m Positive constant in the attractive interaction term of Mie's potential energy function

N Total number of molecules in a system

n Number of moles in a closed system

n Positive constant in the repulsive interaction term of Mie's potential energy function

N_{int} Number of intervals into which the temperature range is divided for the calculation of m in the modified van der Waals equation of state

P Pressure $[P] = \text{kPa}$

p Number of degrees of freedom of a heterogeneous system

P^c Critical pressure $[P_c] = \text{bar}$

$P_{vap_i}^{actual}$ The vapour pressure of a pure compound determined using an approximation from the property data bank in Poling et.al. [27]

$P_{vap_i}^{predicted}$ The vapour pressure of a pure compound predicted by the van der Waals equation of state

P_{vap} Vapour pressure of a pure compound $[bar]$

Q Heat transfer to a closed system from it's surroundings $[Q] = \frac{\text{J}}{\text{mol}}$

Q Magnitude of quadrupole moment $[Q] = \text{D}$

q_i Magnitude of point a charge $[q_i] = \text{C}$

Q_{surr} Heat transfer from closed system to it's surroundings $[Q_{surr}] = \frac{\text{J}}{\text{mol}}$

R Ideal Gas Constant $8.314 \frac{\text{J}}{\text{molK}}$

r Distance between two point charges $[r] = \text{m}$

S Total entropy of a system $[S] = \frac{\text{J}}{\text{molK}}$

S^E Excess entropy of a real mixture $\left[S^E\right] = \frac{\text{J}}{\text{molK}}$

S^{ideal} Entropy of an ideal mixture $[S_{ideal}] = \frac{\text{J}}{\text{molK}}$

S_i^{ig} Entropy of component i as an ideal gas $\left[S_i^{ig}\right] = \frac{\text{J}}{\text{mol}}$

S_i Entropy of pure component i in a mixture $[S_i] = \frac{\text{J}}{\text{molK}}$

S_{surr} Total entropy of the surroundings of a closed system $[S_{surr}] = \frac{\text{J}}{\text{molK}}$

T Temperature $[T] = \text{K}$

T^c Critical temperature $[T_c] = \text{K}$

T_R Relative temperature

T_{surr} Temperature of the surroundings of a closed system $[T_{surr}] = \text{K}$

U Internal energy of system $[U] = \frac{\text{J}}{\text{mol}}$

U^E Excess internal energy of a real mixture $\left[U^E\right] = \dfrac{\mathrm{J}}{\mathrm{mol}}$

U_i^{ig} Internal energy of component i as an ideal gas $\left[U_i^{ig}\right] = \dfrac{\mathrm{J}}{\mathrm{mol}}$

V Total volume of a pure gas or mixture $[V] = \mathrm{cm}^3$

v Molar volume $[v] = \dfrac{\mathrm{cm}^3}{\mathrm{mol}}$

V^E Excess volume of a real mixture $\left[V^E\right] = \dfrac{\mathrm{cm}^3}{\mathrm{mol}}$

V^{ideal} Molar volume of an ideal mixture $[V_{ideal}] = \dfrac{\mathrm{cm}^3}{\mathrm{mol}}$

V_i Molar volume of pure component i in a mixture $[V_i] = \dfrac{\mathrm{cm}^3}{\mathrm{mol}}$

v_i Molar volume of species i in a mixture $[v_i] = \dfrac{\mathrm{cm}^3}{\mathrm{mol}}$

x_{ij} Mole fraction of species i around a molecule of species j in a mixture

x_i Mole fraction of component i in a liquid mixture

z Number of binary interactions between neighbouring molecules for a system of N molecules

z_i Fractional volume occupied by species i around itself in a mixture

z_i Ionic valence of a charged molecule or ion

Chapter 1

Literature Survey and Theoretical Background

1.1 Fluid Thermodynamics

1.1.1 Intermolecular Forces

The intermolecular forces present between individual molecules ultimately determine the thermodynamic properties of pure substances and mixtures alike. In the case of pure compounds only interactions between like molecules take place. In the case of mixtures, however, the additional interactions between dissimilar molecules also contribute to the overall properties of the fluid [27, 28].

Quantitative models as well as analytical relations from statistical mechanics are often only applied to simple, idealised systems of real matter. Consequently, our limited understanding of intermolecular interactions are used in an approximate manner to extrapolate from simple cases the overall properties of complex systems and mixtures.The theory of intermolecular forces do nonetheless provide useful insights into the thermodynamic properties and phase behaviour of real systems. In addition, molecular simulation with the aid of modern computer capabilities can provide predictions of bulk fluid properties from quantitative knowledge of the governing intermolecular forces [28].

The interactions between molecules in close proximity to one another can be either attractive or repulsive. The ultimate consequences of these interactions are observed, for example, when a vapour condenses from a liquid; which would not be possible in the absence of attractive intermolecular forces. Similarly, the virtual incompressibility of condensed phases are a testament to the presence

of repulsive intermolecular forces. Configurational properties of matter are determined by the balance of attractive and repulsive interactions [28].

The most significant of intermolecular interactions are electrostatic, induction, dispersion and chemical forces. These intermolecular forces are expressed with the aid of potential energy functions; similar to moving particles which have kinetic energy due to their relative motion, the potential energy of a particle results from the position of particles relative to each other. In general the force, F, acting between two molecules is given by [28]:

$$F\left(r,\theta,\phi...\right) = -\nabla\Gamma\left(r,\theta,\phi...\right) \tag{1.1.1}$$

Where Γ denotes the potential energy shared by these two molecules, and r, θ, ϕ etc. are the parameters required to express the separation between and orientation of two non-spherical molecules relative to each other. For two spherically symmetric particles, separated by distance r [28]:

$$F = -\frac{\mathrm{d}\Gamma}{\mathrm{d}r} \tag{1.1.2}$$

Theoretically, the work required to separate two spherical particles from some finite r to infinity is given by $-\Gamma\left(r\right)$.

Electrostatic Forces

Electrostatic forces are observed between permanently charged particles, such as ions and dipoles. The magnitude of this kind of interaction is determined using Coulomb's law in equation 1.1.3. Whereas most intermolecular forces are inversely related to higher orders of the distance between molecules, the electrostatic forces are inversely proportional to the square thereof. Electrostatic forces consequently operate over much longer ranges and the resulting potential energy is therefore also larger in magnitude.The long range of these forces is one of the complications in the modelling of electrolyte solutions. The electrostatic forces are also the main cause for the high melting points of ionic salt crystals. [28].

$$F = \frac{q_i q_j}{4\pi\varepsilon_0 r^2} \tag{1.1.3}$$

Where F denotes the resulting force between two point charges, a distance of r apart, with magnitude q_i and q_j. Also, the dielectric permittivity of a vacuum, ε_0, is taken as $8.85419 \times 10^{-12}\ \frac{\mathrm{C}^2}{\mathrm{Jm}}$. When the electrostatic forces need to be calculated in a medium other than a vacuum, the dielectric constant, ε_r, is used to determine the absolute permittivity, ε [28]:

$$\varepsilon = \varepsilon_0 \varepsilon_r \tag{1.1.4}$$

After integration of equation 1.1.3, the potential energy between two spherical molecules in a vacuum is expressed by equation 1.1.5.

$$\Gamma_{ij} = \frac{q_i q_j}{4\pi\varepsilon_0 r} + C_0 \tag{1.1.5}$$

The constant of integration, C_0, reduces to zero when it is assumed, according to common convention, that $\Gamma(r)|_{r=\infty} = 0$. For charged molecules q_i and q_j are multiples of the unit charge e, and consequently the potential energy between two ions can be determined from [28]:

$$\Gamma_{ij} = \frac{z_i z_j e^2}{4\pi\varepsilon r} \tag{1.1.6}$$

In addition to charged particles, electrostatic forces can also be observed between particles that do not have a net charge. For example, in the case of molecules that have electric couples or permanent dipoles. Dipoles arise due to the uneven distribution of electric charge in asymmetric molecules. Generally, the larger the assymetry of a molecule, the larger the resulting dipole moment. For two charges held a distance of d apart, the dipole moment is given by [28]:

$$\mu = ed \tag{1.1.7}$$

For two dipole moments in proximity to each other, the resulting potential energy is a function of the distance between and orientation of the four dipole charges. Figure 1.1.1 illustrates the parameters used to characterise the orientation of the dipole moments relative to each other. If the distance between the dipoles, r, is large in comparison to d_i and d_j the potential energy can be calculated according to [28]:

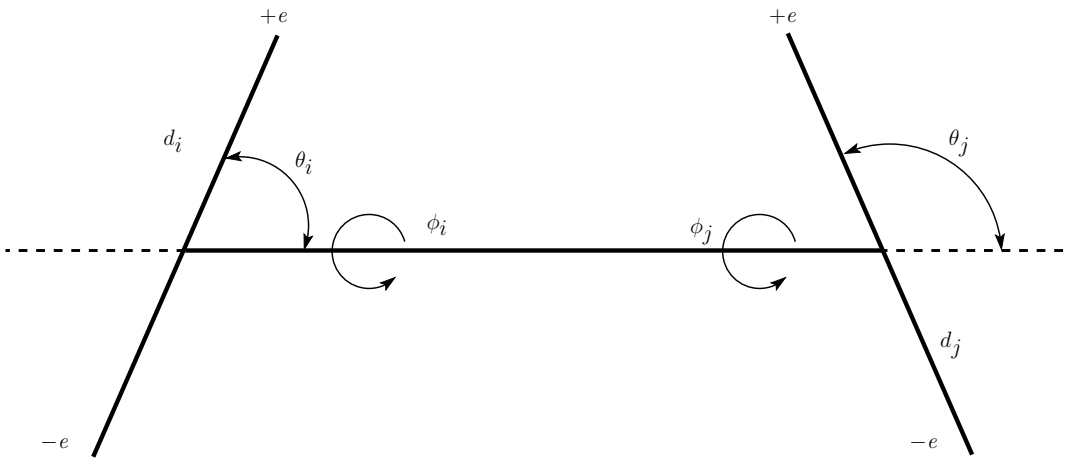

Figure 1.1.1: Orientation of two dipoles

$$\Gamma_{ij} = -\frac{\mu_i \mu_j}{4\pi\varepsilon_0 r^3} \left[2\cos\theta_i \cos\theta_j - \sin\theta_i \sin\theta j \cos\left(\phi_i - \phi_j\right)\right] \tag{1.1.8}$$

A maximum in this resulting potential energy is observed when like charges of each dipole are aligned, whereas a minimum corresponds to the alignment of the opposite charges. The orientation of the two dipole moments is influenced firstly by the electric field created by the charges, and secondly by the kinetic energy of the molecules. The electric field tends to align the dipoles, while the kinetic energy tends to cause random, chaotic movements. Consequently, an increase in temperature corresponds to a decrease in potential energy until the polar effects finally become negligible at some temperature limit [28].

The average potential energy due to polar interactions can be calculated by averaging all Γ_{ij} over all orientations and weighting each orientation according to the Boltzmann factor. For two ideal dipoles i and j ($r \leq d$), a fixed distance r apart in a vacuum, the average potential energy is then: [28]

$$\bar{\Gamma}_{ij} = -\frac{2}{3} \frac{\mu_i^2 \mu_j^2}{\left(4\pi\varepsilon_0\right)^2 kt.^6} + \cdots \tag{1.1.9}$$

Intermolecular interactions due to polar forces can be very significant and small increases in dipole moments can produce large increases in potential energy. This is especially true for small molecules with larger dipole moments [28].

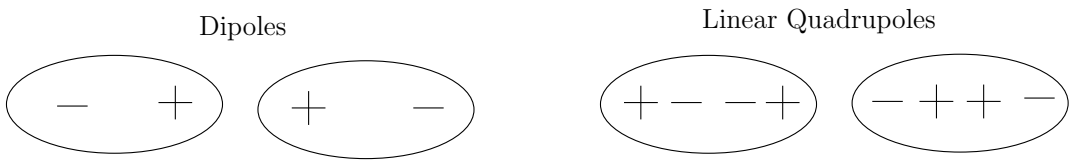

Figure 1.1.2: Schematic representation of linear quadrupoles

Molecules with higher order multiples such as quadrupoles, octapoles, hexadecapoles etc. also exist. Quadrupoles arise when charge concentrates at four seperate locations in a molecule. Intermolecular interactions due to quadrupole forces can have significant effects on the thermodynamic properties of a substance however, the effects are much less pronounced than that of dipole forces. Due to the very short range of higher order multipole forces the effect of these interactions become negligible for higher order multipoles. The quadrupole moment can be calculated by summation of the second moments of the charges, as in equation 1.1.10 below. Figure 1.1.2 provides a schematic representation of molecules with linear quadrupoles [28].

$$Q = \Sigma_i e_i d_i^2 \tag{1.1.10}$$

The potential energy resulting from the interactions of permanent quadrupoles with other quadrupoles or dipoles is determined by the separations and relative orientations. The average potential energy is determined, as in the case of only dipole interactions, by averaging over all orientations and weighting each orientation with the Boltzmann factor [28].

For dipole-quadrupole interactions:

$$\bar{\Gamma}_{ij} = -\frac{\mu_i^2 Q_j^2}{(4\pi\varepsilon_0)^2 kTr^8} + \cdots \tag{1.1.11}$$

For quadrupole-quadrupole interactions:

$$\bar{\Gamma}_{ij} = -\frac{7}{40}\frac{Q_i^2 Q_j^2}{(4\pi\varepsilon_0)^2 kTr^{10}} + \cdots \tag{1.1.12}$$

Induction Forces

Induction forces are encountered when non-polar molecules are in the vicinity of polar molecules. When non-polar molecules are situated in an electric field a dipole moment is induced due to the

displacement of the electrons from their normal positions. Induced dipole forces can also be present between permanent polar molecules however, the magnitude of the potential energy due to induced dipoles is normally small in comparison to that due to permanent dipoles or quadrupoles [28].

In moderate electric fields the induced dipole moment is directly proportional to the field strength. The proportionality constant is termed the polarizability, which is a constant property of the substance for symmetric molecules and a function of orientation for asymmetric molecules [28].

$$\mu^i = \alpha E \tag{1.1.13}$$

The resulting force between a permanent dipole and the nearby induced dipole in the non polar molecule is always attractive. The associated average potential energy can be calculated using the Debye equation [28]:

$$\bar{\Gamma}_{ij} = -\frac{\alpha_i \mu_j^2}{(4\pi\varepsilon_0)^2 r^6} \tag{1.1.14}$$

The average potential energy due to induced dipoles between two permanent dipoles or two quadrupoles are calculated according to equations 1.1.15 and 1.1.16, respectively [28].

$$\bar{\Gamma}_{ij} = -\frac{\alpha_i \mu_j^2 + \alpha_j \mu_i^2}{(4\pi\varepsilon_0)^2 r^6} \tag{1.1.15}$$

$$\bar{\Gamma}_{ij} = -\frac{2}{3}\frac{\alpha_i Q_j^2 + \alpha_j Q_i^2}{(4\pi\varepsilon_0)^2 r^8} \tag{1.1.16}$$

Dispersion Forces

Electrostatic interactions between polar molecules have been widely well understood for much longer than the dispersion interactions between non-polar molecules. Deviation from ideal gas behaviour by non-polar substances, such as that of argon, are explained by the presence of dispersion forces [28].

Continuous movements and oscillations of the electron cloud about the nucleus of non-polar molecules are sufficient to result in small momentary dipole moments. These momentary dipole moments do average to zero over a small period of time however, they do induce instantaneous dipole moments in surrounding molecules. The potential energy associated with the resulting attractive forces between the two temporary dipoles are given by London's equation, equation 1.1.17 below [28].

$$\Gamma_{ij} = -\frac{3}{2}\frac{\alpha_i \alpha_j}{(4\pi\varepsilon_0)^2 r^6}\left(\frac{h\nu_{0i} h\nu_{0j}}{h\nu_{0i} + h\nu_{0j}}\right) \tag{1.1.17}$$

Where h represents Planck's constant and ν_{0i} the characteristic electronic frequency of molecule i. Equation 1.1.17 was first derived by London for two spherically symmetric molecules separated by a large distance. The product $h\nu_{0i}$ is very nearly equal to the first ionization potential of molecule i, I_i. Consequently, equation 1.1.17 is often expressed as [28]:

$$\Gamma_{ij} = -\frac{3}{2}\frac{\alpha_i \alpha_j}{(4\pi\varepsilon_0)^2 r^6}\left(\frac{I_i I_j}{I_i + I_j}\right) \tag{1.1.18}$$

Which reduces to the following expression if molecules i and j are of the same species:

$$\Gamma_{ij} = -\frac{3}{4}\frac{\alpha_i^2 I_i}{(4\pi\varepsilon_0)^2 r^6} \tag{1.1.19}$$

From equations 1.1.18 and 1.1.19 we can deduce that the potential energy due to dispersion forces are independent of temperature and inversely proportional to r^6. This reduced impact of distance of separation, in comparison to polar molecules, explains the relative ease with which nonpolar substances are melted and vaporised. In addition, the potential energy is a stronger function of polarizability than of ionization potential. The latter varies only slightly from species to species while the former varies almost linearly with molecular size [28].

Calculations confirm that dispersion forces tend to be far from negligible, even for polar substances, and are normally much more significant than induction forces. When molecules are in such close proximity that the electron clouds overlap, London's equation does not hold. In such cases interactions between molecules become repulsive and are not well understood. The total potential energy due to attractive and repulsive forces are calculated as follows, according to Mie's equation [28]:

$$\Gamma_{Total} = \frac{A}{r^n} - \frac{B}{r^m} \tag{1.1.20}$$

A, B, n, and m are positive constants. The first term in equation 1.1.20 represents the repulsive interactions and the second term the attractive interactions. It was investigated extensively by Lennard-Jones and is the basis for a variety of physiochemical calculations. It can be rewritten as [28]:

$$\Gamma = \epsilon \frac{\left(\frac{n^n}{m^m}\right)^{\frac{1}{(n-m)}}}{n-m} \left[\left(\frac{\sigma}{r}\right)^n - \left(\frac{\sigma}{r}\right)^m\right] \tag{1.1.21}$$

Where $\epsilon = -\Gamma_{min}$ and $\sigma = r$ at $\Gamma = 0$. London proved that $m = 6$ and normally n is taken as 12 for computational convenience, although better agreement with experimental data is obtained when allowing n to be an adjustable parameter. When $n = 6$ and $m = 12$ are substituted into equation 1.1.21, an expression for the Lennard-Jones potential is obtained [28]:

$$\Gamma = 4\epsilon \left[\left(\frac{\sigma}{r}\right)^n - \left(\frac{\sigma}{r}\right)^m\right] \tag{1.1.22}$$

The Lennard-Jones potential yields the potential energy between two molecules as a function of the distance of seperation between them, with two parameters ϵ and σ. Then energy parameter, ϵ, is equal to the negative of the minimum in energy and the distance parameter, σ, is the seperation between molecules when the potential energy is zero. The constants ϵ, σ and n can all be estimated from numerous physical properties and experimental measurements, such as viscosity, compressibility, specific heat and second virial coefficients [28].

Mie's potential, and consequently equations 1.1.20 through 1.1.22, are only valid for isolated, non-polar, spherically symmetric molecules. Consequently, certain simplifying assumptions are required in order to derive a relationship which holds for non-dilute media and condensed phases. For a condensed phase at conditions similar to that at the triple point, we assume that only interactions between neighbouring pairs of molecules make a significant contribution to the potential energy. Then, for N molecules and z binary interactions, the total potential energy of the system [28]:

$$\Gamma_T = \frac{1}{2} N z \Gamma \tag{1.1.23}$$

Upon substitution of equation 1.1.23 into equation 1.1.20:

$$\Gamma_T = \frac{1}{2} N z \left(\frac{A}{r^n} - \frac{B}{r^m} \right) \tag{1.1.24}$$

Equation 1.1.24 can be modified to account for interactions between non-neighbouring molecules by introducing two parameters s_n and s_m, as in equation 1.1.25. These constants are normally close to unity and can be calculated from lattice geometry for crystalline substances [28].

$$\Gamma_T = \frac{1}{2} N z \left(\frac{s_n A}{r^n} - \frac{s_m B}{r^m} \right) \tag{1.1.25}$$

Structural Effects

Intermolecular forces between non-spherical molecules are influenced by distance of separation as well as spacial orientation. Structural effects are most pronounced at low temperatures and in condensed phases, when intermolecular distances are small. The consequences of these effects are demonstrated by the pronounced differences in boiling points between the isomers of many organic compounds; branched carbon chains have significantly lower boiling points than their straight chain counterparts and the more numerous the branches the lower the boiling point of the chain [28].

Organic molecules will approach a spherical shape as branching increases. The reduced surface area of a branched molecule versus that of a straight chain molecule results in weaker intermolecular attractions. Consequently less kinetic energy is required to overcome these attractions and a reduction in boiling point is observed [28].

Another important structural effect is observed when studying amphiphiles. Such molecules have a hydrophilic part as well as a hydrophobic part, and as a result display unique behaviour in an aqueous medium. These molecules will group together to form aggregates, termed micelles, which keep them in solution. The hydrophobic part, like a long hydrocarbon chain, is kept away from the water whilst the uncharged or ionic hydrophilic part orientates itself toward the water. Reverse micelles can also form when small amounts of water are added to non-polar organic phases that contain surfactants. Figure 1.1.3 illustrates cross-sectional representations of arrangements of micelles and reverse micelles [28].

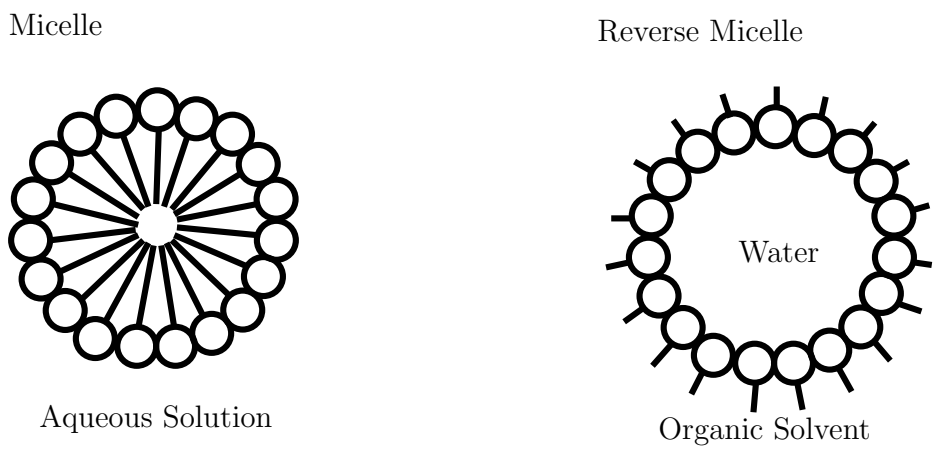

Figure 1.1.3: Schematic representation of a micelle and reverse micelle

Hydrophobic effects are mainly responsible for the insolubility of non-polar and organic substances in water. These effects differ from the numerous other intermolecular effects in that they are mainly an entropic phenomenon rather than enthalpic; when a solute is introduced to the structured nature of liquid water, the hydrogen bonds present between the water molecules have to be disrupted to accommodate the solute molecules. However, in many cases, the hydrogen bonds are not completely broken but only rearranged or distorted. The water molecules still partake in hydrogen bond formation whilst achieving a larger degree of order and thereby resulting in a decrease in entropy. This decrease in entropy, rather than a large enthalpy of mixing, is responsible for the unfavourable Gibbs energy of solubilization of non-polar substances in water [28].

Chemical Forces

Chemical forces are specific attractions which lead to the formation of new chemical species. Not surprisingly, chemical forces contribute significantly to the thermodynamic properties of mixtures or solutions. No simple, quantitative equations, as for physical interactions, can be formulated to describe chemical interactions between molecules and consequently only qualitative relations are used to link these to overall mixture properties. Among the numerous chemical interactions of import to solution thermodynamics is complex formation, electron-donor and -acceptor interactions, hydrogen bonding and acid-base reactions [28].

Chemical interactions are considered saturated where physical interactions are considered unsaturated; after a chemical reaction has taken place between two molecules the resulting species is

usually stable and will not undergo further changes, unless another species is present which can interact chemically with this new compound. For example, when two hydrogen atoms collide they will tend to form a H_2 molecule. However, upon collision with another H atom a H_3 molecule will probably not form. Therefore, the chemical force between the two hydrogen atoms is satisfied or saturated. Physical attractions meet no such saturation and the resulting aggregates can contain any number of atoms [28].

Chemical effects are normally classified into one of two categories namely, association and solvation. Association occurs when molecules of the same species form polymers and solvation when molecules of different species form complexes. Solvation effects are very common and may result in negative deviations from Raoult's law. Association effects are a strong function of composition and the presence of another species can have a very distinct effect on the extent thereof. Both association and solvation effects are related to the electron structure of the molecule at hand. For example, in the case of $AlCl_3$ the aluminium atom has only 6 electrons in it's outer shell i.e. the chemical forces are not satisfied. It will consequently have a strong tendency to add another two by interacting with other molecules by solvation [28].

The most commonly encountered chemical interaction is hydrogen bonding. This effect takes place when molecules containing hydrogen linked to an electronegative atom associate with each other. Studies of substances such as hydrogen fluoride and ice show that the hydrogen atoms form one normal bond with an electronnegative atom and another auxiliary bond with an electronegative atom. These compounds therefore tend to associate with one another and solvate with other molecules containing accessible electronegative atoms [28].

Although the strength of hydrogen bonds are much smaller than that of normal covalent bonds, their presence can have a marked effect on thermodynamic properties. These effects are best illustrated when comparing the properties of chemical isomers. For example, it is noted that the normal boiling point, enthalpy of vaporization and water solubility of ethyl alcohol is much larger than that of dimethyl ether. These are as a result of the additional attractive forces between the ethyl alcohol molecules due to hydrogen bonding. In addition to pure component or isomer properties, the behaviour of hydrogen bonding compounds when mixed with non-polar solvents also illustrate the effects of hydrogen bonding. When a non-polar substance like benzene is mixed isothermally with a non-polar paraffinic solvent, a small amount of heat is absorbed and a small volumetric expansion takes place. On the other hand, when a substace containing strong hydrogen bonds like

ethanol is mixed with the same solvent, a much larger amount of energy is absorbed because it is required to break the hydrogen bonds. Inter-atomic distances between hydrogen bonded molecules tend to be less than the non-bonded molecules and therefore a significant volumetric expansion also takes place. Both heat of mixing and volumetric expansion exhibit highly non-linear behaviour as functions of composition for hydrogen bonding molecules [28].

Even though hydrogen bonding are most commonly encountered, chemical forces also arise from other kinds of complex formations between electron-donor and -acceptor molecules. The existence of these complexes can be determined, from ultraviolet spectroscopy, nuclear magnetic resonance studies, molar absorptivity and various other experimental techniques [28].

Measurements of thermodynamic properties also confirm complex formation in some cases, for example the mixtures 1 , 2 , 4 - trichlorobenzene with benzene, toluene and p - xylene. The volume of mixing is negative in all three cases over the entire composition range. The interactions also tends to increase with increasing electron-donating potential of the hydrocarbon. In fact, the volume of mixing, at 0.5 mol 1 , 2 , 4 - trichlorobenzene, has been found to be a linear function of the ionization potential of the hydrocarbon [28].

The profound influence of chemical forces on thermodynamic properties are even illustrated by some well known separation processes used in the petrochemical industry; for example the tendency of polar solvents to form complexes with unsaturated hydrocarbons and not with saturated hydrocarbons [28].

1.1.2 Mixture Theory and Thermodynamics

It has been found useful in many fields of science to develop simplified models or theories of natural phenomena. These theories will initially contain only essential behaviour and are then expanded to include many possible exceptions and details. The additional terms are used to describe behaviour which was initially neglected and therefore accounts for deviations of reality from the ideal. This approach has been applied quite successfully in the field of solution thermodynamics.

Fundamental Thermodynamic Properties

We have the following expression for the Gibbs energy of a closed system at a specific temperature and pressure [37]:

$$\mathrm{d}\left(nG\right) = \left(nV\right)\mathrm{d}P - \left(nS\right)\mathrm{d}T \tag{1.1.26}$$

If no chemical reaction occurs the composition of the system is constant and we have [37]:

$$\left[\frac{\partial\left(nG\right)}{\partial P}\right]_{T,n} = nV \tag{1.1.27}$$

and

$$\left[\frac{\partial\left(nG\right)}{\partial T}\right]_{P,n} = -nS \tag{1.1.28}$$

If however, the single phase system interacts with it's surroundings and consequently the number of moles of the composite species are variable [37]:

$$\mathrm{d}\left(nG\right) = \left[\frac{\partial\left(nG\right)}{\partial P}\right]_{T,n}\mathrm{d}P + \left[\frac{\partial\left(nG\right)}{\partial T}\right]_{P,n}\mathrm{d}T + \sum_{i}\left[\frac{\partial\left(nG\right)}{\partial n_i}\right]_{P,T,n_j}\mathrm{d}n_i \tag{1.1.29}$$

which leads to the definition of the chemical potential of species i in a mixture [28, 37]:

$$\mu_i \equiv \left[\frac{\partial\left(nG\right)}{\partial n_i}\right]_{P,T,n_j} \tag{1.1.30}$$

By substituting the chemical potential and equations 1.1.28 and 1.1.27 into equation 1.1.29, we obtain the following fundamental property relation for an open system with variable composition [37]:

$$\mathrm{d}\left(nG\right) = \left(nV\right)\mathrm{d}P - \left(nS\right)\mathrm{d}T + \sum_{i}\mu_i\mathrm{d}n_i \tag{1.1.31}$$

This equation forms the basis of solutions thermodynamics. When the Gibbs energy is expressed, as is the case in equation 1.1.31, as a function of it's canonical variables it implicitly provides complete property information. All other thermodynamic properties of the system at hand can then be calculated by mathematical operations and manipulations [28, 37].

Ideal Mixture and Excess Functions

The concept of defining an ideal mixture, and subsequent excess properties to relate this ideal mixture to reality, is similar to how the ideal gas model serves as a reference state for the behaviour of real gasses, and is completed by the introduction of residual properties [28, 37].

An ideal mixture is defined as one for which:

$$\bar{G}_i^{ideal}(T, P, x) = G_i(T, P) + RT \ln x_i \tag{1.1.32}$$

Where $\bar{G}_i^{ideal}$ represents the partial molar Gibbs energy of component i in an ideal mixture, and G_i represents the molar Gibbs energy of that component at the same conditions as the mixture. All thermodynamic properties of the ideal mixture are derived from or based on equation 1.1.32 [28, 37].

The partial entropy can now be determined from:

$$\bar{S}_i^{ideal} = -\left(\frac{\partial \bar{G}_i^{ideal}}{\partial T}\right)_{P,x} \tag{1.1.33}$$

Therefore

$$\bar{S}_i^{ideal} = -\left(\frac{\partial G_i}{\partial T}\right)_P - R \ln x_i \tag{1.1.34}$$

And since $-S_i = \left(\frac{\partial G_i}{\partial T}\right)_P$, we have:

$$\bar{S}_i^{ideal}(T, P, x) = S_i(T, P) - R \ln x_i \tag{1.1.35}$$

In a similar manner we can derive:

$$\bar{V}_i^{ideal} = V_i \tag{1.1.36}$$

$$\bar{H}_i^{ideal} = H_i \tag{1.1.37}$$

Since the principal of summability holds for the partial properties of ideal mixtures, similar to general partial properties, we finally also have the following for ideal mixtures:

$$G^{ideal}(T, P, x) = \Sigma_i x_i G_i(T, P) + RT \Sigma_i x_i \ln x_i \tag{1.1.38}$$

$$S^{ideal}(T,P,x) = \Sigma_i x_i S_i(T,P) - R\Sigma_i x_i \ln x_i \tag{1.1.39}$$

$$V^{ideal}(T,P,x) = \Sigma_i x_i V_i(T,P) \tag{1.1.40}$$

$$H^{ideal}(T,P,x) = \Sigma_i x_i H_i(T,P) \tag{1.1.41}$$

Therefore, formation of an ideal mixture takes place without any evolution or absorption of heat and without change of volume [20, 28, 37].

It can be shown that, for an ideal mixture, equation 1.1.42 holds at a specific temperature and pressure, and all temperatures and pressures in the immediate vicinity. Where f_i^{ideal}, c_i and x_i is the ideal mixture fugacity, proportionality constant and mole fraction, respectively, of component i in the liquid mixture. The liquid fugacity is however also conveniently related to the activity coefficient, γ_i, and liquid mole fraction by equation 1.1.43[20, 28].

$$f_i^{ideal} = c_i x_i \tag{1.1.42}$$

$$f_i^{ideal} = \gamma_i x_i f_i^0 \tag{1.1.43}$$

where f_i^0 is the fugacity of i at some arbitrary reference state.

If we let $f_i^0 = c_i$, then $\gamma_i = 1$. If this relationship holds for the entire composition range it follows that c_i is equal to the fugacity of the pure liquid at the same temperature. Raoult's law is then obtained if the fugacity in equation 1.1.42 is set to the partial pressure of i. Therefore, for an ideal solution a relation, known as the Lewis/Randall rule, can be derived [28, 37]:

$$f_i^{ideal}(T,P,x) = f_i^{pure}(T,P)\, x_i \tag{1.1.44}$$

Real mixtures of similar components often exhibit near-ideal behaviour however, for most liquids ideal behaviour only holds for a small range of compositions. Very dilute mixtures of non-electrolytes behave ideally and Henry's law for ideal dilute solutions is also derived from equation 1.1.42. Correction terms which account for the non-idealities of real mixtures can be included and are termed excess functions [28, 37].

As the name suggests, excess properties are thermodynamic properties which are in excess of that of an ideal mixture's at a specified temperature, pressure and composition. The excess Gibbs energy of a mixture is defined as [28, 37]:

Table 1.1: Summary of similarities between Total property and excess property relations

Total Property Relation	**Excess Property Relation**
$S = -\left(\frac{\partial G}{\partial T}\right)_{P,x}$	$S^E = -\left(\frac{\partial G^E}{\partial T}\right)_{P,x}$
$V = \left(\frac{\partial G}{\partial P}\right)_{T,x}$	$V^E = \left(\frac{\partial G^E}{\partial P}\right)_{T,x}$
$H = G + TS$ $= G - T\left(\frac{\partial G}{\partial T}\right)_{P,x}$ $= -RT^2\left[\frac{\partial\left(\frac{G}{RT}\right)}{\partial T}\right]_{P,x}$	$H^E = G^E + TS^E$ $= G^E - T\left(\frac{\partial G^E}{\partial T}\right)_{P,x}$ $= -RT^2\left[\frac{\partial\left(\frac{G^E}{RT}\right)}{\partial T}\right]_{P,x}$

$$G^E(T,P,x) = G(T,P,x) - G^{ideal}(T,P,x) \tag{1.1.45}$$

The excess volume, V^E, excess entropy, S^E, excess enthalpy, H^E, excess internal energy, U^E, and excess Helmholtz energy,A^E, are all defined in a similar manner. Excess property relations are similar to that of total thermodynamic and residual properties. Table 1.1 summarises these similarities.

In addition, we can derive a fundamental excess-property relation. Firstly, with the use of the chain rule, we have [37]:

$$\mathrm{d}\left(\frac{nG}{RT}\right) \equiv \frac{1}{RT}\mathrm{d}(nG) - \frac{nG}{RT^2}\mathrm{d}T \tag{1.1.46}$$

If we now substitute G with $H - TS$, and $\mathrm{d}(nG)$ with equation 1.1.31, we obtain a fundamental overall property relation [37]:

$$\mathrm{d}\left(\frac{nG}{RT}\right) = \frac{nV}{RT}\mathrm{d}P - \frac{nH}{RT^2}\mathrm{d}T + \sum_i \frac{\bar{G}_i}{RT}\mathrm{d}n_i \tag{1.1.47}$$

Finally, by rewriting equation 1.1.47 for an ideal mixture and subtracting it from the original a fundamental excess property relation is obtained [28, 37]:

$$\mathrm{d}\left(\frac{nG^E}{RT}\right) = \frac{nV^E}{RT}\mathrm{d}P - \frac{nH^E}{RT^2}\mathrm{d}T + \sum_i \frac{\bar{G}_i^E}{RT}\mathrm{d}n_i \tag{1.1.48}$$

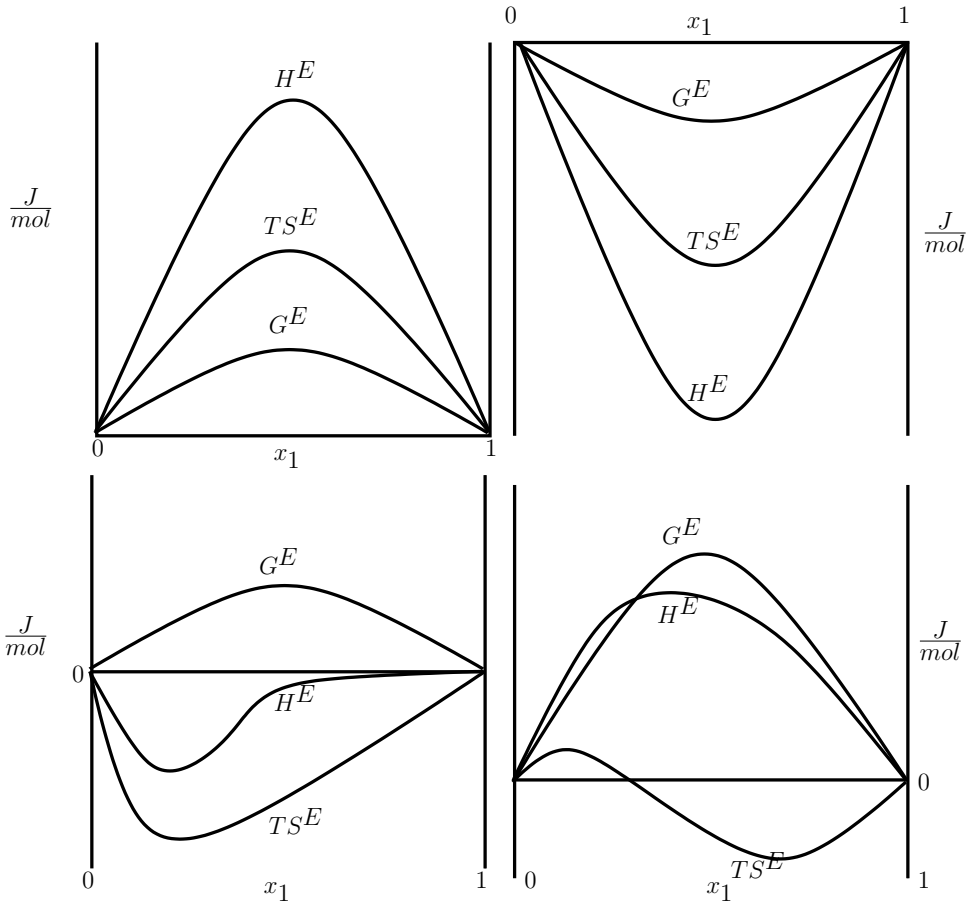

Figure 1.1.4: Typical excess properties for real mixtures

Depending on whether the excess Gibbs energy is positive or negative, real mixtures are said to exhibit positive or negative deviations from the ideal. Characteristic behaviour of liquid mixtures are often explained upon investigation of excess thermodynamic properties. The excess Gibbs energy can be determined from experimental vapour-liquid equilibrium data, and the excess enthalpy from mixing experiments. Since the excess entropy cannot be determined experimentally, the following relationship is used [37]:

$$S^E = \frac{H^E - G^E}{T} \tag{1.1.49}$$

Figure 1.1.4 illustrates quantitatively the excess properties of some real binary mixtures. The excess properties of all mixtures become zero as the composition approaches a pure substance; since that property will obviously approach that of the pure substance. It has also been observed from experimental data that if an excess property does not change sign in the composition range, it will often have it's extreme value near the equimolar composition [37].

Changes on Mixing

When combining the definition of excess properties with equations 1.1.38 to 1.1.41 the following relationships result [37]:

$$G^E = G - \sum_i x_i G_i - RT \sum_i x_i \ln x_i \tag{1.1.50}$$

$$S^E = S - \sum_i x_i S_i + R \sum_i x_i \ln x_i \tag{1.1.51}$$

$$V^E = V - \sum_i x_i V_i \tag{1.1.52}$$

$$H^E = H - \sum_i x_i H_i \tag{1.1.53}$$

The first two terms on the right hand side of equations 1.1.50 through 1.1.53 express the property changes upon mixing. For example, the change of Gibbs energy on mixing, ΔG, is defined as:

$$\Delta G \equiv G - \sum_i x_i G_i \tag{1.1.54}$$

Other properties of mixing are defined similarly. From these definitions it is apparent that the excess volume of a mixture is equal to the change of molar volume on mixing, $V^E = \Delta V$, and similarly the excess enthalpy is equal to the change in molar enthalpy on mixing, $H^E = \Delta H$. The following expressions for G^E and S^E can therefore also be written [37]:

$$G^E = \Delta G - RT \sum_i x_i \ln x_i \tag{1.1.55}$$

$$S^E = \Delta S + R \sum_i x_i \ln x_i \tag{1.1.56}$$

The change of enthalpy and volume on mixing is of greatest interest as these can be measured experimentally, and are equal to the corresponding excess properties.

Similar to excess properties, change of properties on mixing are obviously zero for pure species. If mixing occurs, the change of the Gibbs energy on mixing is negative. In general, the change in entropy on mixing is positive however, negative values are observed in rare cases. The second law of thermodynamics places no restriction on the entropy of mixing for systems open to their

surroundings; it forbids negative changes of entropy only for systems which are isolated from their surroundings [37].

Mixture Activity Coefficients and Fugacities

The chemical potential of a species is an abstract theoretical term and it is difficult to make a connection between it and physical reality. The fugacity of a species conveniently relates pure thermodynamics to physical variables. It was first considered by G.N. Lewis in an attempt to simplify the the expression for chemical equilibrium [28].

For the chemical potential of a pure species we have:

$$\left(\frac{\partial \mu_i}{\partial P}\right) = V_i \tag{1.1.57}$$

For an ideal gas, we substitute $V_i = \dfrac{RT}{P}$, and then integrate with respect to pressure at constant temperature:

$$\mu_i - \mu_i^0 = RT \ln \frac{P}{P^0} \tag{1.1.58}$$

This is a significant result as it relates the chemical potential to an experimentally measurable variable, namely pressure. It is however only valid for an ideal gas and consequently Lewis defined, for an isothermal change, the fugacity of a species in any system, in any state as [28]:

$$\mu_i - \mu_i^0 = RT \ln \frac{f_i}{f_i^0} \tag{1.1.59}$$

Where f_i is the fugacity of species i in a mixture. Either μ_i^0 or f_i^0, but not both, can be chosen arbitrarily. For an ideal gas $f_i = P$, and for an ideal gas mixture $f_i = y_i P$. All systems approach ideal gas behaviour at very low pressures and consequently we have a complete definition for fugacity by including [28, 37]:

$$\lim_{P \to 0} \frac{f_i}{y_i P} = 1 \tag{1.1.60}$$

The importance of the partial molar excess Gibbs energy in mixture thermodynamics is due to it's direct relation to the activity coefficient of a species in a mixture. With the use of equation

1.1.59 [28]:

$$\bar{G}_i - \bar{G}_i^{id} = RT \ln \frac{f_i}{f_i^{ideal}} \tag{1.1.61}$$

And by substituting the definition of the partial molar excess Gibbs energy and the Lewis/Randall rule, equation 1.1.44, into equation 1.1.61 we obtain the following significant relationship [28]:

$$\bar{G}_i^E = RT \ln \frac{f_i}{x_i f_i^{pure}} \tag{1.1.62}$$

The activity of a species in a mixture is the ratio of the fugacity of i in the mixture to the fugacity in some standard reference state. It is an indication of the isothermal change in the chemical potential of species i from the reference state to that of the mixture; how "active" species i is at the mixture state. When the activity coefficient of a species i is defined as

$$\gamma_i \equiv \frac{f_i}{x_i f_i^{pure}} \tag{1.1.63}$$

the expressions, in equations 1.1.64 through 1.1.66 are obtained. They are of significant importance in mixture phase-equilibrium thermodynamics. Equation 1.1.66, for example, is a consequence of applying the Gibbs-Duhem equation to the partial molar excess Gibbs energy and is extensively used in practice to determine the thermodynamic consistency of experimental data [20, 28, 37].

$$\bar{G}_i^E = RT \ln \gamma_i \tag{1.1.64}$$

$$\therefore G^E = RT \sum_i x_i \ln \gamma_i \tag{1.1.65}$$

$$\therefore \sum_i x_i \mathrm{d} \ln \gamma_i = 0 \tag{1.1.66}$$

The pressure and temperature derivatives of the activity coefficients are related to the partial molar excess volume and partial molar excess enthalpy, respectively, of the mixture [28]:

$$\left(\frac{\partial \ln \gamma_i}{\partial P} \right)_{T,x} = \frac{\bar{V}_i^E}{RT} \tag{1.1.67}$$

$$\left(\frac{\partial \ln \gamma_i}{\partial T} \right)_{P,x} = \frac{\bar{H}_i^E}{RT^2} \tag{1.1.68}$$

1.2 Phase Equilibrium Thermodynamics

1.2.1 The Gibbs Phase Rule

A homogeneous phase is one for which all intensive properties are the same throughout, where intensive properties, for example temperature, pressure, composition etc., are those which are not dependent on the size or mass of the phase. Conversely, a heterogeneous system is considered to consist of two or more phases. A phase does not necessarily have to be a continuous whole and it is permissible for one phase to be distributed throughout another. For example the dispersion of gas bubbles in a liquid or a dispersion of one liquid phase inside another [28, 37].

The state of single pure homogeneous phase is fixed when 2 intensive variables are specified. The degrees of freedom of a heterogeneous system composed of numerous species is given by the Gibbs phase rule:

$$p = m + 2 - \pi \tag{1.2.1}$$

Where p, m, and π represent the degrees of freedom, the number of species and the number of phases, respectively. Therefore, the phase rule establishes the number of intensive variables that must be specified in order to fix the state of the system. The remaining intensive variables are subsequently also fixed and cannot be chosen arbitrarily or independently from the rest. It is important to note that equation 1.2.1 only applies to a non-reacting system at equilibrium [37].

A system is completely determined when all intensive and extensive variables are fixed. Duhem's theorem states that if two independent variables are fixed, then the equilibrium state of a closed system, containing specified masses of a given number of species, is completely determined. These two variables may be extensive or intensive however, the number of intensive variables that must be independently specified is given by the Gibbs phase rule, and the remaining may be extensive [37].

1.2.2 Phase Equilibrium

An isolated system comprising of two phases will exchange material until the compositions of each system attains a constant value, or an equilibrium. Even though material still migrates from one phase to another on a microscopic level, after equilibrium is reached there is no net change in the macroscopic system properties. This natural phenomena of phase equilibrium is of fundamental

importance in many natural and industrial processes and is consequently an important topic in the natural and physical sciences. Phase equilibrium thermodynamics is concerned with establishing the relations between variables, such as temperature, pressure and composition, that prevail at equilibrium [28, 37].

Since equilibrium denotes a static state or the absence of change, it also implies the absence of some driving force which brings about change. For example, the driving force behind heat transfer is a temperature gradient, and an imbalance of mechanical forces cause the transfer of work. The chemical potential, as defined by Gibbs in 1875, denotes the driving force responsible for phase transition. Phase equilibrium occurs only when the chemical potential μ_i of each component is the same in each phase. Therefore, for any phase equilibrium problem we initially have [28]:

$$\mu_i^{\alpha} = \mu_i^{\beta} \tag{1.2.2}$$

Where α and β denote the phases. In order to solve the phase equilibrium problem, the relation between the chemical potential and temperature, pressure and composition has to be established for each phase. Auxiliary variables, like fugacity and activity, are normally used to link these physical variables to the abstract concept of chemical potential.

1.2.3 Phase Equilibria and Stability

Consider a closed system that consists of a number of phases and components. Assume that this system is at uniform, but variable, temperature and pressure. It is initially not in a state of equilibrium with regard to mass transfer between phases and chemical reaction. In addition, we assume that the system is at the same temperature and pressure as it's surroundings and therefore all heat exchange with it's surroundings and expansion takes place reversibly [37].

Consequently we have:

$$\mathrm{d}S_{surr} = \frac{\mathrm{d}Q_{surr}}{T_{surr}} = -\frac{\mathrm{d}Q}{T} \tag{1.2.3}$$

Where S_{surr}, Q_{surr} and T_{surr} represents the entropy, the heat transferred to and the temperature of the surroundings, respectively. In order for the heat transfer to take place reversibly $T_{surr} = T$. The second law of thermodynamics requires that:

$$\mathrm{d}S + \mathrm{d}S_{surr} \geq 0 \tag{1.2.4}$$

Upon combination of equations 1.2.3 and 1.2.4 we obtain:

$$\mathrm{d}Q \leq T\mathrm{d}S \tag{1.2.5}$$

And lastly, by applying the first law of thermodynamics we have:

$$\mathrm{d}U + P\mathrm{d}V - T\mathrm{d}S \leq 0 \tag{1.2.6}$$

It is noted that the expression in equation 1.2.6 involves only properties and is consequently relevant to changes in state of any system with uniform temperature and pressure, not only for systems in mechanical and thermal equilibrium with their surroundings. The following is applicable to equation 1.2.6 [37]:

- the inequality holds for any incremental change between non-equilibrium states
- it dictates the direction in which change of the properties will occur towards equilibrium
- the equality applies to changes between equilibrium states i.e. reversible processes

For a process occurring at constant temperature and pressure, equation 1.2.6 becomes [37]:

$$\mathrm{d}U_{T,P} + \mathrm{d}\left(PV\right)_{T,P} - \mathrm{d}\left(TS\right)_{T,P} \leq 0 \tag{1.2.7}$$

$$\therefore \mathrm{d}\left(U + PV - TS\right)_{T,P} \leq 0 \tag{1.2.8}$$

$$\therefore \mathrm{d}\left(H - TS\right)_{T,P} \leq 0 \tag{1.2.9}$$

$$\therefore \mathrm{d}G_{T,P} \leq 0 \tag{1.2.10}$$

The result in equation 1.2.10 is significant. It indicates that all irreversible changes in a process occur in such a way to accomplish a minimum in Gibbs energy of the system. Therefore, the equilibrium state of a closed system, at constant temperature and pressure, is that for which the Gibbs energy of the system is at a minimum. In addition, as indicated by the equality, at the state of equilibrium differential changes in the system can occur, at constant temperature and pressure,

without yielding a change in the Gibbs energy of the system [25, 32, 37].

A general criterion for calculating the equilibrium state is provided by equation 1.2.10. It is most useful for complex systems containing phase equilibrium, chemical reaction equilibrium and systems containing both phase- and chemical reaction equilibrium. The equilibrium conditions are found by determining the mole numbers which bring about a minimum in the Gibbs energy of the system, whilst satisfying the constraints of conservation of mass [6, 17, 25, 27, 32, 36, 37, 43].

Equation 1.2.10 also provides an important criterion which is applied to determine the stability of a single phase. The total Gibbs energy of a system has to decrease if two liquids mix. Therefore, if mixing occurs, the mixed state must result in a negative change in Gibbs energy of the system:

$$G - \sum_i x_i G_i < 0 \tag{1.2.11}$$

$$\therefore \Delta G < 0 \tag{1.2.12}$$

A phase is considered unstable if upon mixing it can achieve a lower overall Gibbs energy by forming multiple phases rather than remaining in a single phase. Figure 1.2.1 illustrates typical shapes of the ΔG_{mix} curve as a function of composition. The usual shape represented in (a) is that of a stable mixture; it is everywhere less than or equal to zero. The mixture in the case of curve (b) however is unstable. For a mixture with an overall composition $\alpha < z_1 < \beta$ the system will split into two phases with $x_1 = \alpha$ and $x_1 = \beta$ [6, 24, 25, 32, 36, 37].

Therefore, for stability in a binary mixture at constant temperature and pressure ΔG_{mix} and it's first and second order derivatives must be continuous functions of x_1 and the second derivative must be everywhere positive [37].

$$\frac{d^2 \Delta G_{mix}}{dx_1^2} > 0 \tag{1.2.13}$$

1.2.4 Liquid-liquid Equilibria

Many chemical species form unstable liquid mixtures and split to form two liquid phases in equilibrium. Liquid-liquid equilibrium forms an important topic in liquid separation processes by

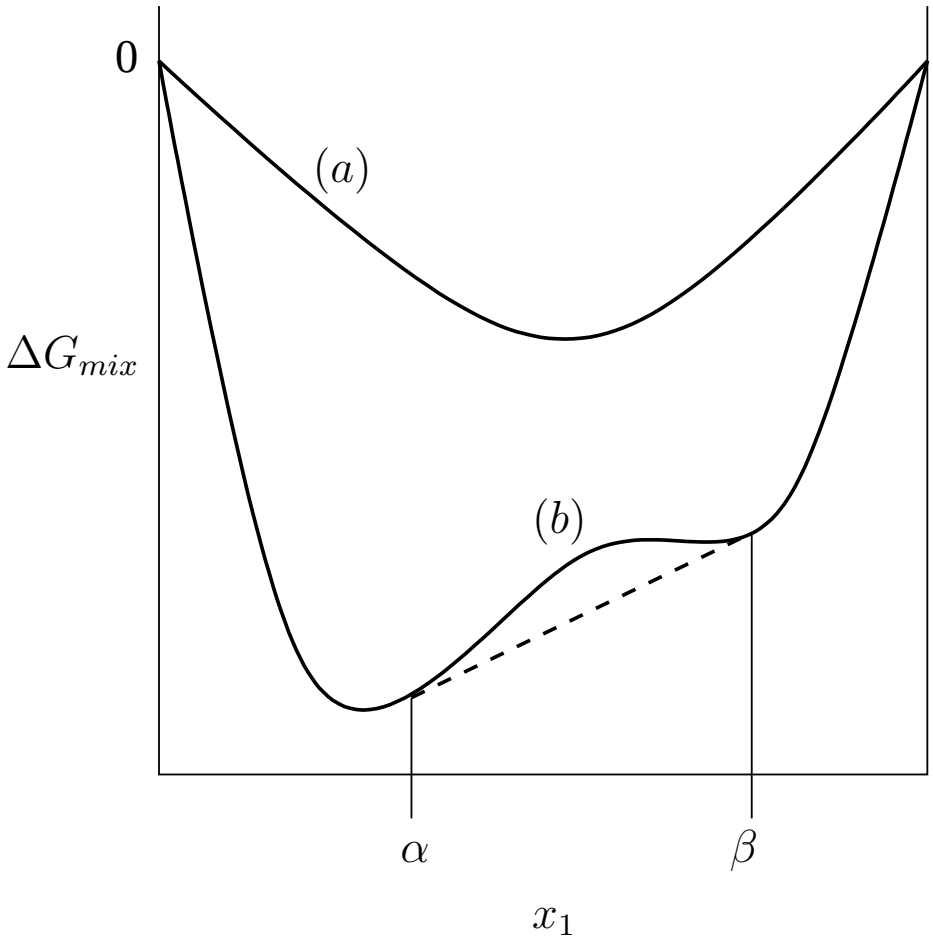

Figure 1.2.1: Typical excess properties for real mixtures

extraction. The phenomena of liquid-liquid equilibria requires that, similar to vapour-liquid equilibria, the chemical potential or fugacities of each component be equal in each phase. In addition to the regular requirements of uniform temperature and pressure throughout the system [6, 37].

Four kinds of binary liquid-liquid equilibria have been observed. They are quantitatively represented in the solubility diagrams in figure 1.2.2 [25, 27, 37].

At constant pressure, or under conditions where pressure effects are negligible, equilibrium compositions of the two liquid phases are determined by the intersections of a isothermal tie-line with the phase boundary. In figure 1.2.2 (a) an isolated region, with an upper and lower temperature boundaries, of partial solubility is observed. At temperatures outside of these boundaries the binary mixture becomes completely mixable. It is only between these temperature bounds that liquid-liquid equilibria is observed for a certain overall mixture composition range. The upper

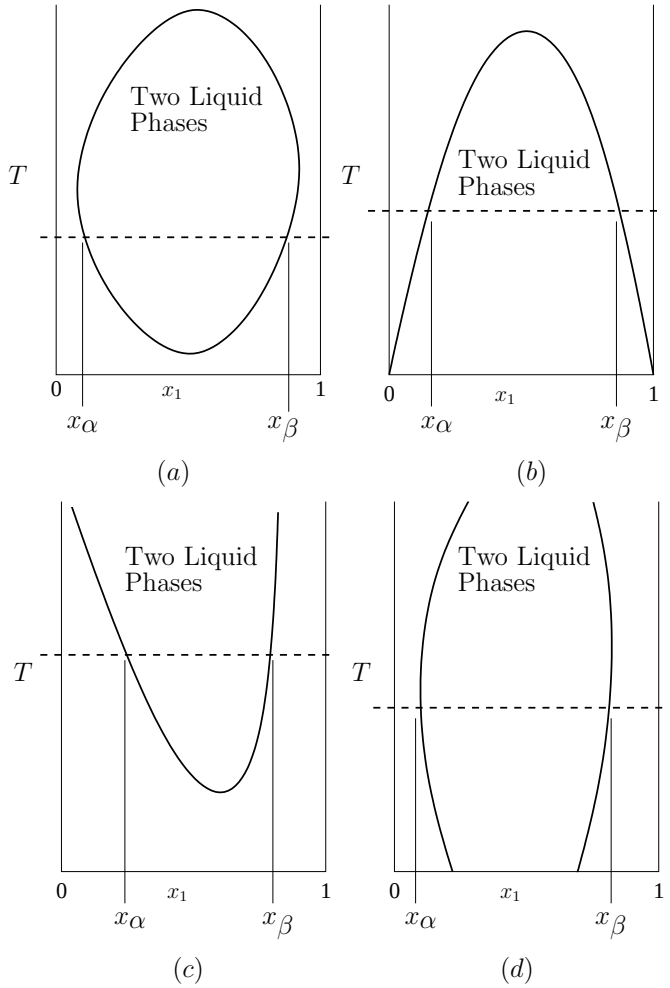

Figure 1.2.2: Solubility diagrams of three kinds of binary liquid-liquid equilibria

temperature bound is termed the upper consolute temperature, or the upper critical solution temperature. Similarly the lower temperature bound is called the lower consolute temperature, or the lower critical solution temperature. Similar to the liquid/gas critical point of pure fluids, these critical solution points represent limiting states at which the properties of the two phases become identical [4, 27, 37].

Liquid-liquid equilibria of the type in figure 1.2.2 (a) is however observed much less frequently experimentally than the behaviour depicted in figure 1.2.2 (b) and (c). The kind of liquid-liquid equilibria depicted in 1.2.2 (b) is encountered when the solubility curve intersects the freezing curve and consequently only the upper critical solution point is observed. In a similar manner, the behaviour observed in 1.2.2 (c) occurs when the vapour-liquid bubble-point curve is intersected. Lastly, the solubility diagram in figure 1.2.2 (d) is observed when both the freezing- and the bubble-point curve is intersected. In such a case no critical solubility points are present [4, 37].

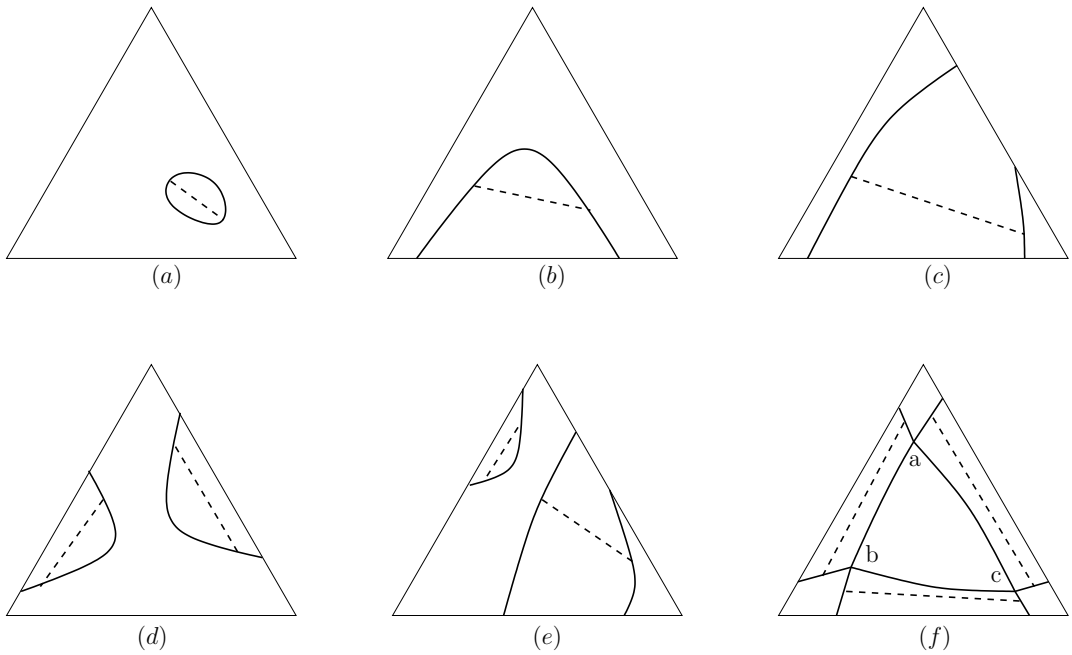

Figure 1.2.3: Solubility diagrams of six kinds of ternary liquid-liquid equilibria

Solubility diagrams for the six kinds of liquid-liquid equilibria that have been observed experimentally for ternary systems are depicted in figure 1.2.3. With the exception of the type of system represented in figure 1.2.3 (f), which may have three liquid phases in equilibrium, unstable ternary mixtures are only observed to split into two equilibrium phases [17, 25, 38].

1.3 Thermodynamic Models

Equilibrium based separation processes are common in chemical industry, for example distillation, extraction and absorption. In order to design such process equipment accurate knowledge of transport properties, phase equilibrium data etc. is essential. However, the list of possible mixtures is endless, even at only a limited set of temperatures and pressures. It is therefore understandably inconceivable that experimental data would be available for every possible combination of species. It is in fact often the case that experimental data is not available for a specific system at the applicable temperature, pressure and composition. In such cases reliable methods of correlation are required. Thermodynamic models provide such methods by which the required properties of mixtures can be deduced, extrapolated or correlated from available pure component and mixture data. The judicious use of suitable thermodynamic models is therefore a vital tool in the chemical engineering design industry [4, 27, 37].

In the case of Liquid-liquid equilibria thermodynamic models may take the form of excess Gibbs energy models and equations of state. Equations of state find widespread application for both property and phase equilibrium predictions. They are the preferable method by which high-pressure vapour-liquid equilibria is calculated for systems of non-associating molecules. Excess Gibbs energy or activity coefficient models, i.e. expressions for $\frac{G^E}{RT}$ from which activity coefficients are calculated, normally provide more accurate predictions for associating systems [4].

Whether a specific model is suitable for the problem at hand is determined by it's ability to accommodate the specific type of liquid-liquid phase equilibria. The ability of a activity coefficient model to accurately predict liquid-liquid equilibria poses a significant problem; seeing as the activity coefficients it predicts are the only thermodynamic contributions used in the equilibrium calculation, as opposed to the supplementary role played by thermodynamic models in vapour-liquid equilibria calculations [27, 37].

1.3.1 Equations of State

Equations of state are semi-theoretical, empirically derived functions of state variables, i.e. pressure, temperature, molar volume and composition. They provide a method for calculation of configurational and residual thermodynamic properties, normally based on theoretical analysis of molecular interactions combined with parametrisations which allow for the reproduction of experimental data. The virial equation of state, for example, is derived from molecular theory. Cubic and quartic equations of state are semi-theoretical equations which can be solved analytically and are applicable to a wide range of compounds. Equations of state which are derived purely empirically are applicable over a much larger temperature and pressure range for many more compounds. Empirical equations of state can however not be solved analytically and normally require large amounts of property data in order to fit the numerous parameters involved [4, 27].

Some equations of state are applicable to the gas phase, some to the liquid phase, some are simultaneously applicable, in the same form, to both the gas and liquid phase. The virial equation of state is suitable for representing slight deviations from ideal gas behaviour. Cubic and quartic equations are applicable to both the gas and liquid phases. However, no equation of state is simultaneously applicable to the gas, liquid and solid phase. [4, 27].

van der Waals Equation of State

The simplest equation of state is known as the ideal gas law, which can be stated as follows for an ideal gas mixture:

$$P = \sum_i n_i \frac{RT}{V} \tag{1.3.1}$$

As interest and research about the transition from liquid to vapour phase enjoyed more attention the van der Waals equation of state evolved from the ideal gas law. It is cubic in the molar volume and contains two adjustable parameters a and b, see equation 1.3.2. It is the simplest cubic equation of state and is never very accurate for real fluids. It does however have sound theoretical basis and the behaviour that it predicts is qualitatively correct [4, 20].

$$P = \frac{RT}{v - b} - \frac{a}{v^2} \tag{1.3.2}$$

Term 1 of equation 1.3.2 represents the effects of the repulsive interactions between molecules on the pressure and term 2 that of the attractive interactions. It was the first equation of state capable of predicting both gas and liquid phase properties and many modern empirical equations of state are derived from it. More complex equations of state are available and provide more accurate predictions however, the cubic equations of state are fairly accurate and relatively simple to apply. In the derivation of the van der Waals equation the following assumptions were made [4]:

- Each individual molecule, in a fluid of interacting molecules, moves independently in a uniform potential field produced by other molecules.
- A molecule cannot occupy the same space as the core of another molecule.
- Molecules are rigid spheres between which there is an infinitesimal attractive force with infinite range.
- The distribution of molecules around any one molecule is random.

Equation 1.3.2 has three real roots below the critical temperature. For a specific vapour pressure the smallest root corresponds to the liquid molar volume, the largest to that of the vapour and the intermediate has no known physical significance. As the critical temperature is approached these roots converge on the critical volume. The parameters, a and b, are calculated at the critical point by utilising the following [4]:

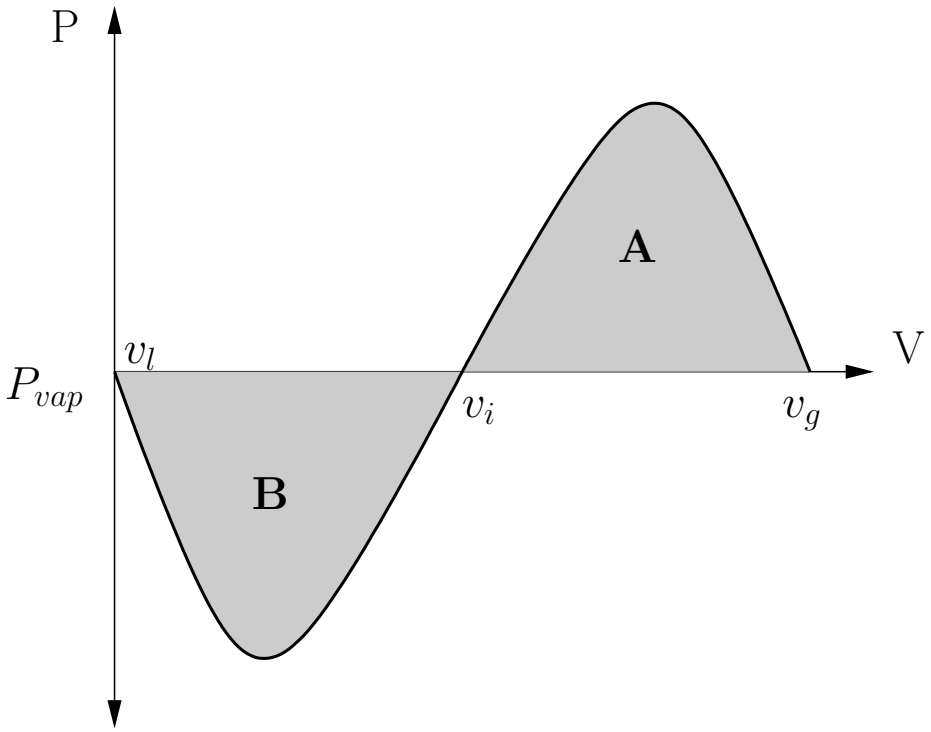

Figure 1.3.1: Roots of the Van der Waals equation of state

$$\left(\frac{\partial P}{\partial V}\right)_T = 0 \tag{1.3.3}$$

$$\left(\frac{\partial^2 P}{\partial V^2}\right) = 0 \tag{1.3.4}$$

These are solved to find expressions for a and b:

$$a = \frac{27\left(RT^c\right)^2}{64P^c} \tag{1.3.5}$$

$$b = \frac{RT^c}{8P^c} \tag{1.3.6}$$

Figure 2.2.1 illustrates how the vapour-liquid equilibrium pressure and the roots of the van der Waals equation are related.

The van der Waals equation is applied to mixtures by utilising suitable combining rules. It is common practice to calculate the attractive parameter a for a mixture by [4]:

$$a = \left(\sum_i x_i\sqrt{a_i}\right)^2 \tag{1.3.7}$$

And the repulsive parameter simply as the mole weighted average of the pure component parameters [4]:

$$b = \sum_i x_i b_i \tag{1.3.8}$$

These combining- or mixing rules are regularly used in conjunction with modern cubic equations of state. In more complex cases, binary interaction parameters are introduced in the calculation of the attractive parameter a [4].

General Cubic Equations of State

The predictions provided by the standard van der Waals equation are usually found to be qualitatively accurate but quantitatively rather poor. Predicted densities in the region of the critical point are particularly inaccurate and the vapour-liquid equilibrium curve is found to deviate from reality. The two most apparent ways in which the van der Waals equation can be improved are [4, 20]:

- The crude expression for the free volume which neglects many body interactions can be improved by using the correct rigid sphere model for the repulsive term.
- The attractive term, which assumes a uniform distribution of molecules over the entire temperature range, can be improved by utilising empirical modifications for term 1 of 1.3.2.

The application of equations of state are however usually at sub-critical temperatures and under these conditions the contribution to inaccuracy of the repulsive term is considered insignificant in comparison to that of the attractive term. Consequently, most modifications to the van der Waals equation took the form of improvements to the attractive term [4, 21].

Cubic equations of state are very well suited for application to vapour-liquid equilibrium and many of the modifications for these functions originated in that field, such as the cohesion function [26]. A commonly used modification to the van der Waals equation is that of Adachi-Lu, displayed below in equation 1.3.9 [2]:

$$\frac{a\,(T)}{a_c} = \exp\left[m\,(1 - T_R)\right] \tag{1.3.9}$$

$$T_R = \frac{T}{T^c} \tag{1.3.10}$$

Most modified cubic equations of state take the following form [4]:

$$P = \frac{RT}{v-b} - \frac{a\left(T\right)}{\left(v+c_1 b\right)\left(v+c_2 b\right)} \tag{1.3.11}$$

Parameters c_1 and c_2 are integer variables which determine the shape of the specific cubic equation of state. In addition, the variable a is considered to be temperature dependant in all modified cubic equations of state; the functional form of which was determined by fitting experimental vapour pressure data. Modern cubic equations of state which find widespread practical application are summarised in table 1.2 [4, 21, 27].

Which form of cubic equation is used is determined by which properties are to be predicted. The most common approach is to choose a formulation in such a way that produces the most accurate liquid densities and vapour pressures [27].

The modifications introduced in the Redlich-Kwong equation has no theoretical basis but is rather a successful empirical improvement. The parameters of this equation are considered functions of T^c and P^c, whereas most other modifications also take into the account the acentric factor of the molecules. As a result it provides accurate results only for simple fluids. Many modifications of the Redlich-Kwong equation were developed, among these is the Soave-Redlich-Kwong equation. It assumes the attractive term to be a more complex function of temperature, which includes the acentric factor. Similarly, the Peng-Robinson equation of state also incorporates the acentric factor along with the critical temperature and pressure. This latter form of the cubic equation of state does however provide improved liquid density predictions when compared to the former equations [4, 20].

Thermodynamic Properties from Equations of State

The common P-V-T equation of state may be used to derive expressions for configurational and residual thermodynamic properties within it's domain of applicability. Equations of state which can be used to describe liquid and gas phase behaviour are necessarily pressure explicit with temperature and volume the independent variables. Using Maxwell's relations we have the following expressions for the internal energy and entropy of a system [28]:

Table 1.2: Cubic Equations of State

van der Waals

$$P = \frac{RT}{v-b} - \frac{a}{v^2}$$
$$a_i = \frac{27\left(RT_i^c\right)^2}{64P_i^c}, \qquad b_i = \frac{RT_i^c}{8P_i^c}$$
$$a = \left(\sum_i x_i\sqrt{a_i}\right)^2$$

Redlich - Kwong

$$P = \frac{RT}{v-b} - \frac{a}{v\left(v+b\right)\sqrt{T}}$$
$$a_i = 0.42748\frac{R^2\left(T_i^c\right)^{2.5}}{P_i^c}, \qquad b_i = 0.08664\frac{RT_i^c}{P_i^c}$$
$$a = \sum_i\sum_j x_i x_j\left(1-k_{ij}\right)\sqrt{a_i a_j}$$

Soave-Redlich-Kwong

$$P = \frac{RT}{v-b} - \frac{a\alpha}{v\left(v+b\right)}$$
$$a_i = 0.42747\frac{\left(RT_i^c\right)^2}{P_i^c}, \qquad b_i = 0.08664\frac{RT_i^c}{P_i^c}$$
$$\alpha_i = \left[1+n_i\left(1-\sqrt{T_{R,i}}\right)\right]^2$$
$$n_i = 0.48508 + 1.55171\omega_i - 0.15613\omega_i^2$$
$$a\alpha = \sum_i\sum_j x_i x_j\left(1-k_{ij}\right)\sqrt{a_i\alpha_i a_j\alpha_j}$$

Peng-Robinson

$$P = \frac{RT}{v-b} - \frac{a\alpha}{v\left(v+b\right)+b\left(v-b\right)}$$
$$a_i = 0.45724\frac{\left(RT_i^c\right)^2}{P_i^c}, \qquad b_i = 0.07780\frac{RT_i^c}{P_i^c}$$
$$\alpha_i = \left[1+n_i\left(1-\sqrt{T_{R,i}}\right)\right]^2$$
$$n_i = 0.37464 + 1.54226\omega_i - 0.26992\omega_i^2$$
$$a\alpha = \sum_i\sum_j x_i x_j\left(1-k_{ij}\right)\sqrt{a_i\alpha_i a_j\alpha_j}$$

$$\mathrm{d}U = \left[T \left(\frac{\partial P}{\partial T} \right)_{v,n} - P \right] \mathrm{d}v \tag{1.3.12}$$

$$\mathrm{d}S = \left(\frac{\partial P}{\partial T} \right)_{v,n} \mathrm{d}v \tag{1.3.13}$$

Combining equations 1.3.12 and 1.3.13 with fundamental thermodynamic property relations yields equations 1.3.14 to 1.3.19, which can be used to determine property values from pressure explicit equations of state [4, 28].

$$nU = \int_V^\infty \left[P - T \left(\frac{\partial P}{\partial T} \right)_{V,n} \right] \mathrm{d}V + \Sigma_i n_i U_i^{ig} \tag{1.3.14}$$

$$nH = \int_V^\infty \left[P - T \left(\frac{\partial P}{\partial T} \right)_{V,n} \right] \mathrm{d}V + PV + \Sigma_i n_i U_i^{ig} \tag{1.3.15}$$

$$nS = \int_V^\infty \left[\frac{nR}{V} - \left(\frac{\partial P}{\partial T} \right)_{V,n} \right] \mathrm{d}V + R\Sigma_i n_i \ln \frac{V}{n_i RT} + \Sigma_i n_i S_i^{ig} \tag{1.3.16}$$

$$nA = \int_V^\infty \left[P - \frac{nRT}{V} \right] \mathrm{d}V - RT\Sigma_i n_i \ln \frac{V}{n_i RT} + \Sigma_i n_i \left(U_i^{ig} - TS_i^{ig} \right) \tag{1.3.17}$$

$$nG = \int_V^\infty \left[P - \frac{nRT}{V} \right] \mathrm{d}V - RT\Sigma_i n_i \ln \frac{V}{n_i RT} + PV + \Sigma_i n_i \left(U_i^{ig} - TS_i^{ig} \right) \tag{1.3.18}$$

$$\mu_i = \int_V^\infty \left[\left(\frac{\partial P}{\partial n_i} \right)_{T,V,n_j} - \frac{RT}{V} \right] \mathrm{d}V - RT \ln \frac{V}{n_i RT} + RT + U_i^{ig} - TS_i^{ig} \tag{1.3.19}$$

Equation 1.3.19 can subsequently be used to derive an expression for the fugacity of component i [4, 28]:

$$RT \ln \frac{f_i}{y_i P} = \int_V^\infty \left[\left(\frac{\partial P}{\partial n_i} \right)_{T,V,n_j} - \frac{RT}{V} \right] \mathrm{d}V - RT \ln \frac{PV}{nRT} \tag{1.3.20}$$

The molar volume of the system corresponding to the lower bound of the integral can be determined at the relevant conditions from the applicable equation of state, which is an iterative process for pressure explicit equations of state. Similar expressions can be derived from volume explicit equations of state as functions of temperature and pressure. The latter approach enjoyed more attention historically as it does not require iterative calculations, which were highly undesirable before the arrival of modern computers [20, 28].

1.3.2 Activity Coefficient Models

Equations of state can conveniently be used to derive thermodynamic properties of a system, as demonstrated in section 1.3.1. When used to predict phase-equilibrium by calculation of fugacity coefficients however, cubic equations of state are only suitable for systems of non-associating molecules. For such systems activity coefficient models yield better results when used to calculate the liquid phase fugacities, in conjunction with an equation of state method for the vapour phase [4, 10, 17, 31].

Activity coefficient models are all empirically derived functions involving sets of parameters fitted to experimental data. Activity coefficient models can be identified as one of two approaches [4, 20, 30]:

- Model parameters are determined by fitting of experimental binary equilibria at some temperature. Equilibria of higher order multi-component systems are predicted using calculated parameters of constituent binary pairs.
- Group contribution methods are used to determine model parameters by regression against large collections of experimental phase equilibrium data. These models are predictive and do not require any experimental data.

The former approach is normally preferred as they are known to provide more accurate predictions. However, the requirement of binary experimental data can be an obstacle. Examples of such models include the NRTL, UNIQUAC, Wilson and T-K-Wilson models, whereas the UNIFAC model is an example of the a group contribution method [1, 4, 20].

Wilson and T-K-Wilson Models

In 1964 Wilson recognised that the arrangement of molecules around one another are not purely random and that non-ideal behaviour is as a result of this behaviour. The model proposed by Wilson is subsequently termed a local composition model. According to this theory, for a mixture of two compounds, the composition around a molecule from species 1 will usually not be equal to the bulk composition. Instead, Wilson proposed that the mole fractions of species 1 and 2 around a molecule of species 1, x_{11} and x_{21} respectively, are given by a Boltzmann-weighted average of the bulk mole fractions [4, 20, 28, 30]:

$$\frac{x_{11}}{x_{21}} = \frac{x_1 \exp\left(-\dfrac{\varepsilon_{11}}{RT}\right)}{x_2 \exp\left(-\dfrac{\varepsilon_{21}}{RT}\right)} \tag{1.3.21}$$

$$= \frac{x_1}{x_2} \exp\left(\frac{\lambda_{12}}{RT}\right) \tag{1.3.22}$$

Where ε_{11} and ε_{21} are termed energies of interaction, and $\lambda_{12} = \varepsilon_{21} - \varepsilon_{11}$. Equation 1.3.22 illustrates that the absolute magnitude of the molecular interactions does not determine the arrangement of molecules around each other in a mixture. It is in fact determined by the difference between like and unlike interactions instead [4].

We calculate the fractional volume occupied by species 1 around itself as:

$$z_1 = \frac{x_{11} v_1}{x_{11} v_1 + x_{21} v_2} \tag{1.3.23}$$

From equation 1.3.22 we substitute the following into equation 1.3.23.

$$x_{11} = \frac{x_{21} x_1}{x_2} \exp\left(\frac{\lambda_{12}}{RT}\right) \tag{1.3.24}$$

Which, after simplification, yields:

$$z_1 = \frac{x_1}{x_1 + \Lambda_{12} x_2} \tag{1.3.25}$$

Where $\Lambda_{12} = \frac{v_2}{v_1} \exp\left(-\frac{\lambda_{12}}{RT}\right)$. Similarly we have:

$$z_2 = \frac{x_2}{x_2 + \Lambda_{21} x_1} \tag{1.3.26}$$

Where $\Lambda_{21} = \frac{v_1}{v_2} \exp\left(-\frac{\lambda_{21}}{RT}\right)$. For the parameters Λ_{ij} in the Wilson equation [4]:

- $\Lambda_{ij} = 1$ when $i = j$
- $\Lambda_{ij} > 0$
- In general $\Lambda_{ij} \neq \Lambda_{ji}$

Using the Flory-Huggins theory, by which the molar Gibbs energy of a mixture is [45]:

$$G = \sum_{i=1}^{n} x_i \left(\mu_i + RT \ln z_i\right) \tag{1.3.27}$$

And for an ideal mixture:

$$G^{ideal} = \sum_{i=1}^{n} x_i \left(\mu_i + RT \ln x_i\right) \tag{1.3.28}$$

Therefore, by combining equations 1.3.27 and 1.3.28, we have the following expression for the excess free Gibbs energy of a mixture:

$$\frac{G^E}{RT} = \sum_{i=1}^{n} x_i \left(\ln \frac{z_i}{x_i}\right) \tag{1.3.29}$$

If we now substitute the expressions for the fractional volume of species 1 and 2 into the above equation, we have the following relation for a binary mixture:

$$\frac{G^E}{RT} = -x_1 \ln\left(x_1 + \Lambda_{12} x_2\right) - x_2 \ln\left(x_2 + \Lambda_{21} x_1\right) \tag{1.3.30}$$

From which the activity coefficients of each component in the mixture may be derived. The generic multicomponent expressions are shown in table 1.3.

It has proven to be very accurate for both polar and non-polar mixtures and has been found very useful for solutions of associating molecules in non-polar solutions, for which simpler models like the Margules and van Laar are found to be inadequate. In addition, both the Margules and van Laar equations are not readily simplified for multi-component mixtures. The Wilson model conveniently utilises only binary interaction parameters for multicomponent systems [4, 28].

However, the standard Wilson model is unable to predict liquid-liquid equilibrium and consequently many modifications have been developed. The T-K-Wilson model is one such version of the Wilson model. It is also summarised in table 1.3. The T-K-Wilson model accurately correlates binary liquid-liquid equilibria and, given that binary interaction parameters are calculated from reliable experimental data, produces accurate results for multi-component systems. [4, 23].

The Non-Random Two-Liquid (NRTL) Model

Table 1.3: The Wilson Model

Wilson Model

$$\frac{G^E}{RT} = -\sum_{i=1}^{n} x_i \ln\left(\sum_{j=1}^{n} x_j \Lambda_{ij}\right)$$

$$\ln \gamma_i = 1 - \ln\left(\sum_{j=1}^{n} x_j \Lambda_{ij}\right) - \sum_{k=1}^{n} \frac{x_k \Lambda_{ki}}{\sum_{j=1}^{n} x_j \Lambda_{kj}}$$

where

$$\Lambda_{ij} = \frac{v_j}{v_i} \exp\left(\frac{-\lambda_{ij}}{RT}\right)$$

$$\Lambda_{ii} = 1$$

$$\Lambda_{ij} \neq \Lambda_{ji}$$

T-K-Wilson Model

$$\frac{G^E}{RT} = \sum_{i=1}^{n} x_i \ln\left(\frac{\sum_{j=1}^{n} x_j v_{ij}}{\sum_{j=1}^{n} x_j \Lambda_{ij}}\right)$$

$$\ln \gamma_i = \ln\left(\frac{\sum_{j=1}^{n} x_j v_{ij}}{\sum_{j=1}^{n} x_j \Lambda_{ij}}\right) + \sum_{k=1}^{n} x_k \left(\frac{v_{ki}}{\sum_{j=1}^{n} x_j v_{kj}} - \frac{\Lambda_{ki}}{\sum_{j=1}^{n} x_j \Lambda_{kj}}\right)$$

where

$$v_{ij} = \frac{v_j}{v_i}$$

Table 1.4: The NRTL Model

NRTL Model

$$\frac{G^E}{RT} = \sum_{i=1}^{n} x_i \left(\frac{\sum_{j=1}^{n} \tau_{ji} G_{ji} x_j}{\sum_{k=1}^{n} x_k G_{ki}} \right)$$

$$\ln \gamma_i = \frac{\sum_{j=1}^{n} \tau_{ji} G_{ji} x_j}{\sum_{k=1}^{n} x_k G_{ki}} + \sum_{j=1}^{n} \frac{x_j G_{ij}}{\sum_{k=1}^{n} x_k G_{ki}} \left(\tau_{ij} - \frac{\sum_{k=1}^{n} \tau_{kj} G_{kj} x_k}{\sum_{k=1}^{n} x_k G_{kj}} \right)$$

where

$$\tau_{ij} = \frac{g_{ij}}{RT}$$

$$G_{ij} = \exp\left(-\alpha_{ij} \tau_{ij}\right)$$

$$\tau_{ii} = \tau_{jj} = 0, \qquad G_{ii} = G_{jj} = 1$$

Similar to the Wilson model, the NRTL model is based on principles of local composition. It was developed by Renon and Prausnitz in 1968. It is capable of handling liquid-liquid phase equilibria and was in fact developed as an attempt to address the inability of the Wilson model to predict liquid-liquid equilibria. The general form of the NRTL model is shown in table 1.4 [4, 20, 25, 30, 31, 36, 43].

It contains three adjustable parameters per binary interaction. The parameter α_{ij} is related to the non-randomness of the mixture and when it is set equal to zero the model reduces to the two-suffix Margules equation. It typically has a value between 0.2 and 0.5. However, in cases where experimental data is absent α_{ij} may be set arbitrarily [28].

As with the Wilson models, reliable multi-component predictions can only be made with the use of binary interaction parameters which have been determined from accurate binary experimental data [4].

The Universal Quasi-Chemical (UNIQUAC) Model

Developed in 1975 by Abrams and Prausnitz, the UNIQUAC equations form a semi-theoretical model. In addition to the interactions between unlike molecules, the size and shape of the molecules have a significant effect on the behaviour of liquid mixtures. The UNIQUAC model comprises of two terms, each accounting for one of the aforementioned factors: [1, 3, 4, 20, 25, 28]

- Configurational term, G^c, accounts for entropic contributions due to differences in shape and size of molecules.

Table 1.5: The UNIQUAC Model

UNIQUAC Model

$$\frac{G^E}{RT} = \frac{G^c + G^r}{RT}$$

$$\frac{G^c}{RT} = \sum_{i=1}^{n} x_i \ln \frac{\phi_i}{x_i} + \frac{z}{2} \sum_{i=1}^{n} q_i x_i \ln \frac{\theta_i}{\phi_i}$$

$$\frac{G^r}{RT} = -\sum_{i=1}^{n} q_i x_i \ln \sum_{j=1}^{n} \theta_j \tau_{ji}$$

where

$$\theta_i = \frac{x_i q_i}{\sum_{j=1}^{n} x_j q_j}$$

$$\phi_i = \frac{x_i r_i}{\sum_{j=1}^{n} x_j r_j}$$

$$\tau_{ij} = \exp\left(\frac{-u_{ij}}{RT}\right)$$

$$\tau_{ii} = \tau_{jj} = 1$$

$$z = 10$$

- Residual term, G^r, accounts for enthalpic contributions mainly due to intermolecular forces.

And the excess Gibbs energy of the mixture is given simply by:

$$\frac{G^E}{RT} = \frac{G^c + G^r}{RT} \tag{1.3.31}$$

The UNIQUAC model manages to predict multi-component liquid-liquid and vapour-liquid equilibria using only pure component and binary interaction parameters. The model equations are summarised in table 1.5. Pure component parameters r_i are determined from the volume, and q_i from the surface of area of a single molecule. These parameters have been tabulated for large selections of molecules. It has found widespread application largely due to it's realtive accuracy while using only binary interaction parameters [3, 4, 25, 28, 36, 43].

1.3.3 The Gibbs-Duhem Equation

The intensive state of each phase in a heterogeneous system is characterised with $m + 2$ variables, where m is the number of species. These variables can however not all be specified arbitrarily and the degrees of freedom are subsequently calculated with the help of the Gibbs phase rule. The Gibbs-Duhem equation establishes how these variables are related. Suppose M represents some

extensive property of a mixture. It is a function of temperature, pressure and the mole numbers and therefore, the total differential of M is given by [28]:

$$\mathrm{d}M = \left(\frac{\partial M}{\partial T}\right)_{P,n_i} \mathrm{d}T + \left(\frac{\partial M}{\partial P}\right)_{T,n_i} \mathrm{d}P + \sum_i \bar{M}_i \mathrm{d}n_i \tag{1.3.32}$$

where

$$\bar{M}_i \equiv \left(\frac{\partial M}{\partial n_i}\right)_{T,P,n_j} \tag{1.3.33}$$

In addition, the partial molar properties, defined in equation 1.3.33, are related to the extensive property M by Euler's theorem [28]:

$$M = \sum_i \bar{M}_i n_i \tag{1.3.34}$$

which, upon differentiation, yields:

$$\mathrm{d}M = \sum_i \bar{M}_i \mathrm{d}n_i + \sum_i n_i \mathrm{d}\bar{M}_i \tag{1.3.35}$$

Finally, the Gibbs-Duhem equation is obtained upon substitution of equation 1.3.35 into equation 1.3.32:

$$\left(\frac{\partial M}{\partial T}\right)_{P,n_i} \mathrm{d}T + \left(\frac{\partial M}{\partial P}\right)_{T,n_i} \mathrm{d}P - \sum_i n_i \mathrm{d}\bar{M}_i = 0 \tag{1.3.36}$$

When the Gibbs-Duhem equation is applied to the Gibbs energy of a mixture we have [28]:

$$\left(\frac{\partial G}{\partial T}\right)_{P,n_i} = S \tag{1.3.37}$$

$$\left(\frac{\partial G}{\partial P}\right)_{T,n_i} = v \tag{1.3.38}$$

$$\left(\frac{\partial M}{\partial n_i}\right)_{T,P,n_j} = \mu_i \tag{1.3.39}$$

$$\therefore S\mathrm{d}T - V\mathrm{P} + \sum_i x_i \mathrm{d}\mu_i = 0 \tag{1.3.40}$$

or in terms of excess functions

$$\therefore S^E \mathrm{d}T - V^E \mathrm{P} + \sum_i x_i \mathrm{d}\mu_i^E = 0 \tag{1.3.41}$$

However, we have

$$\bar{G}_i^E = \mu_i^E = RT \ln \gamma_i \tag{1.3.42}$$

and therefore, at constant pressure and temperature:

$$\sum_i x_i \mathrm{d} \ln \gamma_i = 0 \tag{1.3.43}$$

1.3.4 Activity Coefficient Models and Equation of State Mixing Rules

As noted previously, equations of state are generally not very accurate for associating or polar substances. The calculation of the equation of state parameters by suitable mixing rules can dramatically improve the predictions obtained. One such method utilises activity coefficient models to determine some or all parameters of a cubic equation of state [4].

Standard practice to incorporate an activity coefficient model into an equation of state is with the use of an expression for the excess Helmholtz free energy of a mixture,A^E, at suitable temperature and pressure. It is defined in a similar manner as all other excess properties as [4]:

$$A^E(T, v, x) = A(T, v, x) - A^{ideal}(T, v, x) \tag{1.3.44}$$

$$A^E(T, v, x) = A(T, v, x) - \sum_{i=1}^{n} [x_i A_i(T, v_i) + x_i RT \ln x_i] \tag{1.3.45}$$

Where A_i is the molar Helmholtz energy of pure component i, A is the total molar Helmholtz energy of the mixture and A^{ideal} is the Helmholtz energy of an ideal mixture.

Seeing as most equations of state are defined with T and v as independent variables, for convenience sake the Helmholtz energy is written as a function of the same variables. Also, in order for equation 1.3.45 to be consistent with the constant pressure requirement, v_i and v are determined

by solving the equation of state at the applicable pressure [4].

The excess Helmholtz free energy is related to the excess Gibbs free energy by:

$$G^E = A^E + Pv^E \tag{1.3.46}$$

$$G^E = A^E + P\left(v - \sum_{i=1}^{n} x_i v_i\right) \tag{1.3.47}$$

Using the generic expression for a cubic equation of state in eqaution 1.3.11 to derive the Helmholtz free energy, as in equation 1.3.17, we obtain the following [4]:

$$\frac{A}{RT} = -\ln\left(\frac{v}{v-b}\right) - \frac{a}{bRT\left(c_1 - c_2\right)}\ln\left(\frac{v + c_1 b}{v + c_2 b}\right) + \frac{A^{ig}}{RT} \tag{1.3.48}$$

$$\begin{aligned}\therefore \frac{G^E}{RT} &= \sum_i x_i \ln\left(\frac{v_i - b_i}{v - b}\right) - \frac{a}{bRT\left(c_1 - c_2\right)}\ln\left(\frac{v + c_1 b}{v + c_2 b}\right) \\ &\cdots + \sum_i x_i \frac{a_i}{b_i RT\left(c_1 - c_2\right)}\ln\left(\frac{v_i + c_1 b_i}{v_i + c_2 b_i}\right) + \frac{Pv}{RT}\end{aligned} \tag{1.3.49}$$

In order to calculate the molar volumes v and v_i in equation 1.3.49, the problem may be simplified by using a method proposed by Huron and Vidal [15, 44]:

- Choosing $P \to \infty$ then $v \to b$ and $v_i \to b_i$.
- Assume $b = \sum_i x_i b_i$ and therefore $v^E = 0$.
- Assume $\lim_{P\to\infty} Pv^E = 0$.

Consequently we have [15]:

$$\frac{G^E}{RT} = \left(-\frac{a}{RTb} + \sum_i x_i \frac{a_i}{RTb_i}\right)\left(\frac{1}{c_1 - c_2}\right)\ln\left(\frac{1 + c_1}{1 + c_2}\right) \tag{1.3.50}$$

This now provides a convenient method by which the composition dependence of a may be determined; by equating equation 1.3.50 to an activity coefficient model suitable equation of state mixing rules are defined. A similar method, with a different mixing rule for b, was applied by Wong and Sandler. In addition, several other schemes, such as low-pressure and zero-pressure methods, have been developed in order to equate equations of state with activity coefficient models. [4, 14, 48**?**].

1.4 Computational Aspects

1.4.1 Challenges in and Importance of Phase Equilibrium Calculation

1.4.2 Data Sources and Data Reduction

1.4.3 Phase Stability

Tangent Plane Analysis

In liquid-liquid equilibria, the requirement that the chemical potential or fugacity of each component be equal in each phase, is only a necessary condition. A necessary and sufficient condition is, as discussed in sections 1.2.3 and 1.2.4, that the overall Gibbs energy be at a global minimum.

In order to illustrate the method whereby the stability of a mixture is determined consider the following; a mixture has an initial composition z_1 and chemical potential $\mu(z_1)$. An infinitesimally small amount, δn, of a new phase, with composition z_2, forms. The change in Gibbs energy of the mixture upon formation of the new phase is given by [20]:

$$\delta G = \delta n \sum_{i=1}^{C} m_i \left[\mu_i(z_2) - \mu_i(z_1)\right] \tag{1.4.1}$$

The amount of component i is given by $m_i \delta n$. In order for the mixture to be stable at composition z_1, eqaution 1.4.1 must evaluate to a value larger or equal to zero, for any composition z_2 and a positive δn. This results in the Gibbs tangent plane condition [20]:

$$\sum_{i=1}^{C} m_i \left[\mu_i(z_2) - \mu_i(z_1)\right] \geq 0 \tag{1.4.2}$$

Consider now the Gibbs energy of mixing of the binary mixture depicted in figure 1.4.1. The mixture at composition z_1 splits into two phases with compositions x_α and x_β. The Gibbs energy of mixing of the resulting system and the change in Gibbs energy is given in equation 1.4.3 and equation 1.4.4, respectively [20].

$$G_{new} = \kappa G_{mix}(x_\alpha) + (1-\kappa) G_{mix}(x_\beta) \tag{1.4.3}$$

$$\Delta G_{mix} = \kappa G_{mix}(x_\alpha) + (1-\kappa) G_{mix}(x_\beta) - G_{mix}(z_1) \tag{1.4.4}$$

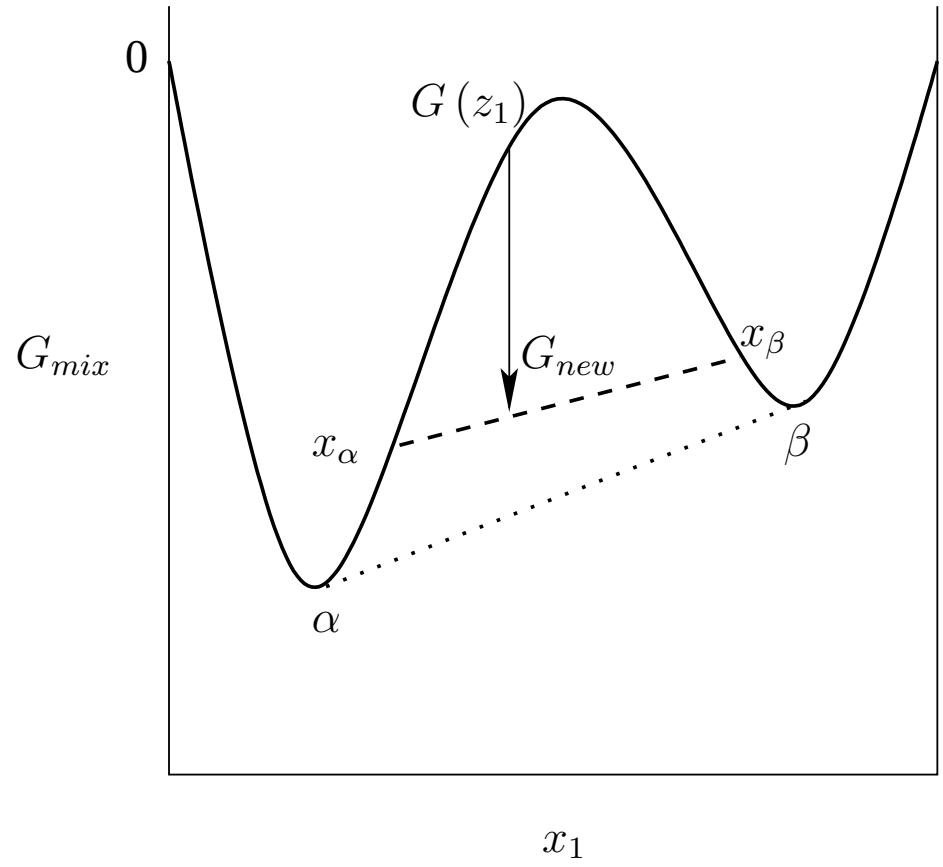

Figure 1.4.1: Gibbs energy of mixing for binary mixture liquid-liquid phase separation, and the tangent plane at the incipient equilibrium phases

Where κ represents the fraction of the mixture in the phase at composition x_α. The tie-line connecting the two points at x_α and x_β, on the G_{mix} curve is given by [20]:

$$G_{tieline}(x) = G_{mix}(x_\alpha) + \frac{G_{mix}(x_\beta) - G_{mix}(x_\alpha)}{x_\beta - x_\alpha}(x - x_\alpha) \tag{1.4.5}$$

The expression in equation 1.4.5 is, upon inspection, at $x = z_1$ equivalent to the expression for the G_{new}. The phase split will therefore result in a decrease of the overall Gibbs energy if $G_{tieline}(z_1) < G_{mix}(z_1)$. Equilibrium is achieved when the tie-line corresponds to the common tangent at compositions α and β. The equation for the line tangent to the G_{mix} at z is given by [20]:

$$f(x) = G_{mix}(z) + \frac{\mathrm{d}G_{mix}}{\mathrm{d}z}|_z (x - z) \tag{1.4.6}$$

And, finally, the distance from the tangent line, to the Gibbs energy surface:

$$s\left(x\right) = G_{mix}\left(x\right) - G_{mix}\left(z\right) + \frac{\mathrm{d}G_{mix}}{\mathrm{d}z}|_{z}\left(x - z\right) \tag{1.4.7}$$

Therefore, if for a composition z the tangent plane distance in equation 1.4.7 becomes negative for any composition within the allowable simplex, the mixture is unstable at z [20].

The Hessian Matrix and Phase Diagram Construction

In liquid-liquid phase equilibria, the binodal curve is analogous to the dew point or bubble point curve in vapour-liquid equilibria. The binodal curve depicts the locus of points where one liquid phase becomes saturated and a second phase forms which coexists, in equilibrium, with the first. As such, and related to the way in which it is determined experimentally, it is also referred to as the cloud point curve. The extreme point of the binodal curve, the point at which the length of the tie-line between the two phases becomes zero, is the plait point. At this point the composition of the two equilibrium phases become equal [33].

The spinodal curve represents the absolute limits to which a phase can be metastable. Inside the spinodal curve the smallest variations in composition will result in phase split. It coincides with the inflection points of the Gibbs energy versus composition curve, in the case of binary mixtures, or in the case of ternary mixtures, the Gibbs energy surface. Inside the region between the binodal and spinodal curves, the mixture is metastable with respect to small fluctuations [33].

Figure 1.4.2 depicts the binodal and spinodal curves for a ternary mixture.

The Hessian matrix of the Gibbs energy of a mixture can be defined as follows:

$$\bigtriangledown^{2} g = \begin{vmatrix} \dfrac{\partial g^{2}}{\partial x_{1}^{2}} & \dfrac{\partial g^{2}}{\partial x_{1}\partial x_{2}} & \cdots & \dfrac{\partial g^{2}}{\partial x_{1}\partial x_{n-1}} \\ \dfrac{\partial g^{2}}{\partial x_{2}\partial x_{1}} & \dfrac{\partial g^{2}}{\partial x_{2}^{2}} & \cdots & \dfrac{\partial g^{2}}{\partial x_{2}\partial x_{n-1}} \\ \vdots & & & \\ \dfrac{\partial g^{2}}{\partial x_{n-1}\partial x_{1}} & \dfrac{\partial g^{2}}{\partial x_{n-1}\partial x_{2}} & \cdots & \dfrac{\partial g^{2}}{\partial x_{n-1}^{2}} \end{vmatrix} \tag{1.4.8}$$

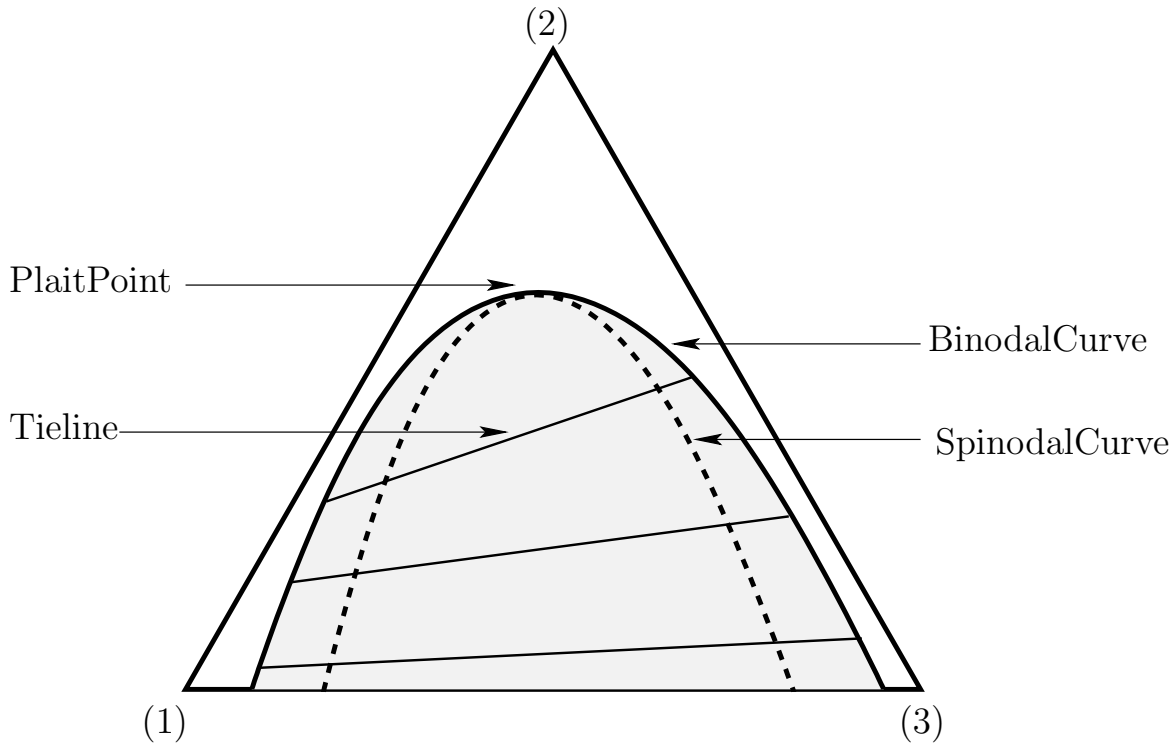

Figure 1.4.2: Ternary liquid-liquid phase diagram depicting the binodal and spinodal curves

Where $g = \dfrac{G}{RT}$ and x_i represents the mole fraction of component i in the mixture.

According to the stability criterion discussed in section 1.2.3, a mixture is stable if the Hessian matrix is positively defined [40]. A matrix is positively defined if its determinant and all constituent diagonal minors are positive. Equivalently, a square matrix is positively defined if all its eigenvalues are positive [7, 40].

Therefore, the regions of stability of a multicomponent mixture can be determined by evaluating the signs of the eigenvalues of the Hessian matrix at different compositions. The regions where the different eigenvalues have constant signs are separated by lines where each eigenvalue is zero. Consequently the shape of the phase diagram is often calculated by solving equation 1.4.9 [40].

$$\det\left(\bigtriangledown^2 g\right) = 0 \tag{1.4.9}$$

However, care has to be taken when using this approach for determining the shape of the spinodal curves; while all spinodal curves are zero determinant lines, not all zero determinant lines separate

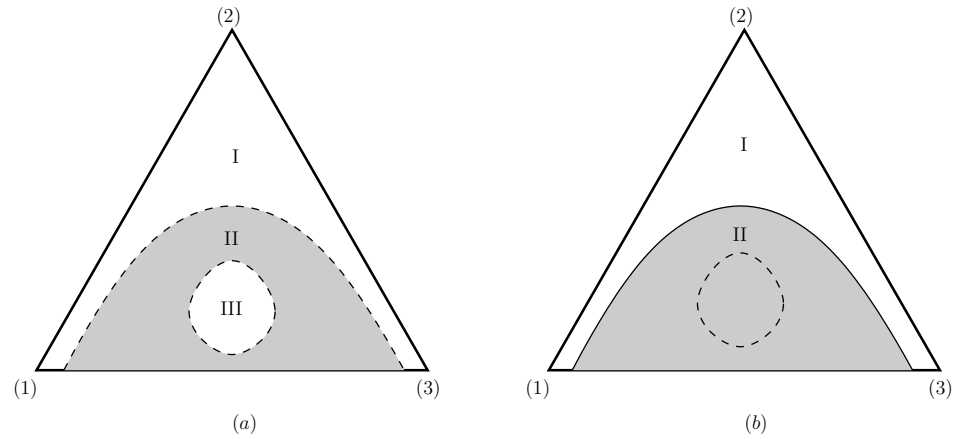

Figure 1.4.3: Ternary liquid-liquid phase diagrams and zero eigenvalue lines of the Hessian Matrix

regions of stability. For illustration, a ternary mixture, as depicted in figure 1.4.3, has two zero determinant curves. In region I all eigenvalues are positive and therefore the mixture is stable. In region II, $\lambda_1 < 0$ and $\lambda_2 > 0$, the mixture will be unstable. In region III, λ_2 is also negative and the resulting matrix determinant is positive. However, since both eigenvalues are negative, the Hessian is not positively defined and the stability criterion is not satisfied. Since the mixture will be unstable in both the regions II and III, the deviding zero determinant line will therefore not coincide with a spinodal curve [40].

The structure of liquid-liquid phase diagrams at different operating conditions are used to select extracting agents and construct process flow sheets. Experimental data are often scarce and the experimental procedures to determine such data are often costly and complicated. Determining the structure of the liquid-liquid phase diagram experimentally for initial design purposes, for example, at various operating temperatures is normally not viable. Moreover, once the operating conditions are chosen, this information remains important in order to optimize and establish the parametric stability of the system. The process can be severely impacted by small fluctuations in operating conditions if the structure of the phase diagram is a strong function of temperature. For these reasons the mathematical modelling of phase separation is an invaluable process design and optimization tool [39, 40].

Although reliable methods exist whereby two-phase equilibria can be accurately calculated, for example by the tangent plane analysis discussed in the previous section, methods used to predict multi-phase equilibria are not as formalised or efficient. This is due to the fact that such methods normally involve the stability analysis of the Gibbs energy at a specific composition point, and

therefore it is impossible to consider all geometric features of the Gibbs energy function simultaneously. In order to obtain true, unambiguous phase separation information at a specific composition the structure of the entire phase diagram is required [39].

The following algorithm provides a method for the automated synthesis of a ternary phase diagram. It can, in principle, be applied to higher order systems [39].
Assuming that a constituent binary system can contain only one phase seperation:

1. Determine the stability of the binary system at successive compositions, starting from the middle composition of the side of the first binary constituent. If no instability is detected, perform the stability analysis at the concentration points halving the segments on either side of the previous point. Continue this process until instability is revealed or a pre-set tolerance is reached. If no region of instability is detected, repeat the evaluation for the next binary constituent. If no instability is detected for any binary pair, continue to step 7. Else, proceed to the next step.

2. Once the phase compositions are determined for the binary split, take a step normal to that tie-line, into the viable concentration region. The step-size is predetermined and the direction is such that the scalar product of the normal vector and the previous tie-line is positive. Perform the stability analysis and calculate the phase separation, if applicable, at the new composition. Continue in this manner until:

   - The last step reaches a new initial point which falls outside the feasible concentration simplex. In this case continue to stage 3.
   - The stability analysis at the last point converged to a single stable composition, then continue to stage 4.
   - The numerical method at the last point converged to a three-phase region, then continue to stage 5.
   - The numerical method at the last point converged to a three-phase region which was previously examined, then return to stage 6.

3. If the previous step has resulted in an initial point outside the viable composition range, the binodal curve is open. The binary phase split of the constituent binary is calculated as in stage 1.

4. If the previous step has converged to a single stable composition, the pre-set step-size can be halved and the consecutive process of normal step, stability analysis, phase split calculation and step-size reduction can be continued until a predetermined tolerance is reached. The final point can then be taken as the plait point.

5. If a three-phase region is revealed, scrap the calculations from the stage 2 calculations which revealed the three phase region and initiate stage 2 calculations from all three binary constituent sides of the ternary diagram.

6. If the previous step terminated in an already discovered three-phase region, then the previous tie-line is saved as the last one and the calculation terminated.

7. If all phase split regions starting from the constituent binary pairs have been completed, or if no binary splits where detected, the interior of the phase diagram can be scanned for instability. Seeing as such systems are rare, this can be considered an additional step.

1.4.4 Phase Equilibrium Calculation Strategies

Assuming that a liquid mixture is unstable at some overall composition, the resulting phase equilibrium can be calculated using one of two approaches: [42]

- Equation solving methods.
- Gibbs energy minimization methods.

The equation solving approach is based on the requirement that the chemical potential, or activity, of each component must be equal in all phases. As such, it is also commonly known as the iso-activity method. The combination of expressions for the activity of each component, with component and overall mass balances yield a set of equations. The resulting set of equations can then be solved, either directly or by means of some numerical method [42].
The Gibbs free energy approach

Equation Solving Approaches

Gibbs Free Energy Minimization

1.4.5 Model Parameter Estimation

Chapter 2

Method

2.1 The Double Weighted Power Mean Mixture Model for the Gibbs Energy of Fluid Mixtures

The liquid phase is characterised by short range intermolecular forces and is consequently conceptualised as a collection of clusters of molecules, each with a central reference molecule and an arrangement of the nearest molecules around it. Due to the short range of intermolecular forces in the condensed phase, the binary interactions between like and unlike molecules in these clusters ultimately determine the overall properties of a mixture. Mixing rules based on this assumption must therefore prescribe a method to calculate cluster properties, from binary interactions, between molecules arranged around a central reference molecule. Then they must provide a method to combine the cluster properties to yield an estimate of the overall mixture property [11, 18, 49].

When both the cluster and overall combination methods are taken as composition weighted power means, a double weighted power mean mixture model results. The double weighted power mean is expressed as [11, 49]:

$$f\left(\bar{c},\bar{x}\right)=\lim_{p\to r^{+}}\left(\sum_{i=1}^{n}x_{i}\left[\lim_{q\to s^{+}}\left(\sum_{k=1}^{n}x_{k}c_{ik}^{q}\right)^{\frac{1}{q}}\right]^{p}\right)^{\frac{1}{p}} \tag{2.1.1}$$

For $r,s\neq 0$ we have:

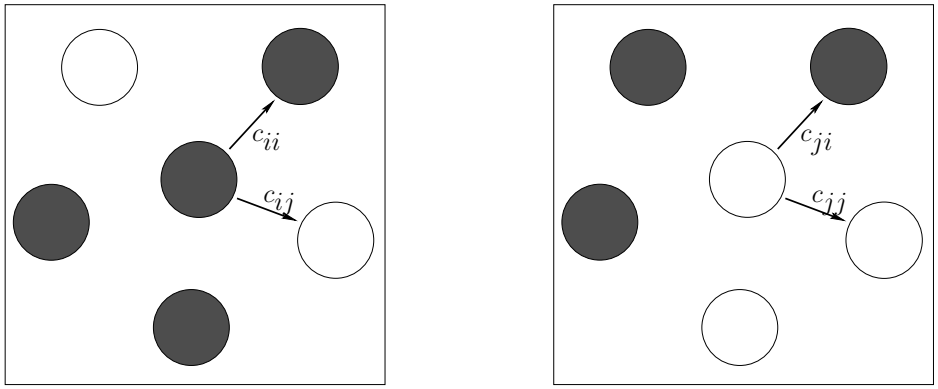

Figure 2.1.1: Illustration of cluster orientation and binary interaction parameter syntax

$$f\left(\bar{c},\bar{x}\right)=\left[\sum_{i=1}^{n}x_i\left(\sum_{j=1}^{n}x_jc_{ij}^{s}\right)^{\frac{r}{s}}\right]^{\frac{1}{r}} \tag{2.1.2}$$

Where x_i represents the mole fraction of component i in the mixture. The coefficients c_{ij} denote the binary interactions assumed in a cluster, where i refers to the central cluster molecule and j to the neighbouring cluster molecule. For a pure component, all molecular interactions are identical and the pure fluid property is referred to by c_{ii}, which therefore also denotes the pure fluid property in a mixture. Figure 2.1.1 illustrates the syntax used for the binary interactions in a cluster [11, 49].

The model in equation 2.1.2 contains two types of adjustable parameters. The first represents the binary interactions between neighbouring molecules in a cluster, and the second kind determines the combination methods. The s parameter determines the method whereby cluster properties are obtained from the binary interactions, and the r parameter determines how the cluster properties are combined to give the overall mixture property [11, 49].

In order to model fluid mixtures, it has been suggested to use equation 2.1.2 to model the Gibbs energy as follows [11]:

$$f(\bar{c},\bar{x}) = \frac{G}{RT} - \sum_{i=1}^{n} x_i \ln x_i \tag{2.1.3}$$

$$= \frac{G^E}{RT} + \sum_{i=1}^{n} \left(\frac{G_i}{RT} x_i \right) \tag{2.1.4}$$

Where G represents the overall Gibbs energy of the mixture, G^E the excess Gibbs energy, G_i the Gibbs energy of component i, R the ideal gas constant and T the applicable temperature.

When the indices in equation 2.1.2 are set equal to 1, 0, or -1, the relevant averaging method corresponds to an arithmetic, geometric and harmonic mean, respectively. Therefore, the double weighted power mean mixture model can be seen as a generalisation of a number of mixture models. Including the Porter, Margules and Wassiljewa-NRTL models. For example, when $r = 1$ and $s = -1$, the model's composition dependence becomes similar to that of the NRTL model [11]:

$$\frac{G^E}{RT} = \sum_{i=1}^{n} c_{ii} x_i \left[\frac{\sum_{j=1}^{n} (1 - \Lambda_{ij}) x_j}{\sum_{k=1}^{n} \Lambda_{ik} x_k} \right] \tag{2.1.5}$$

Where $\Lambda_{ij} = \dfrac{c_{ii}}{c_{ij}}$. The result in equation 2.1.5 is of interest since it is derived by performing a composition weighted harmonic mean to obtain the cluster properties, and a weighted arithmetic mean to obtain the overall mixture property. The relationship in equation 2.1.5 was therefore obtained without invoking the concept of local compositions. In addition, Focke has shown that this form of the model, which requires only two parameters per binary pair, can be related to the classic expressions for the multi-component NRTL model [11].

It is now proposed to use eqution 2.1.1 to model liquid mixtures by setting $r = 0$ and $s \neq 0$. $f(\bar{c},\bar{x})$ then becomes [11, 49]:

$$f(\bar{c},\bar{x}) = \prod_{i=1}^{n} \left(\sum_{j=1}^{n} x_j c_{ij}^{s} \right)^{\frac{x_i}{s}} \tag{2.1.6}$$

Which is assumed to be related to the Gibbs energy by:

$$-\ln f\left(\bar{c},\bar{x}\right)=\frac{G}{RT}-\sum_{i=1}^{n}x_i\ln x_i \tag{2.1.7}$$

$$=\frac{G^E}{RT}+\sum_{i=1}^{n}\left(\frac{G_i}{RT}x_i\right) \tag{2.1.8}$$

$$\therefore\frac{G^E}{RT}=-\frac{1}{s}\sum_{i=1}^{n}x_i\ln\left(\sum_{j=1}^{n}x_j\Lambda_{ij}^{s}\right) \tag{2.1.9}$$

In this case, as in equation 2.1.9, Wilson equations are generated. It may also be argued that the s parameter is related to the nature of the cluster, in which case:

$$\frac{G^E}{RT}=-\sum_{i=1}^{n}\frac{x_i}{s_i}\ln\left(\sum_{j=1}^{n}x_j\Lambda_{ij}^{s_i}\right) \tag{2.1.10}$$

However, equations 2.1.1 and 2.1.6 are only applicable to properties which have well defined absolute values. This is obviously not the case for the Gibbs energy of mixtures, as it is defined with respect to some arbitrary reference state [11].

Finally, a method proposed by Wong and Sandler provides a convenient way by which the pure component binary parameters in equation 2.1.6 can be determined. They proposed that the excess Helmholtz free energy of mixing is independent of pressure, P. Therefore, the excess Helmholtz energy at infinite pressure yields an approximation to the excess Gibbs free energy for the liquid state. [11, 48]:

$$G^E(T,x_i)=G^E(T,P\approx 0,x_i)\approx A^E_{EOS}(T,P\to 0,x_i) \tag{2.1.11}$$

$$\approx A^E_{EOS}(T,P\to\infty,x_i) \tag{2.1.12}$$

Where A^E_{EOS} represents the excess Helmholtz free energy determined from the cubic equation of state.

As the pressure approaches infinity the free volume approaches zero. Therefore, in the case of a cubic equation of state for a pure compound and for a mixture, respectively, $v\to b$ and $v_i\to b_i$. Consequently the Gibbs excess energy at infinite pressure can be expressed as [15, 44]:

$$\frac{G^E}{RT} \approx \frac{A^E_\infty}{RT} = -\frac{\Phi}{RT}\frac{a_{mix}}{b_{mix}} - \sum_{i=1}^{n}\left(\frac{-\Phi}{RT}\frac{a_{ii}}{b_i}\right)x_i \tag{2.1.13}$$

$$\frac{G}{RT} = \frac{G^E}{RT} + \sum_{i=1}^{n} x_i \frac{G_i}{RT} \tag{2.1.14}$$

$$\therefore \frac{G}{RT} = \frac{G^E}{RT} + \sum_{i=1}^{n}\left(\frac{-\Phi}{RT}\frac{a_{ii}}{b_i}\right)x_i = \frac{-\Phi}{RT}\frac{a_{mix}}{b_{mix}} \tag{2.1.15}$$

Φ is a characteristic constant of the cubic equation of state used and

- $\Phi = 1/\left(1+\phi_1\right)$ for $\phi_1 = \phi_2$ or
- $\Phi = \ln\left[\left(1+\phi_1\right)/\left(1+\phi_2\right)\right]/\left(\phi_1 - \phi_2\right)$ for $\phi_1 \neq \phi_2$

Where the general form of the cubic equation of state is:

$$P = \frac{RT}{(v-b)} - \frac{a}{(v+\phi_1 b)(v+\phi_2 b)} \tag{2.1.16}$$

When comparing equations 2.1.6 and 2.1.13, the following relationship between the c_{ii} constants in the double weighted power mean and the equation of state parameters is apparent:

$$c_{ii} = \frac{-\Phi}{RT}\frac{a_{ii}}{b_i} \tag{2.1.17}$$

It is also clear that since $a_{ii}, b_i > 0$, the parameters $c_{ii} < 0$ when $\Phi > 0$.

Due to the close proximity of molecules, resulting in more frequent molecular interaction, non-ideal behaviour in the liquid phase is more pronounced in the liquid phase than in the vapour phase. Thermodynamic models play a very significant role in the prediction of liquid-liquid phase equilibria and the applicability of a specific model to a specific problem is determined by it's ability to accommodate variations from the ideal. An investigation is launched into the ability of the double weighted power mean model, as stated in equation 2.1.10, to accommodate liquid-liquid phase equilibria.

Three models for the excess free Gibbs energy of a mixture are fitted to experimental liquid-liquid phase equilibrium data namely, the NRTL, UNIQUAC and the proposed double wiegthed power mean mixture model (DWPM). The NRTL and UNIQUAC models are used to confirm the reliability of the software routines used. These were developed to perform parameter and equilibrium calculations, to investigate the applicability of the DWPM model. In addition, the computational efficiency and relative ease, or difficulty, with which the DWPM model is used to model liquid-liquid equilibria can be evaluated.

The component properties and parameters required for the DWPM model is determined by fitting a modified van der Waals equation to the pure compound experimental vapour-liquid equilibrium data obtained from the property data bank in Poling, Prausnitz and O'Connell [27]. The experimental liquid-liquid phase equilibrium data of all mixtures are obtained from the Dechema liquid-liquid data collection [25].

2.2 Calculation of the Pure Component Parameters for the Double Weighted Power Mean Mixture Model

The van der Waals equation of state, as discussed in section 1.3.1, was derived from the ideal gas law. It is cubic in the molar volume, v, and contains two adjustable parameters a and b:

$$P = \frac{RT}{v - b_c} - \frac{a_c}{v^2} \tag{2.2.1}$$

The parameters a_c and b_c are calculated from [4]:

$$a_c = \frac{27\left(RT_c\right)^2}{64P_c} \tag{2.2.2}$$

$$b_c = \frac{RT_c}{8P_c} \tag{2.2.3}$$

The second term in equation 2.2.1 represents the attractive interactions between particles .In subcritical regions, the inaccuracy of this term dominates and can be improved by using a relatively simle, yet effective, method proposed by Adachi and Lu [2]:

$$\frac{a\,(T)}{a_c} = \exp\left[m\,(1 - T_R)\right] \tag{2.2.4}$$

Where

$$T_R = \frac{T}{T_c} \tag{2.2.5}$$

Therefore the attraction parameter becomes a function of temperature and equation 2.2.1 becomes:

$$P = \frac{RT}{v - b_c} - \frac{a\,(T)}{v^2} \tag{2.2.6}$$

In order to determine the adjustable parameter m in equation 2.2.4, the modified van der Waals equation can be fit to vapour-liquid equilibrium data at different temperatures. A method for calculating the vapour pressure by evaluating the roots of equation 2.2.1, was also discussed earlier. Below the critical temperature, the van der Waals eqaution has three real roots, the smallest corresponding to the liquid molar volume and the largest to that of the vapour. The roots converge on the critical volume as the critical temperature is approached.

For the purposes of this investigation, the vapour-liquid equilibrium data of pure substances were obtained from the property data bank in Poling et.al. [27]. The data is given in the form of equations that describe the vapour pressure over a range of applicable temperatures. The vapour pressure of each compound is determined by one of the following:

method 1.

$$\ln\left(\frac{P_{vap}}{P_c}\right) = \frac{1}{(1-x)}\left[A_{vp}x + B_{vp}x^{1.5} + C_{vp}x^3 + D_{vp}x^6\right] \tag{2.2.7}$$

where $x = 1 - \frac{T}{Tc}$

method 2.

$$\ln P_{vap} = A_{vp} - \frac{B_{vp}}{T} + C_{vp}\ln T + D_{vp}\frac{P_{vap}}{T^2} \tag{2.2.8}$$

method 3.

$$\ln P_{vap} = A_{vp} - \frac{B_{vp}}{T + C_{vp}} \tag{2.2.9}$$

Due to the manner whereby the vapour pressure is calculated, the Adachi-Lu parameter estimation is done by means of a bi-level optimization. The steps for calculating the Adachi-Lu parameter, m, from the vapour-liquid equilibrium data is as follows:

1. Import the compound critical point data and vapour pressure parameters, for equations 2.2.7 through 2.2.9, from a saved data file.

2. Generate an array of temperatures, with a selected interval size, ΔT_{int}, within the applicable range for equations 2.2.7 to 2.2.9.

3. Generate an array of vapour pressures for the elements in the temperature array using the suitable method from equations 2.2.7 to 2.2.9.

4. Calculate b_c.

5. Using a suitable numerical algorithm:

$$\min_{m} E = \Delta T_{int} \sum_{i=1}^{N_{int}} \left(P_{vap_i}^{predicted} - P_{vap_i}^{actual} \right) \tag{2.2.10}$$

Where N_{int} is the number of intervals into which the temperature range is divided, ΔT_{int} the size of the temperature intervals, $P_{vap_i}^{actual}$ the vapour pressure determined using one of equations 2.2.7 to 2.2.9, and $P_{vap_i}^{predicted}$ is the vapour pressure predicted using the van der Waals equation.

(a) In order to calculate the vapour pressure predicted by the van der Waals equation of state, at a selected temperature and the relevant value of m, a suitable numerical algorithm is used to evaluate the integral of equation 2.2.12 between v_l and v_g, to determine the difference in areas A and B as indicated in figure 2.2.1. The goal becomes:

$$\min_{P_{vap_i}^{predicted}} E = \| RT \ln \left(\frac{v_g - b}{v_l - b} \right) + a\left(T\right) \left(\frac{1}{v_g} - \frac{1}{v_l} \right) - P_{vap_i}^{predicted} \left(v_g - v_l \right) \| \tag{2.2.11}$$

Where the molar volumes in 2.2.11 are determined as follows:

i. Rewrite the van der Waals equation as:

$$P_{vap} v^3 - \left(RT + P_{vap} b \right) v^2 + a\left(T\right) v - a\left(T\right) b = 0 \tag{2.2.12}$$

ii. Solve for the roots of equation 2.2.12, where $a\left(T\right)$ is calculated at the specified temperature and relevant value of m.

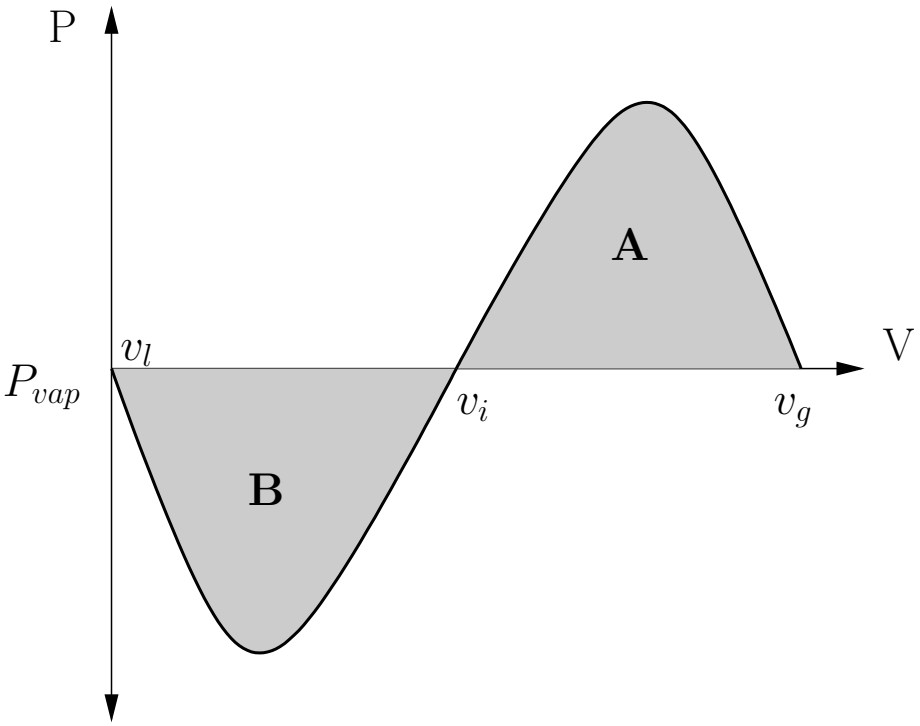

Figure 2.2.1: Roots of Van der Waals EOS for Determining Vapor Pressure

iii. Sort the 3 resulting roots and assign the largest to the vapour molar volume, the smallest to the liquid molar volume, and the one partway between them to v_i.

(b) Terminate the optimization initiated in step 5a once the function in 2.2.11 reaches a specified tolerance.

6. Terminate the optimization initiated in step 5 once the function in 2.2.10 is minimised.

7. Write the calculated m parameter to a data file for use at a later time.

The method described above was implemented in the Python programming language. The details and parameters of the optimisation methods used to determine the predicted van der Waals vapour pressures and Adachi-Lu parameter are summarised in tables 2.1 and 2.2 respectively.

Assuming the Adachi-Lu modification for the van der Waals equation of state, the expression for the pure component parameters, in equation 2.1.17, becomes:

$$c_{ii} = -\frac{a_i(T)}{RTb_i} \tag{2.2.13}$$

Parameter	Value
Design Variable	$P_{vap}^{predicted}$
Bounds	$P_{vap_{min}}^{actual} \leq P_{vap}^{predicted} \leq P_{vap_{max}}^{actual}$
Goal Function	Equation 2.2.11
Termination Tolerance on Design Variable	10^{-4}
Maximum Number of Function Evaluations	500
Maximum Number of Iterations	500
SciPy Optimiser	fminbound
Algorithm	Brent's Method

Table 2.1: Optimisation parameters for the vapour pressure prediction using the van der Waals equation of state

Parameter	Value
Design Variable	m
Bounds	$0 \leq m \leq 5$
Goal Function	Equation 2.2.10
Termination Tolerance on Design Variable	10^{-4}
Maximum Number of Function Evaluations	500
Maximum Number of Iterations	500
SciPy Optimiser	fminbound
Algorithm	Brent's Method

Table 2.2: Optimisation Parameters for the adjustable parameter m in the modified van der Waals equation of state

Once the optimal value for m has been determined the form of the temperature dependence of $a(T)$ is known. Consequently the pure component parameters, c_{ii}, required for the double weighted power mean model, in equation 2.1.10, can be calculated as needed at the relevant temperatures.

2.3 Binary Interaction Parameter Calculation from Binary Liquid-liquid Equilibrium Data

2.3.1 Bi-Level Optimization Method

As discussed in section 1.4.5, a method proposed by Bollas et.al. and Mitsos et.al. employs a bi-level optimization technique to estimate the binary interaction parameters for activity coefficient models. A similar method was applied to calculate the binary parameters for the NRTL, UNIQUAC and DWPM models from experimental binary mixture liquid-liquid equilibrium data [6, 22].

In order to use this method, complete experimental tie-line data is required at each temperature. In other words, phase envelope data with measured compositions of only one of the phases at a selected temperature, is insufficient. For the purposes of this investigation tie-line data for a number of binary systems were obtained from the Dechema liquid-liquid data collection [25]. The binary mixtures for which interaction parameters are calculated, and the corresponding original sources are given in table 2.3.

For each model, the set of binary interaction parameters at a specified temperature determines the shape of the Gibbs energy function versus composition, and ultimately the predicted liquid-liquid equilibrium. However, the suitability of a set of binary parameters is determined by the accuracy with which the predicted equilibrium phase splits can match the experimentally measured compositions, or the overall phase diagram of that mixture. A bi-level optimization technique contains two nested optimizations, where:

- The outer loop varies the model parameters to minimize the overall goal function.
- The inner loop solves the phase equilibrium problem.

Binary Mixture	Data Source
2-Hexanol and Water	Ginnings and Webb,(1938) [13]
13-Dimethyl Benzene and Water	Chernoglazova and Simulin,(1976) [9]
Aniline and Water	Campbell,(1945) [8]
Diethylene Glycol and 12-Dimethyl Benzene	Lesteva et al.,(1972) [16]
Dipropyl Ether and Water	Bennet and Philip,(1928) [5]
Ethyl Ester Acetic Acid and Water	Merriman,(1913) [19]
Methanol and Heptane	Tagliavini and Arich,(1958) [41]
Methanol and Hexane	Radice and Knickle,(1975) [29]

Table 2.3: Binary mixtures for which binary interaction parameters are calculated and experimental data sources

The overall goal function for this approach should minimize some measure of total error over all experimental measurements, either at each specified temperature or over an entire range of temperatures. For the purposes of this investigation, equation 2.3.1 below is used to calculate the optimum set of parameters at each temperature.

$$\min_{\overline{\Lambda}} E = \sum_{k=1}^{P} \left[x_k - x'_k \left(\overline{\Lambda} \right) \right]^2 \tag{2.3.1}$$

Where P represents the number of phases in equilibrium. For binary systems, no more than two phases are observed and therefore equation 2.3.1 becomes:

$$\min_{x'_\alpha, x'_\beta} E = \left[x_\alpha - x'_\alpha \left(\overline{\Lambda} \right) \right]^2 + \left[x_\beta - x'_\beta \left(\overline{\Lambda} \right) \right]^2 \tag{2.3.2}$$

Where x_α represents the experimentally measured composition of one of the liquid phases, and x_β that of the second phase. Similarly, $x'_\alpha \left(\overline{\Lambda} \right)$ and $x'_\beta \left(\overline{\Lambda} \right)$ represent the equilibrium phase compositions predicted by the mixture model, and $\overline{\Lambda}$ represents the set of adjustable binary parameters of each model.

To simplify the expressions used to calculate phase equilibrium, the change of Gibbs energy on mixing, ΔG_{mix}, as a function of mixture composition is used to model the Gibbs energy surface. The steps whereby the binary interaction parameters are determined for each of the models are as follows:

1. Import experimental liquid-liquid equilibrium data, pure component parameters for the UNIQUAC model, as well as the pure component parameters for the van der Waals equation of state, which were determined previously, from file.

2. At each experimental temperature:

   (a) If the current model is the DWPM calculate the pure component parameters according to equation 2.2.13.

   (b) Using a suitable numerical algorithm, determine the optimal set of adjustable binary parameters,$\overline{\Lambda}$, by minimizing the goal function in equation 2.3.2. Where the predicted equilibrium phase compositions, x'_α and x'_β, are calculated as follows:

      i. Using a suitable numerical method, find the common tangent to the ΔG_{mix} curve by solving for the two compositions that both satisfy the following equations, within a set tolerance:

$$\frac{\Delta G_{mix}\left(x'_\alpha\right) - \Delta G_{mix}\left(x'_\beta\right)}{x'_\alpha - x'_\beta} - \frac{\mathrm{d}\Delta G_{mix}\left(x'_\alpha\right)}{\mathrm{d}x_1} = 0 \tag{2.3.3}$$

$$\frac{\mathrm{d}\Delta G_{mix}\left(x'_\alpha\right)}{\mathrm{d}x_1} - \frac{\mathrm{d}\Delta G_{mix}\left(x'_\beta\right)}{\mathrm{d}x_1} = 0 \tag{2.3.4}$$

      ii. To ensure that the solution,$\langle x'_\alpha, x'_\beta \rangle$, is in fact an equilibrium solution, check that:

$$T\left(x_m\right) - \Delta G_{mix}\left(x_m\right) \leq 0 \qquad \forall\, 0 \leq x_m \leq 1 \tag{2.3.5}$$

      Where:

$$T\left(x_m\right) = \Delta G_{mix}\left(x'_\alpha\right) - \frac{\Delta G_{mix}\left(x'_\alpha\right) - \Delta G_{mix}\left(x'_\beta\right)}{x'_\alpha - x'_\beta}\left[x'_\alpha - x_m\right]$$

$$m = 1, 2, 3 \cdots M_{int}$$

      And M_{int} is some arbitrary number of intervals into which the composition range is divided.

      To do this, an array with M_{int} number of entries is generated using equation 2.3.5. If all the entries of this array are smaller or equal to zero, proceed to the next step. If any of these entries are positive, the solution obtained in step 2(b)i is not an equilibrium solution. In such a case, generate a new random starting point for the numerical method and return to step 2(b)i.

   (c) Write the binary parameters that yield the best fit, at that temperature, to an output file, to be used later to generate the predicted phase envelope etc.

Parameter	Value
Design Variables	x'_α and x'_β
Bounds	$0 \leq x'_\alpha \leq 1$ and $0 \leq x'_\beta \leq 1$
Goal Function	Solve equations 2.3.3 and 2.3.4
Termination Tolerance on Design Variables	10^{-5}
Termination Tolerance on Function Values	10^{-5}
Maximum Number of Function Evaluations	1000
Maximum Number of Iterations	500
Optimiser	fsolve
Algorithm	MINPACKs hybrd and hybrj

Table 2.4: Optimisation Parameters for Phase Equilibrium Calculation

Parameter	Value
Design Variables	Model Adjustable Parameters
Goal Function	Equation 2.3.1
Termination Tolerance on Design Variables	10^{-5}
Termination Tolerance on Function Values	10^{-5}
Maximum Number of Function Evaluations	1000
Maximum Number of Iterations	500
Optimiser	fmin-l-bfgs-b
Algorithm	L-BFGS-B

Table 2.5: Optimisation Parameters for Model Parameter Calculation

The method described above was implemented in the Python programming language. All ΔG_{mix} function evaluations were performed using wrapped FORTRAN 95 code, in order to improve the execution time required for the optimizations. The details and parameters of the numerical methods used for the phase equilibrium calculation and the parameter estimation are summarised in tables 2.4 and 2.5.

2.3.2 Pseudo Analytical Approach

Calculating the binary model parameters using a bi-level optimization method, does not fully utilise the already known information about the equilibrium compositions. Instead, the parameter estimation step is completely separate from the phase equilibrium calculation. Although this approach is logical and intuitive, it has 3 important disadvantages:

- Solving the phase equilibrium problem in itself, is already a deceptively simple one. By nesting this problem into the parameter optimization, another complex optimization problem, it becomes that much more complex and computationally very expensive.
- The complexity and computational inefficiency becomes even more significant for higher order mixtures.
- The known experimental compositions are never matched exactly. Strictly speaking, even if the optimizer routine converges successfully, the error made by the model prediction is still only minimized.

A method combining the idea of common tangent calculation with the direct equation solving approach is now considered. If a binary mixture is unstable at some temperature, the following is known at the compositions of the two incipient phases:

$$g(x_\alpha) = f(x_\alpha) \tag{2.3.6}$$
$$\frac{\mathrm{d}g(x_\alpha)}{\mathrm{d}x} = \frac{\mathrm{d}f(x_\alpha)}{\mathrm{d}x} \tag{2.3.7}$$
$$g(x_\beta) = f(x_\beta) \tag{2.3.8}$$
$$\frac{\mathrm{d}g(x_\beta)}{\mathrm{d}x} = \frac{\mathrm{d}f(x_\beta)}{\mathrm{d}x} \tag{2.3.9}$$

Where x_α and x_β are the compositions of the two liquid phases in equilibrium, $g(x) = \dfrac{G(x)}{RT}$, and $f(x)$ is the common tangent line which intercepts the Gibbs energy curve at the two equilibrium compositions:

$$f(x) = mx + c \tag{2.3.10}$$

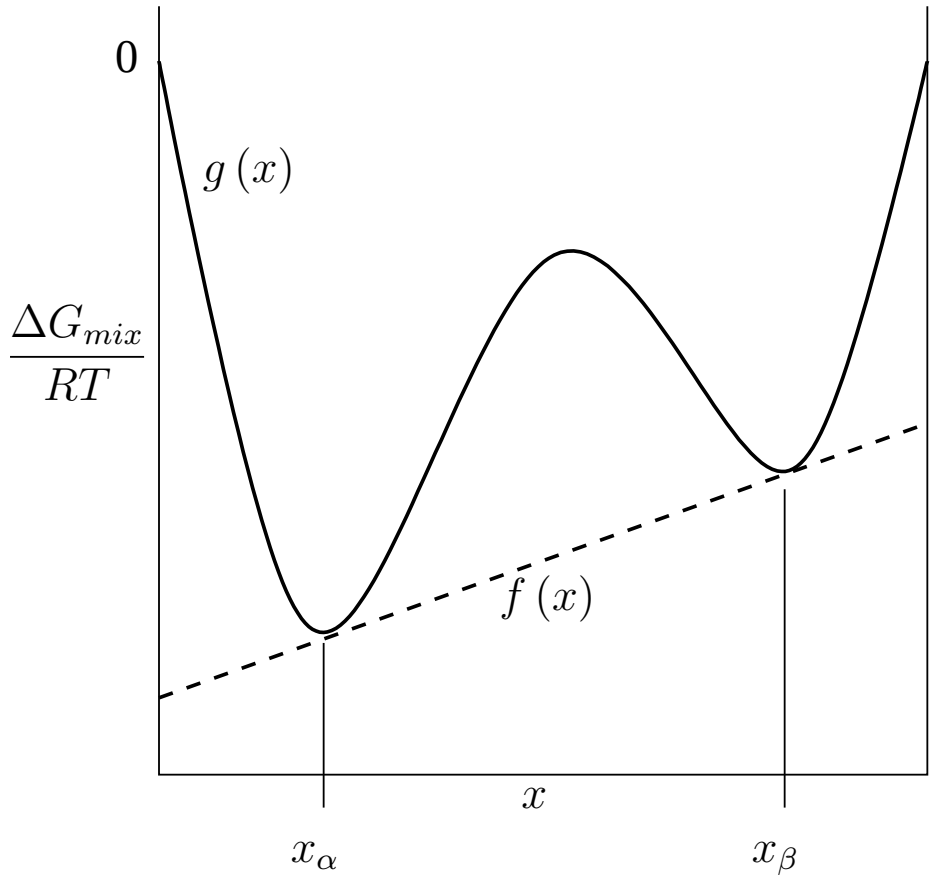

Figure 2.3.1: Illustration of cluster orientation and binary interaction parameter syntax

See figure 2.3.1 for clarification. For binary systems, the NRTL, UNIQUAC and DWPM models each have two binary interaction parameters, which are unknown and assumed to be temperature dependant. Also, in equation 2.3.10, m and c are unknown. Therefore, at a given temperature and with the equilibrium compositions already known, the properties in equations 2.3.6 through 2.3.9 describe a fully defined system of 4 equations, with 4 unknowns. If a solution to this system can be found, the model parameters calculated thereby will predict the measured phase equilibrium exactly.

The benefits of this pseudo-analytic approach are:

- The given experimental data is used directly and therefore the measured phase compositions are matched exactly.
- The approach is simple to implement.
- It can be applied in reverse to calculate the predicted phase equilibrium, and the phase

diagram, when the two binary model parameters are known and the two equilibrium compositions, instead, are unknown.

Considering the system of equations reveals that, given that which is known about the phase equilibrium, the number of properties that can be enforced on the shape of the ΔG_{mix} curve etc., is fixed. In other words, given the system of 4 equations, one can only solve for 4 unknowns and not 3 or 5. If, for example, a mixture model requires 5 interaction parameters to model a binary system, all 5 parameters can not be determined independently. Alternatively, additional degrees of freedom need to be fixed, either by enforcing another desired property by means of an equation, or by arbitrarily fixing the superfluous parameters.

The system of equations, for each model, cannot be solved analytically and therefore a numerical method is utilised to solve it; hence the name, pseudo-analytical method. When the model parameters are known and the phase equilibrium compositions are calculated, a number of constraints are implemented to ensure physically insignificant solutions are disregarded. The constraints which are enforced are as follows:

- $c \leq 0$
- $f\left(1\right) \leq 0$
- $x'_{\alpha} - x'_{\beta} \geq 0.1$, to ensure that the solution does not converge to the trivial solution $x'_{\alpha} = x'_{\beta}$.

This pseudo-analytical approach was implemented using Python, and again all ΔG_{mix} evaluations were done using wrapped FORTRAN code, to improve the required running time. The pseudo-analytical method was used to determine the binary interaction parameters for the same binary mixtures as before, in table 2.3.

2.4 Binary Interaction Parameter Calculation from Ternary Liquid-liquid Equilibrium Data

2.4.1 Pseudo Analytical Approach

The bi-level optimization method for the estimation of model interaction parameters, can be applied to higher order systems. And again, although the concept is intuitive and straight-forward,

the application thereof becomes more difficult for systems of higher dimensions. In addition, the increase in dimensions results in a further increase in computational complexity.

The common tangent line which determines the phase equilibrium compositions in binary mixture liquid-liquid equilibria, translates to a common tangent plane for ternary mixtures. The problem of parameter estimation and phase stability analysis for ternary mixtures is a problem in three dimensions. Also, unlike binary mixtures, more than one tie-line exists at a single temperature and more than 2 phases may co-exist simultaneously. The pseudo-analytical approach for the calculation of activity coefficient model parameters, as discussed in section 2.3.2, can be easily extrapolated for application to ternary mixtures.

In the case of ternary mixtures, the mole fractions of two components can be specified and the other is implied. Such that:

$$x_1 + x_2 + x_3 = 1 \tag{2.4.1}$$

For two phases, α and β in liquid-liquid equilibrium, we know:

$$g\left(x_1^\alpha, x_2^\alpha\right) = f\left(x_1^\alpha, x_2^\alpha\right) \tag{2.4.2}$$

$$g\left(x_1^\beta, x_2^\beta\right) = f\left(x_1^\beta, x_2^\beta\right) \tag{2.4.3}$$

$$\frac{\mathrm{d}g}{\mathrm{d}x_1}\left(x_1^\alpha, x_2^\alpha\right) = \frac{\mathrm{d}f}{\mathrm{d}x_1}\left(x_1^\alpha, x_2^\alpha\right) \tag{2.4.4}$$

$$\frac{\mathrm{d}g}{\mathrm{d}x_1}\left(x_1^\beta, x_2^\beta\right) = \frac{\mathrm{d}f}{\mathrm{d}x_1}\left(x_1^\beta, x_2^\beta\right) \tag{2.4.5}$$

$$\frac{\mathrm{d}g}{\mathrm{d}x_2}\left(x_1^\alpha, x_2^\alpha\right) = \frac{\mathrm{d}f}{\mathrm{d}x_2}\left(x_1^\alpha, x_2^\alpha\right) \tag{2.4.6}$$

$$\frac{\mathrm{d}g}{\mathrm{d}x_2}\left(x_1^\beta, x_2^\beta\right) = \frac{\mathrm{d}f}{\mathrm{d}x_2}\left(x_1^\beta, x_2^\beta\right) \tag{2.4.7}$$

Where x_1^α and x_2^α are the compositions of components 1 and 2 in phase α respectively, and similarly x_1^β and x_2^β are the compositions of components 1 and 2 in phase β respectively. And $f\left(x_1, x_2\right)$ is the common tangent plane to both phases α and β:

$$f_1\left(x_1, x_2\right) = a_1 x_1 + b_1 x_2 + c_1 \tag{2.4.8}$$

Therefore, the information from one tie-line yields 6 equations. However, the NRTL, UNIQUAC and DWPM models each have 2 interaction parameters per binary pair, and the equation for the tangent plane has 3 unknown parameters, a_1, b_1 and c_1. The composition information of a single tie-line is therefore insufficient to fix all 9 parameters.

If the information of another tie-line at the same temperature is known however, one can apply the properties in equations 2.4.2 to 2.4.7 at this additional tie-line, yielding 12 equations in total. The additional tie-line will however also be associated with it's own tangent plane:

$$f_2(x_1, x_2) = a_2 x_1 + b_2 x_2 + c_2 \tag{2.4.9}$$

Where a_2, b_2 and c_2 are also unknown. At one experimental temperature however, the ΔG_{mix} surface is defined by the same binary parameters for both tie-lines. Consequently, using information from two experimentally measured tie-lines, and the properties in equations 2.4.2 to 2.4.7, a system of 12 equations and 12 unknowns can be defined. This system may then be solved, using some suitable numerical algorithm, to calculate the 6 unknown model interaction parameters and the 6 parameters, a_1, b_1, c_1, a_2, b_2 and c_2, from then tangent plane equations 2.4.8 and 2.4.9.

The reverse calculation, that of the equilibrium compositions and phase diagram, when the model interaction parameters are known is however not determined using the exact same set of equations. While equations 2.4.2 to 2.4.7 still hold, only one tangent plane is considered for a single tie-line:

$$f(x_1, x_2) = a x_1 + b x_2 + c \tag{2.4.10}$$

If a mixture is known to be unstable at some composition, we know that the two incipient phases will be linearly related to the original composition. In other words, on a T vs x diagram, the line connecting two liquid phases in equilibrium will pass through the original overall mixture composition. The following holds for a line in three dimensions:

$$\frac{x_1 - x_1^\alpha}{x_1^\beta - x_1^\alpha} = \frac{x_2 - x_2^\alpha}{x_2^\beta - x_2^\alpha} = \frac{z - z^\alpha}{z^\beta - z^\alpha} \tag{2.4.11}$$

Where, x^α, x^β and z are all connected with one straight line. In this case the z-direction is the scaled change in Gibbs energy on mixing, $g(x_1, x_2)$. The line that connects the two equilibrium

compositions will also lie in the plane that is tangent to the Gibbs energy curve at these two compositions. And therefore equation 2.4.11 becomes:

$$\frac{x_1 - x_1^\alpha}{x_1^\beta - x_1^\alpha} = \frac{x_2 - x_2^\alpha}{x_2^\beta - x_2^\alpha} = \frac{f\left(x_1, x_2\right) - f^\alpha\left(x_1^\alpha, x_2^\alpha\right)}{f^\beta\left(x_1^\beta, x_2^\beta\right) - f^\alpha\left(x_1^\alpha, x_2^\alpha\right)} \tag{2.4.12}$$

The parametric equations of the line in 2.4.12 can be written as:

$$x_1 = x_1^\alpha + \left(x_1^\beta - x_1^\alpha\right) t \tag{2.4.13}$$

$$x_2 = x_2^\alpha + \left(x_2^\beta - x_2^\alpha\right) t \; g\left(x_1, x_2\right) = g^\alpha\left(x_1^\alpha, x_2^\alpha\right) + \left[g^\beta\left(x_1^\beta, x_2^\beta\right) - g^\alpha\left(x_1^\alpha, x_2^\alpha\right)\right] t \tag{2.4.14}$$

Equation 2.4.14 and 2.4.14 can be combined to eliminate t. The resulting equation is then used together with equations 2.4.2 to 2.4.7 to define a system of 7 equations. Where the model parameters are unknown, the equilibrium compositions x_1^α, x_2^α, x_1^β and x_2^β, and the parameters of the common tangent plane, a, b and c, are unknown. Therefore, a fully specified system of 7 equations and 7 unknowns result, which again can be solved using a suitable numerical method.

A method whereby the unstable composition regions of a ternary mixture can be identified by analysis of the Hessian matrix of the Gibbs energy surface, is described in section 1.4.3. A general algorithm for the calculation of ternary phase diagrams was also discussed. When applying such an algorithm, similar to the one proposed by Solokhin et.al., the aforementioned phase composition calculation method can now be used to calculate a number of tie-lines. The phase diagram for a ternary mixture using a mixture model for which the binary interaction parameters are known can also be predicted. The present algorithm used to calculate a number of ternary phase diagrams is summarised as follows:

1. Import the known model parameters from a saved data file.
2. Create composition arrays for components 1 and 2, with N_{int} intervals over the composition range $0 \leq x_i \leq 1$, for $i = 1, 2$.
3. At each physically significant $\langle x_1 x_2 \rangle$ evaluate the Hessian matrix of the Gibbs energy surface.
4. Using a connected component labelling algorithm, determine the number of unconnected unstable regions.

5. For every unstable region which contains a binary phase separation:

   (a) Starting at the binary mixture, calculate the binary phase separation compositions.

   (b) From the midpoint of the tie-line between the the previously calculated equilibrium phases α and β, take a step to a point m, perpendicular to the tie-line, into the unstable region. The step size is set proportional to the length of the tie-line.

   (c) If the mixture at m is inside the unstable region, and the previous tie-line is not smaller than some predetermined tolerance, calculate the new equilibrium separation at m and return to step 5b.

   (d) If the mixture is stable at this new point m, or the calculated tie-line is smaller than the selected small tolerance, take the halfway point as the plait point of that region, and return to step 5 for remaining regions containing binary splits, or continue to step 6 for remaining regions which contain no binary seperations.

6. For isolated regions of instability:

   (a) Select any random point inside the region as the firs starting point m and calculate the corresponding phase separation through that point.

   (b) From the midpoint of the tie-line between the the previously calculated equilibrium phases α and β, take a step to a point m, perpendicular to the tie-line, in the positive direction. The step size is set proportional to the length of the tie-line.

   (c) If the mixture is unstable at the new point m, and the previous tie-line is not smaller than some predetermined tolerance, calculate the new equilibrium separation at m and return to step 6b.

   (d) If the mixture is stable at m or the calculated tie-line is smaller than the selected small tolerance, take this halfway point as the plait point of that region, and proceed to calculate the tie-lines in the negative direction from the original tie-line in a similar manner until the entire isolated region is explored.

7. Draw cubic-splines through the endpoints of the calculated tie-lines for each region to complete the phase diagram.

Software was developed using the Python programming language to perform the parameter estimation from ternary liquid-liquid equilibria, and to calculat the predicted phase diagrams for

Ternary Mixture	Data Source
1-Hexanol and Nitromethane and Water	Sazonov et al.,(1977) [35]
1-Nonanol and Nitromethane and Water	Sazonov and Chernysheva,(1978) [34]
Cyclohexane and Benzene and Nitromethane	Weck and Hunt,(1954) [46]
Heptane and Hexane and Methanol	Wittrig,(1977) [47]
Water and Dimethyl Sulfoxide and Tetrahydrofuran	Foucault et al.,(1993) [12]

Table 2.6: Ternary mixtures for which binary interaction parameters are calculated and experimental data sources

the DWPM model using the method described here. The ternary mixtures and the corresponding original references are given in table 2.6.

Chapter 3

Results and Discussion

3.1 Binary Mixtures

The bi-level optimization method for parameter estimation, as discussed previously, was successfully applied using the Python programming language. Multi-parameter, constrained optimizers included in the SciPy.Optimize package were used. This method was however found to be very sensitive to initial values and convergence was unreliable. The software would often terminate after a large number of iterations or function evaluations without converging to a feasible solution. This is probably due to the complexity of the unknown overall or underlying mathematical function which is being optimized.

In order to overcome this, calculation of binary interaction parameters at various temperatures required manual tweaking of initial parameter guesses for each system, for each model. This is inconvenient and becomes very problematic for cases where the range or order of magnitude of the interaction parameters is not known, for a specific model or mixture. These optimizations may take hours to perform, with no guarantee of convergence.

Another problem which was encountered using the bi-level optimization approach was that of parameter scaling. When a model requires that the binary interaction parameters differ greatly, in order to match the experimental measurements, scaling issues prevent the optimization technique from converging properly and reliably.

The parameters and phase diagrams for each of the models and each of the binary mixtures in table 2.3 where calculated using the pseudo-analytical approach discussed in section 2.3.2. It was found that this method converged reliably and is relatively insensitive to initial parameter guesses.

Temperature	**NRTL**		**UNIQUAC**		**DWPM**	
(K)	g_{ij}	g_{ji}	u_{ij}	u_{ji}	Λ_{ij}	Λ_{ji}
293.00	-1.011E+02	1.788E+03	1.780E+02	1.659E+02	2.423E-03	1.159E+00
298.00	-1.086E+02	1.850E+03	1.684E+02	1.820E+02	2.169E-03	1.184E+00
303.00	-1.164E+02	1.906E+03	1.607E+02	1.953E+02	2.000E-03	1.209E+00

Table 3.1: Calculated binary interaction parameters for 2-Hexanol and Water

The pseudo analytical approach does apply a random multi-start approach. This is done in order to ensure convergence to physically significant solutions. However, the solution is readily tested for compliance to certain requirements. This process is automated and therefore requires no manual tweaking. For example, in the case of calculated phase equilibrium compositions, $\sum_i^n x_i = 1$ must apply. Also, the predicted tie-line must have a negative value at $x = 0$ and $x = 1$. Nevertheless, the pseudo analytical method converged very rapidly, and reliably, in spite of the use of a multi-start approach.

For the DWPM the values of s_i in equation 2.1.10 are chosen as $1/2$. Therefore, the form of the DWPM model used in this investigation reduces to the 3 parameter Wilson model. The software is however programmed to accommodate any values for each s_i, and the pseudo analytical approach converges equally easily and rapidly for any sensible combination of these parameters. For the NRTL model α is chosen as 0.2, where $\alpha = \alpha_{ij} = \alpha_{ji}$. The pure component constants, r_i and q_i, in the UNIQUAC model are supplied in the Dechema data collection [25]. The calculated binary interaction parameters for each of the binary mixtures, using the NRTL, UNIQUAC and DWPM models are now presented.

The calculated binary interaction parameters for the mixture 2-Hexanol and Water, for each of the models, at the experimental temperatures is displayed in table 3.1. The phase diagram predicted by the DWPM, NRTL and UNIQIAC models, using 10 sets of linearly interpolated parameters, and the original experimentally measured phase compositions are displayed in figures 3.1.1, 3.1.2 and 3.1.3 respectively.

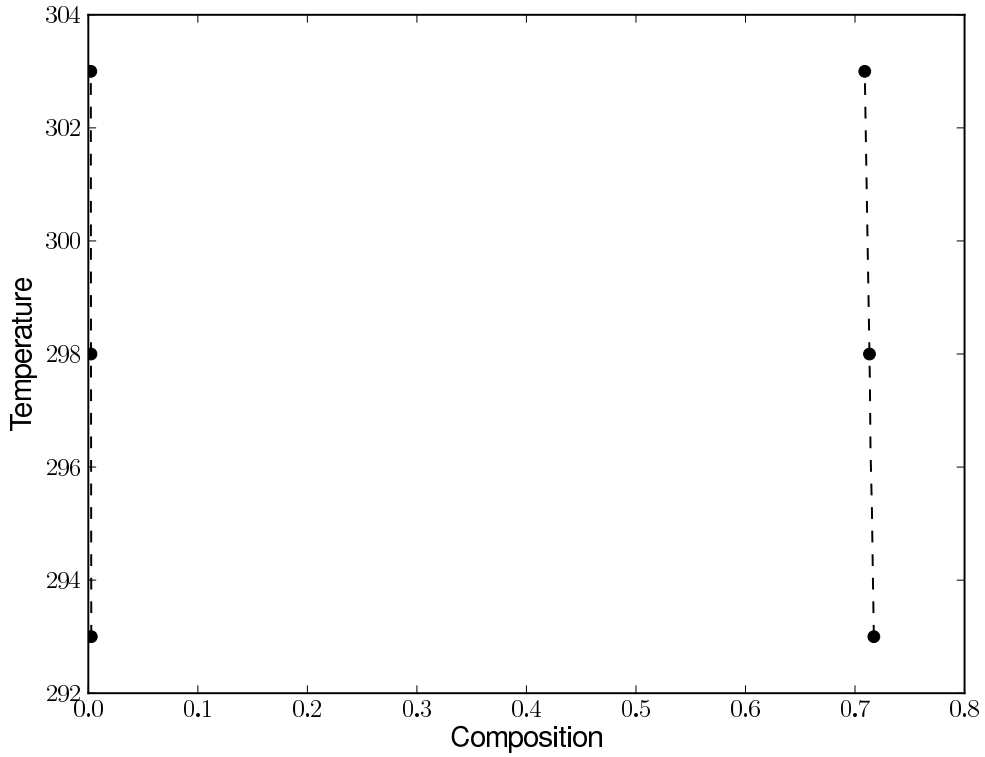

Figure 3.1.1: Calculated phase diagram for 2-Hexanol and Water using the DWPM model

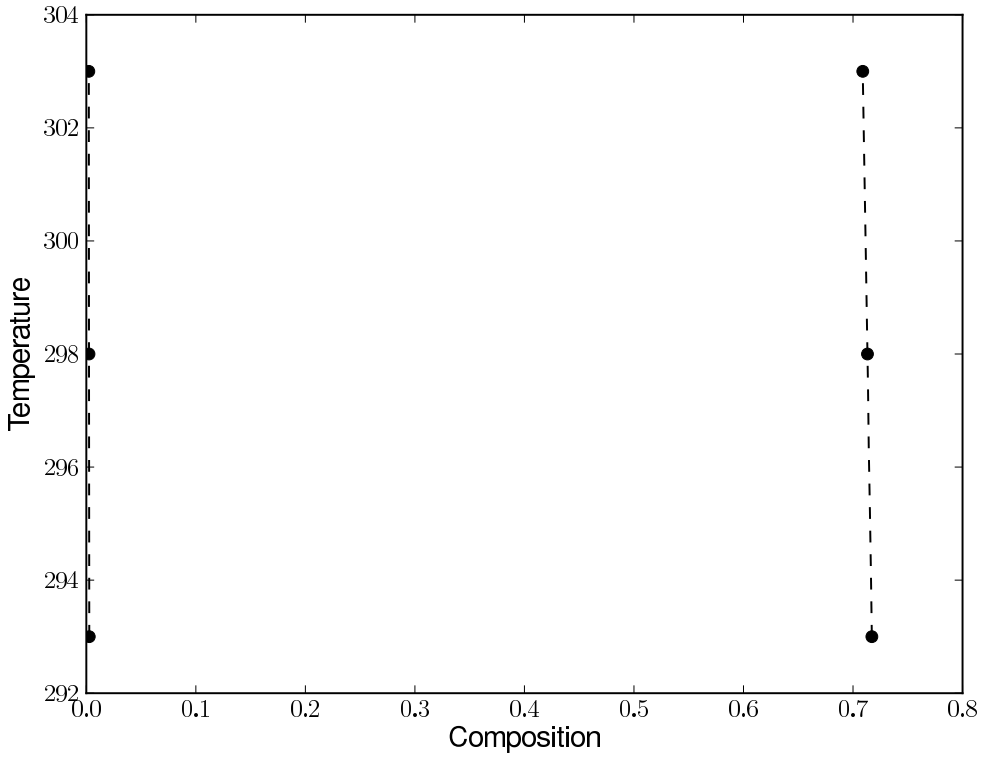

Figure 3.1.2: Calculated phase diagram for 2-Hexanol and Water using the NRTL Model

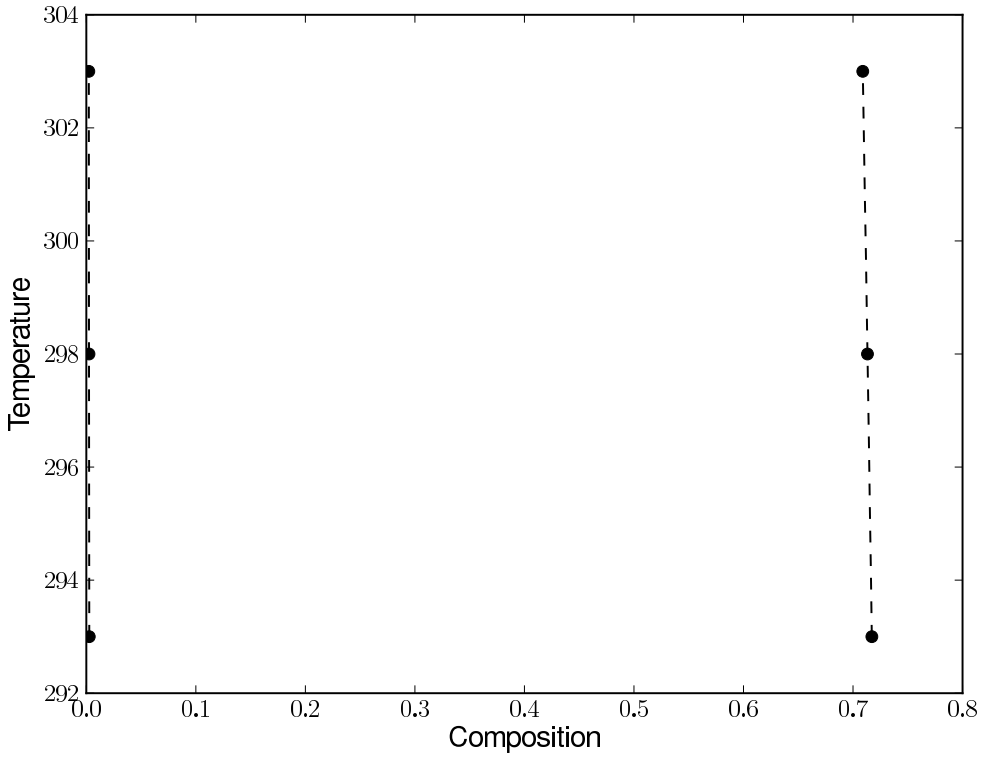

Figure 3.1.3: Calculated phase diagram for 2-Hexanol and Water using the UNIQUAC model

Temperature	**NRTL**		**UNIQUAC**		**DWPM**	
(K)	g_{ij}	g_{ji}	u_{ij}	u_{ji}	Λ_{ij}	Λ_{ji}
292.85	1.386E+03	2.541E+03	1.000E+03	3.371E+02	1.579E-04	1.352E-02
312.85	1.265E+03	2.626E+03	9.282E+02	3.376E+02	1.987E-04	2.588E-02
342.85	1.033E+03	2.741E+03	7.842E+02	3.337E+02	2.808E-04	6.865E-02

Table 3.2: Calculated binary interaction parameters for 13-Dimethyl Benzene and Water

For each of the binary mixtures modelled, the ΔG_{mix} curves, and resulting phase splits, predicted by the NRTL, UNIQUAC and DWPM models are included in the Appendix in section 5.1. For each of these plots the change of Gibbs energy on mixing versus composition is determined using the set of calculated interaction parameters, at the relevant temperatures.

The calculated parameters for 13-Dimethyl Benzene and Water for each model, at the experimental temperatures is displayed in table 3.2. As before, the phase diagram predicted by the DWPM, NRTL and UNIQIAC models, using 10 sets of linearly interpolated parameters, and the original experimentally measured phase compositions are displayed in figures 3.1.4, 3.1.5 and 3.1.6 respectively.

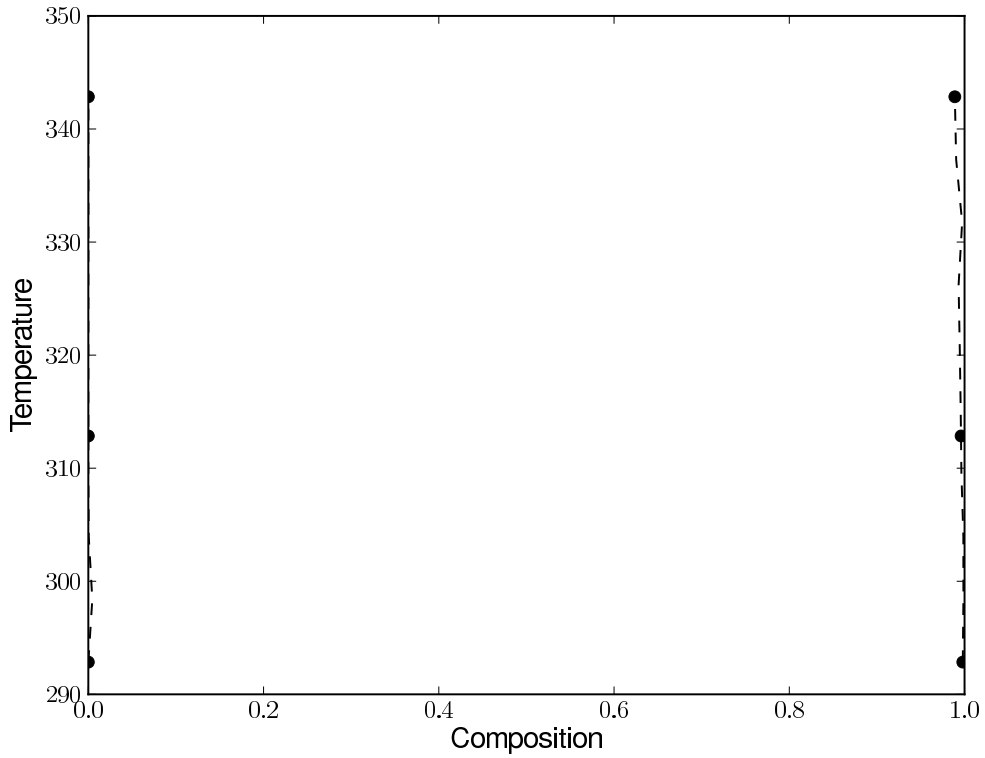

Figure 3.1.4: Calculated phase diagram for 13-Dimethyl Benzene and Water using the DWPM model

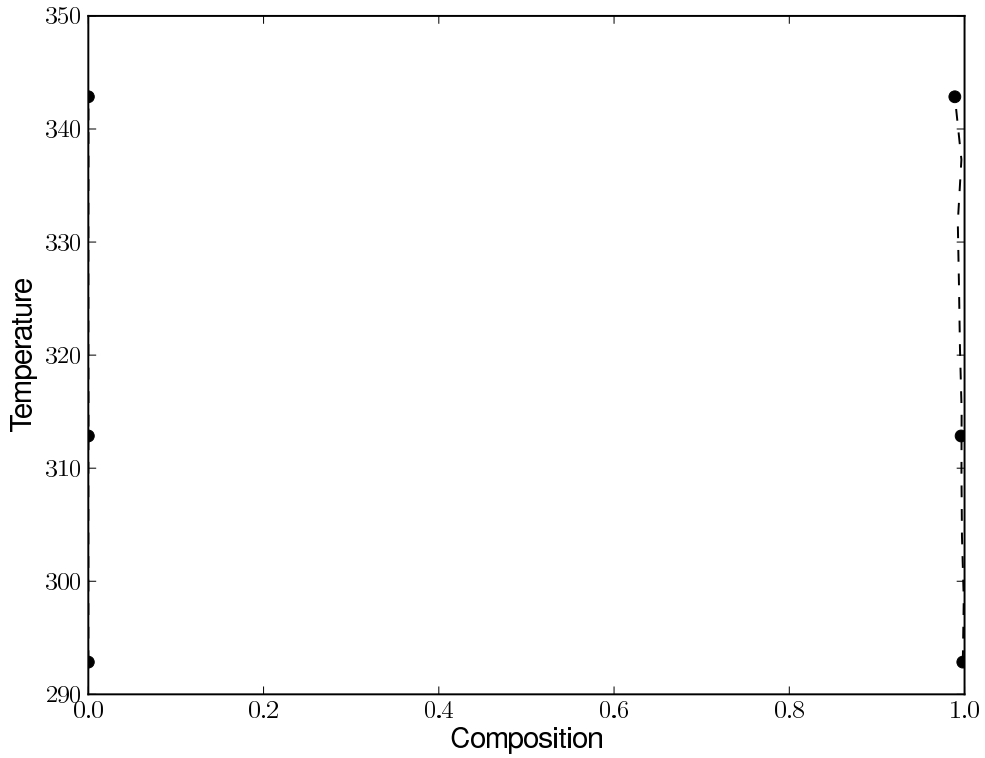

Figure 3.1.5: Calculated phase diagram for 13-Dimethyl Benzene and Water using the NRTL Model

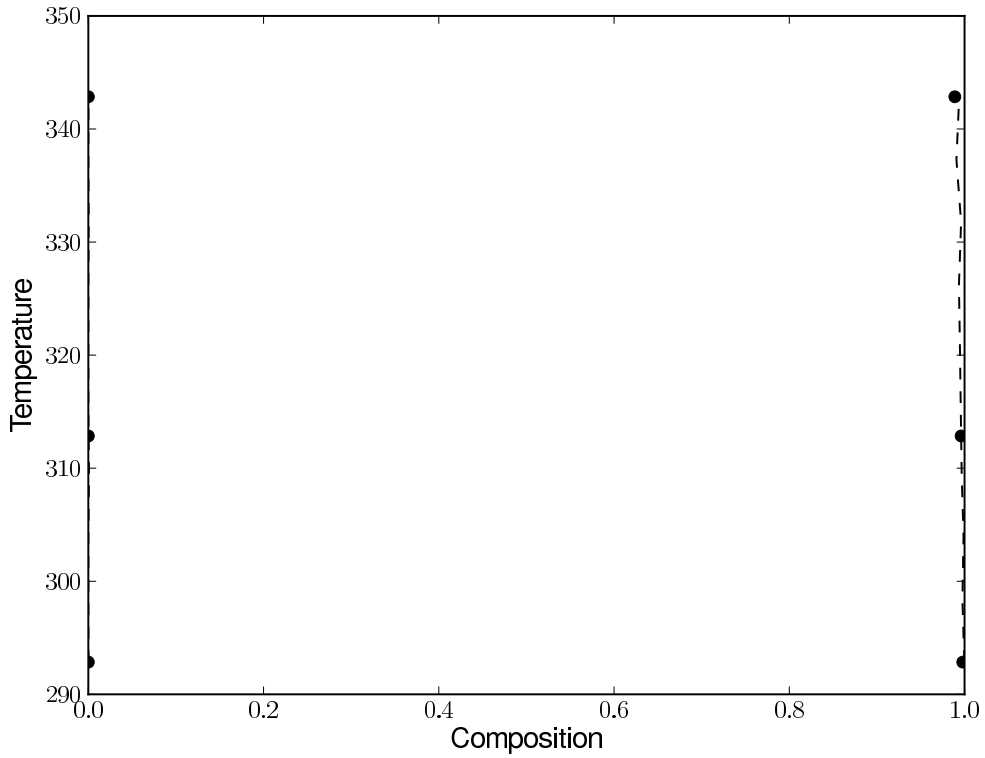

Figure 3.1.6: Calculated phase diagram for 13-Dimethyl Benzene and Water using the UNIQUAC model

Temperature	**NRTL**		**UNIQUAC**		**DWPM**	
(K)	g_{ij}	g_{ji}	u_{ij}	u_{ji}	Λ_{ij}	Λ_{ji}
281.60	1.944E+01	1.384E+03	1.576E+02	1.056E+02	7.805E-03	7.746E-01
298.40	-4.970E+01	1.510E+03	9.818E+01	1.465E+02	6.999E-03	9.409E-01
321.00	-4.920E+01	1.582E+03	1.283E+02	1.290E+02	7.994E-03	9.237E-01
339.30	-9.394E+01	1.655E+03	1.166E+02	1.281E+02	8.663E-03	1.011E+00
369.70	-2.231E+02	1.800E+03	5.003E+01	1.518E+02	9.514E-03	1.273E+00

Table 3.3: Calculated binary interaction parameters for Aniline and Water

The results for the mixture Aniline and Water for each model, at the experimental temperatures are displayed in table 3.3. The calculated phase diagrams using the DWPM, NRTL and UNIQIAC models are presented in figures 3.1.7, 3.1.8 and 3.1.9 respectively. The binary interaction parameters were again linearly interpolated at 9 equally spaced intervals for the construction of the phase diagrams.

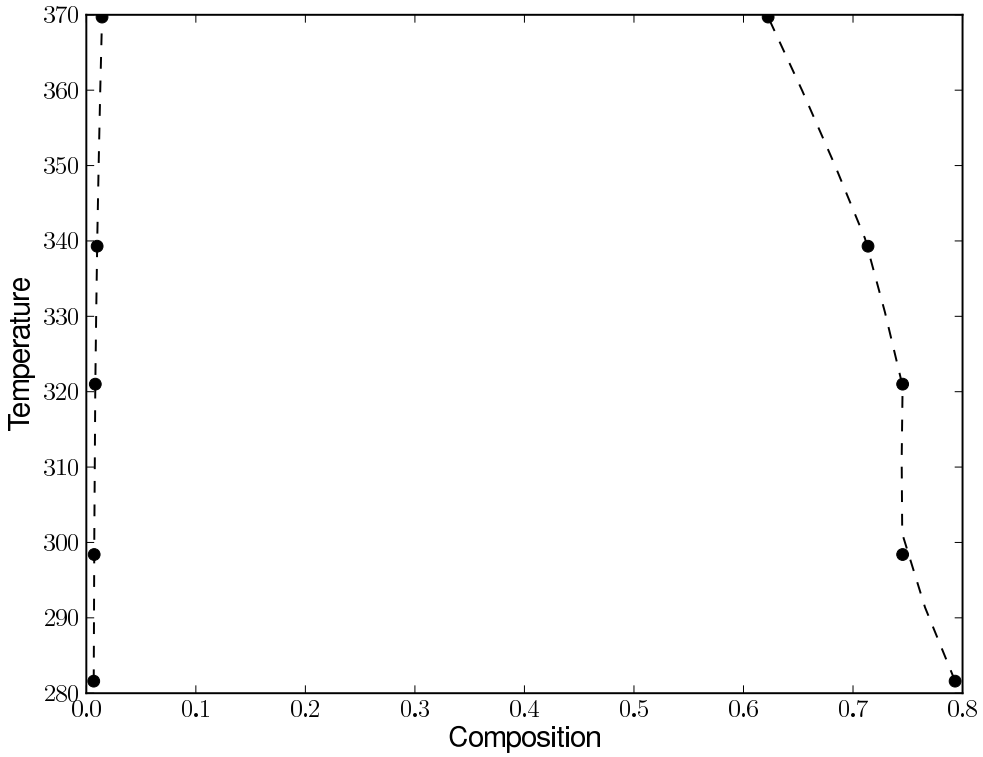

Figure 3.1.7: Calculated phase diagram for Aniline and Water using the DWPM model

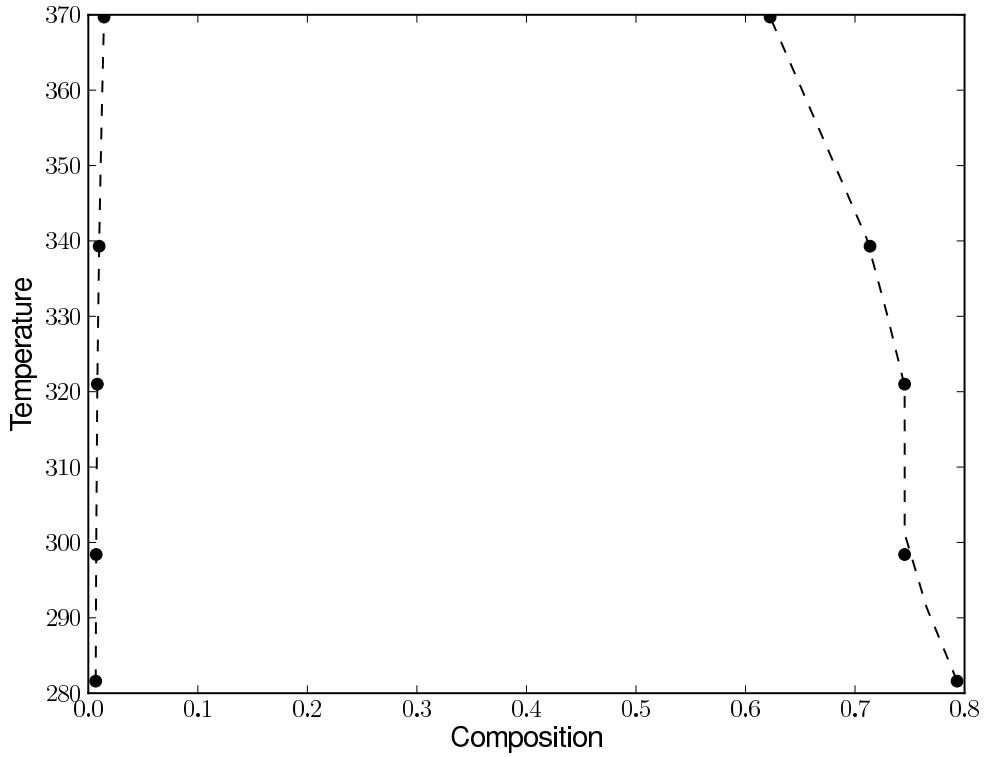

Figure 3.1.8: Calculated phase diagram for Aniline and Water using the NRTL Model

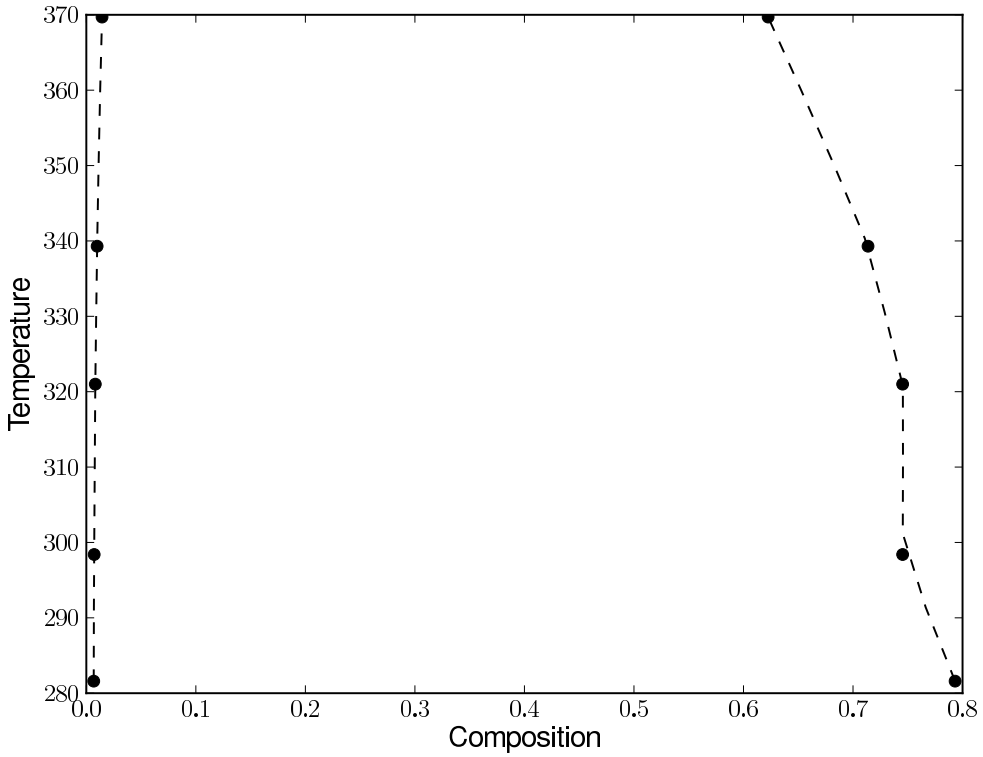

Figure 3.1.9: Calculated phase diagram for Aniline and Water using the UNIQUAC model

Temperature	**NRTL**		**UNIQUAC**		**DWPM**	
(K)	g_{ij}	g_{ji}	u_{ij}	u_{ji}	Λ_{ij}	Λ_{ji}
313.30	2.424E+02	1.463E+03	-3.846E+01	4.915E+02	9.234E-03	4.125E-01
332.80	1.771E+02	1.262E+03	-4.489E+01	4.285E+02	2.315E-02	4.917E-01
353.80	1.817E+02	1.252E+03	-4.372E+01	4.243E+02	3.003E-02	4.967E-01
363.00	2.279E+02	1.064E+03	-1.779E+01	3.525E+02	5.441E-02	4.460E-01
393.00	1.641E+02	1.038E+03	-3.698E+01	3.511E+02	7.420E-02	5.422E-01

Table 3.4: Calculated binary interaction parameters for Diethylene Glycol and 12-Dimethyl Benzene

The calculated binary interaction parameters for Diethylene Glycol and 12-Dimethyl Benzene is displayed in table 3.4. The phase diagram predicted by the DWPM, NRTL and UNIQIAC models, using 10 sets of linearly interpolated parameters, and the original experimentally measured phase compositions are displayed in figures 3.1.10, 3.1.11 and 3.1.12 respectively.

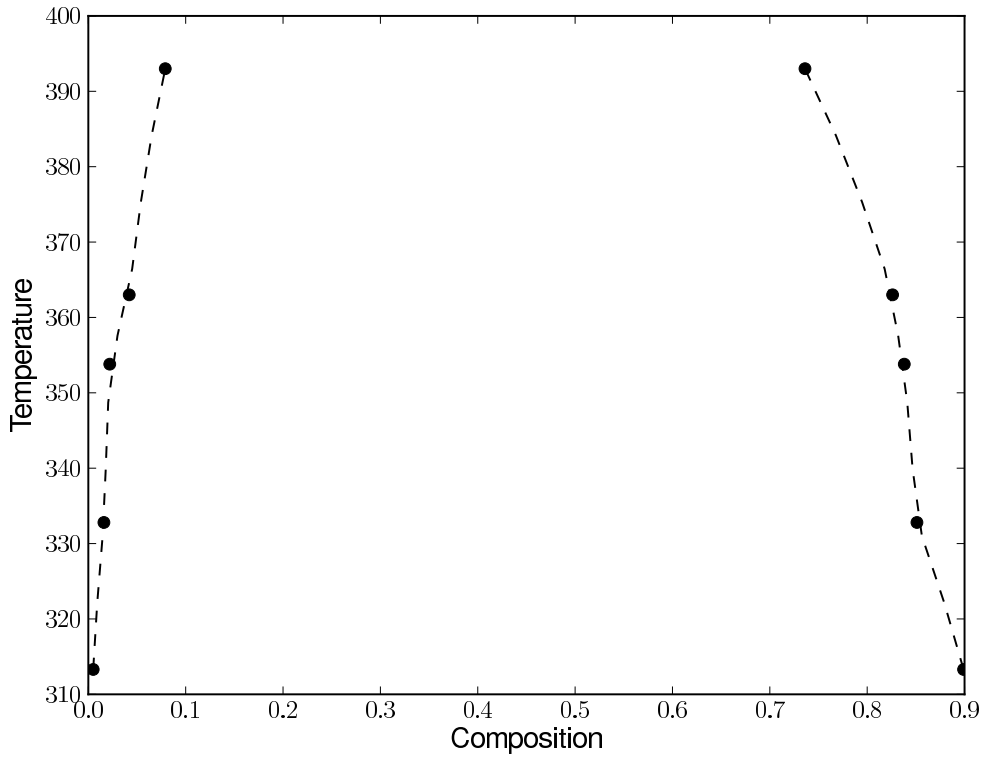

Figure 3.1.10: Calculated phase diagram for Diethylene Glycol and 12-Dimethyl Benzene using the DWPM model

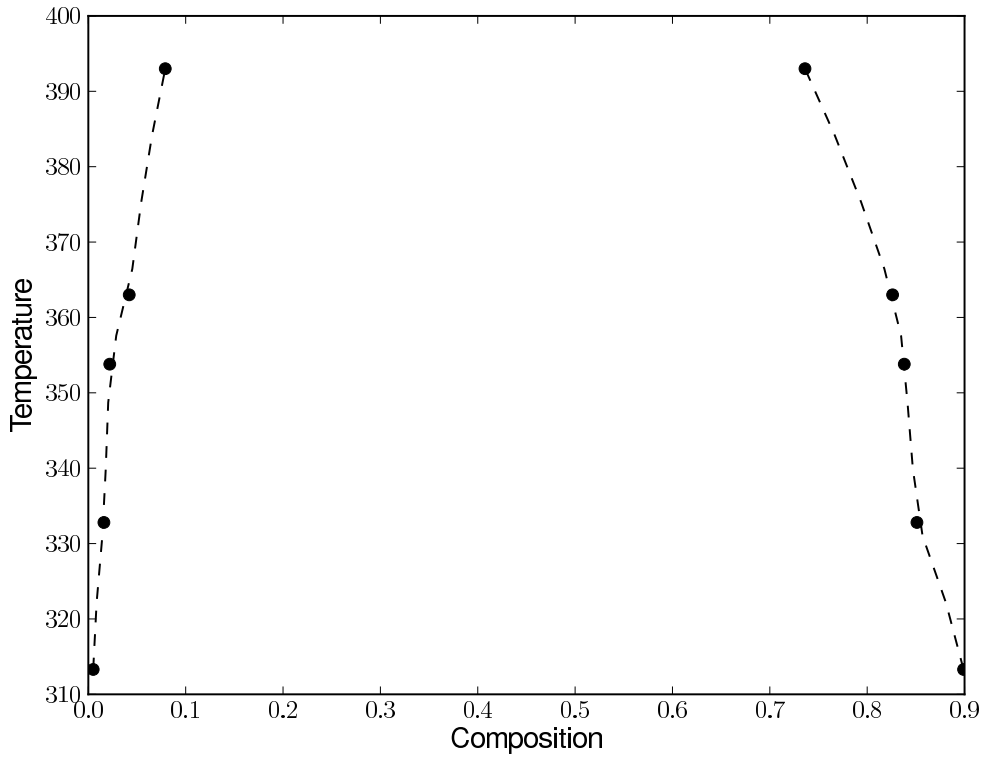

Figure 3.1.11: Calculated phase diagram for Diethylene Glycol and 12-Dimethyl Benzene using the NRTL model

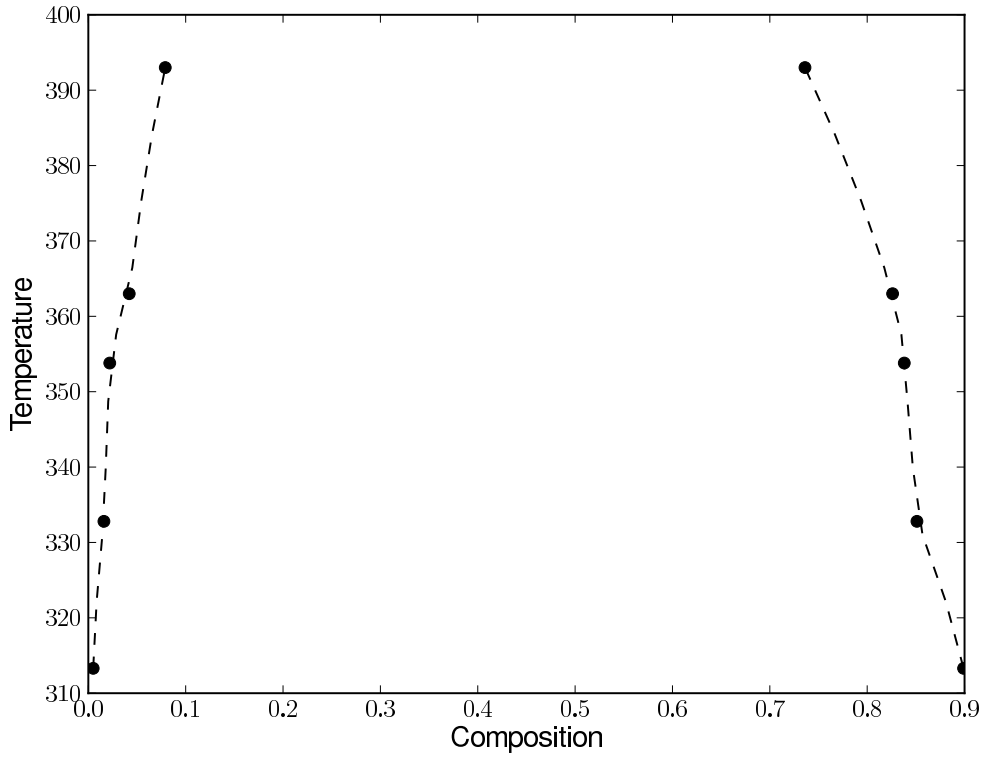

Figure 3.1.12: Calculated phase diagram for Diethylene Glycol and 12-Dimethyl Benzene using the UNIQUAC model

Temperature	**NRTL**		**UNIQUAC**		**DWPM**	
(K)	g_{ij}	g_{ji}	u_{ij}	u_{ji}	Λ_{ij}	Λ_{ji}
273.00	6.092E+02	1.334E+03	7.281E+02	6.859E+01	6.793E-03	1.029E-01
283.00	6.872E+02	1.474E+03	7.732E+02	9.605E+01	4.888E-03	8.704E-02
288.00	6.827E+02	1.548E+03	7.646E+02	1.095E+02	4.128E-03	9.360E-02
293.00	6.418E+02	1.627E+03	7.289E+02	1.234E+02	3.447E-03	1.138E-01
298.00	6.090E+02	1.699E+03	7.003E+02	1.359E+02	2.969E-03	1.336E-01

Table 3.5: Calculated binary interaction parameters for Dipropyl Ether and Water

The calculated binary interaction parameters for Dipropyl Ether and Water is displayed in table 3.5. The phase diagram predicted by the DWPM, NRTL and UNIQIAC models, using 10 sets of linearly interpolated parameters, and the original experimentally measured phase compositions are displayed in figures 3.1.13, 3.1.14 and 3.1.15 respectively.

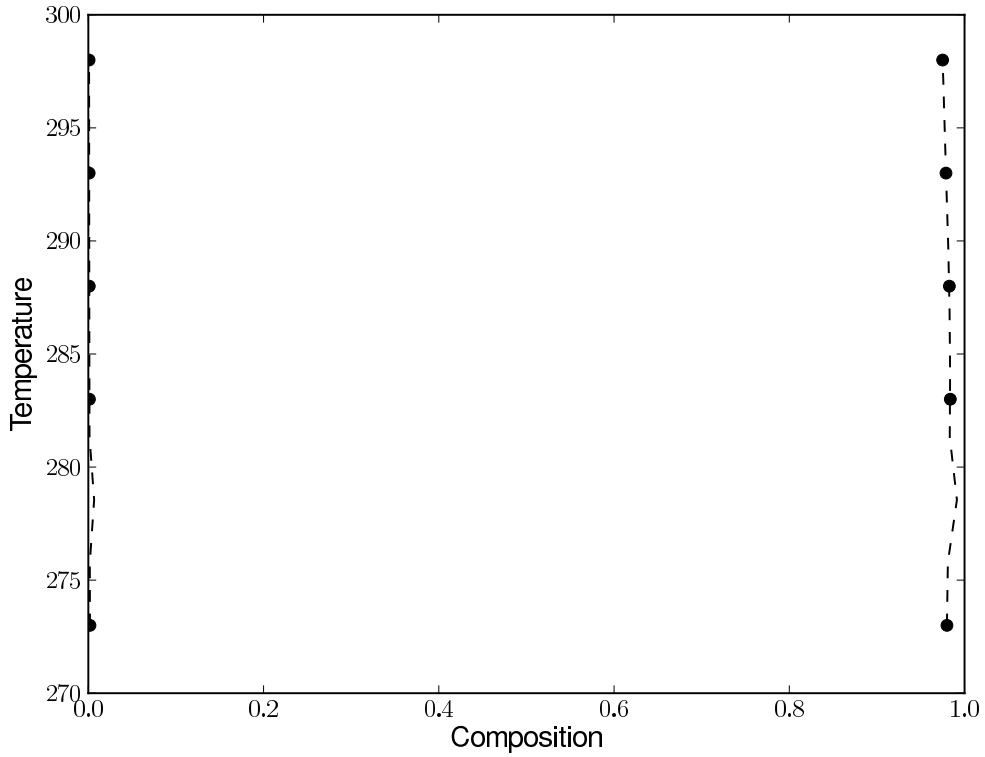

Figure 3.1.13: Calculated phase diagram for Dipropyl Ether and Water using the DWPM model

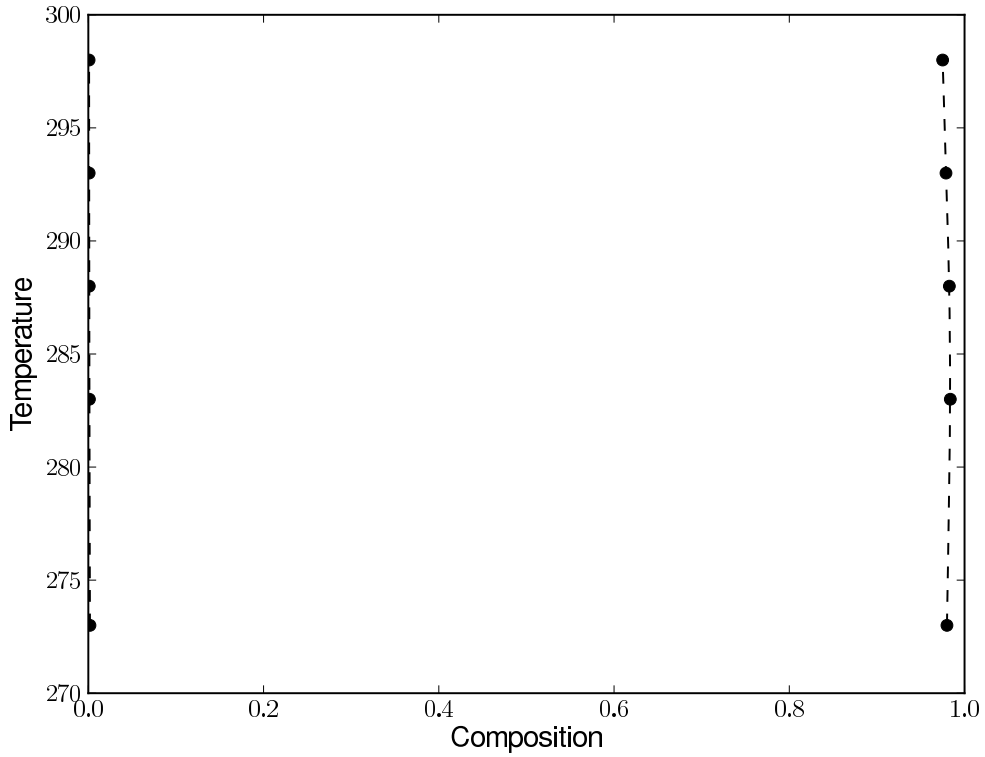

Figure 3.1.14: Calculated phase diagram for Dipropyl Ether and Water using the NRTL model

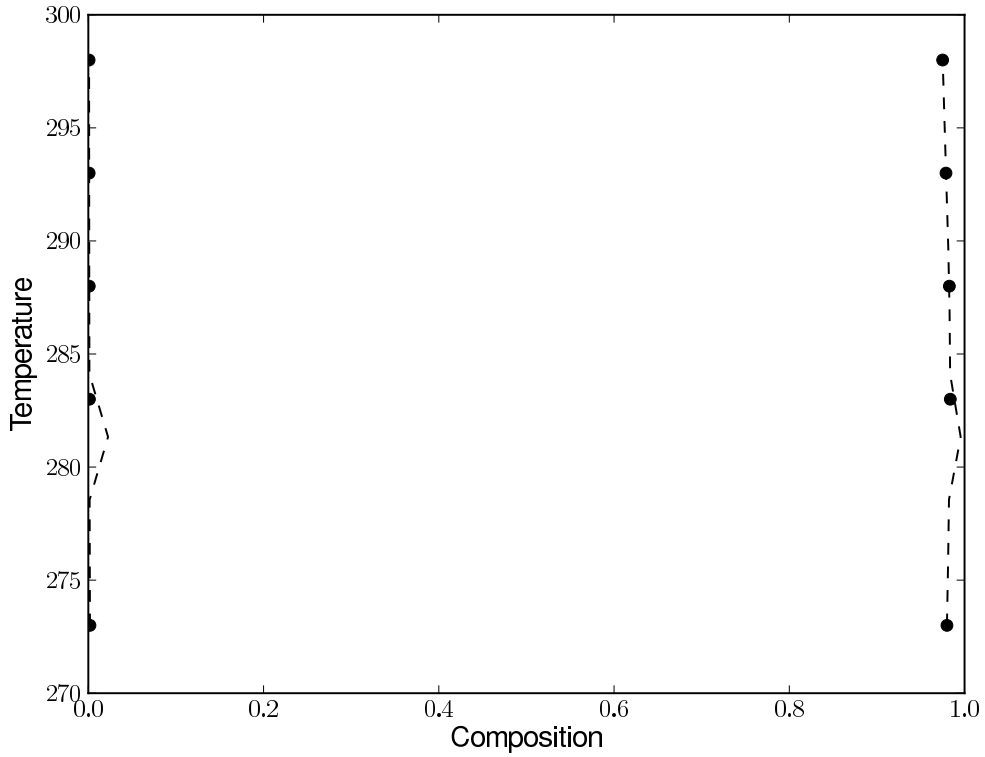

Figure 3.1.15: Calculated phase diagram for Dipropyl Ether and Water using the UNIQUAC model

Temperature	**NRTL**		**UNIQUAC**		**DWPM**	
(K)	g_{ij}	g_{ji}	u_{ij}	u_{ji}	Λ_{ij}	Λ_{ji}
273.00	2.689E+02	8.719E+02	4.731E+02	2.994E+01	4.046E-02	3.195E-01
278.00	2.513E+02	9.204E+02	4.598E+02	3.930E+01	3.626E-02	3.453E-01
283.00	2.337E+02	9.685E+02	4.465E+02	4.882E+01	3.266E-02	3.721E-01
288.00	2.163E+02	1.016E+03	4.332E+02	5.844E+01	2.957E-02	3.997E-01
293.00	1.990E+02	1.063E+03	4.199E+02	6.815E+01	2.692E-02	4.281E-01
298.00	1.809E+02	1.110E+03	4.059E+02	7.808E+01	2.460E-02	4.586E-01
303.00	1.621E+02	1.157E+03	3.914E+02	8.824E+01	2.255E-02	4.908E-01
308.00	1.434E+02	1.203E+03	3.771E+02	9.841E+01	2.078E-02	5.239E-01
313.00	1.241E+02	1.250E+03	3.623E+02	1.088E+02	1.922E-02	5.587E-01

Table 3.6: Calculated binary interaction parameters for Ethyl Ester Acetic Acid and Water

The calculated binary interaction parameters for Ethyl Ester Acetic Acid and Water is displayed in table 3.6. The phase diagram predicted by the DWPM, NRTL and UNIQIAC models, using 10 sets of linearly interpolated parameters, and the original experimentally measured phase compositions are displayed in figures 3.1.16, 3.1.17 and 3.1.18 respectively.

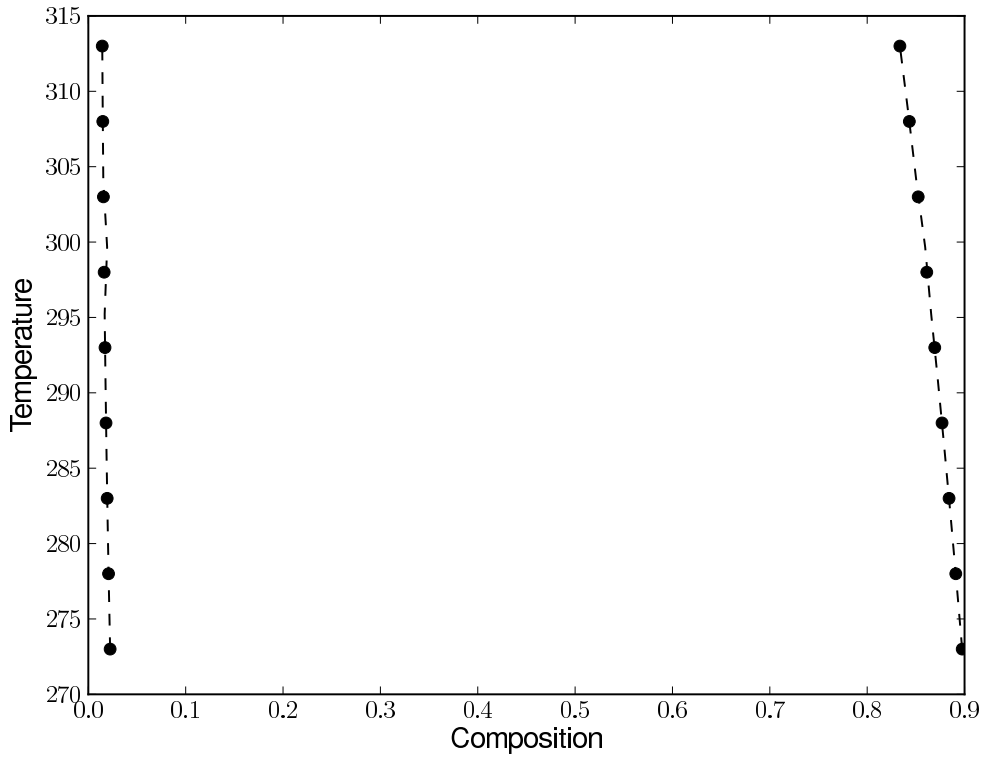

Figure 3.1.16: Calculated phase diagram for Ethyl Ester Acetic Acid and Water using the DWPM model

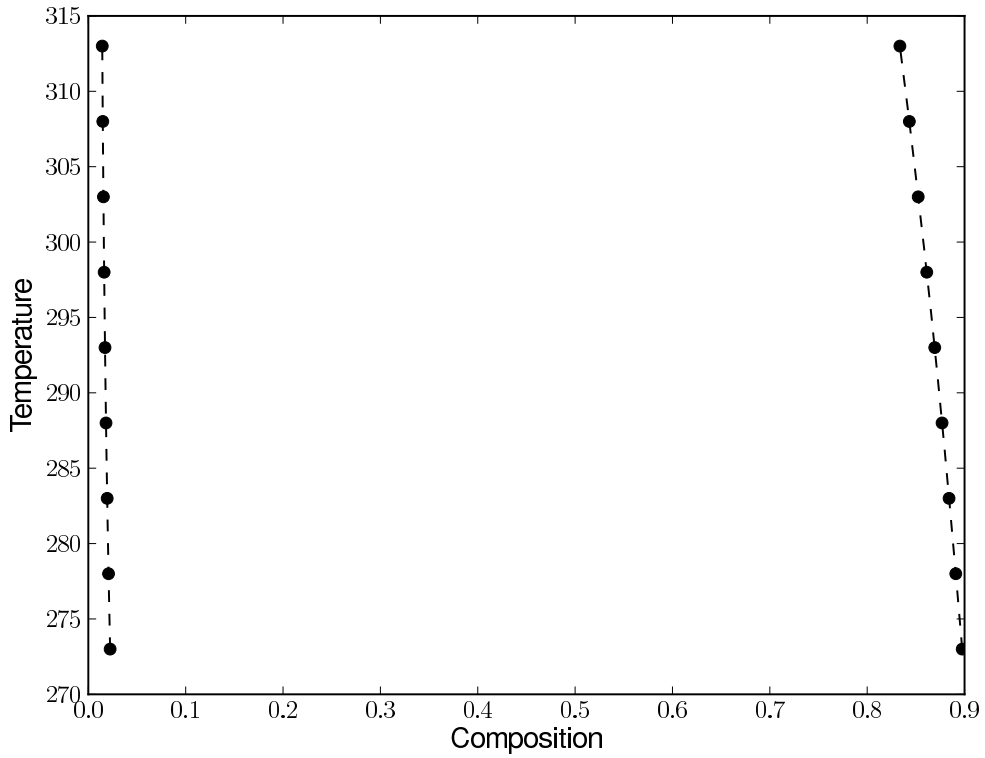

Figure 3.1.17: Calculated phase diagram for Ethyl Ester Acetic Acid and Water using the NRTL model

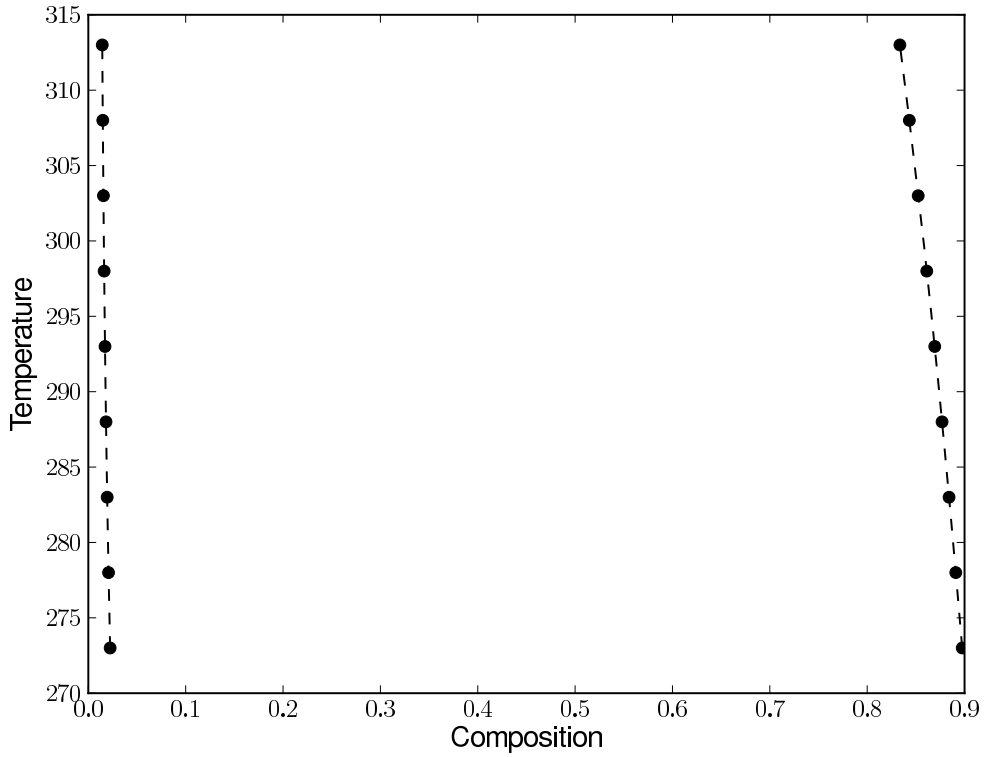

Figure 3.1.18: Calculated phase diagram for Ethyl Ester Acetic Acid and Water using the UNIQUAC model

Temperature	**NRTL**		**UNIQUAC**		**DWPM**	
(K)	g_{ij}	g_{ji}	u_{ij}	u_{ji}	Λ_{ij}	Λ_{ji}
291.00	5.169E+02	4.396E+02	5.751E+00	6.875E+02	2.004E-01	1.574E-01
303.00	5.494E+02	3.490E+02	2.189E+00	6.460E+02	2.828E-01	1.559E-01
313.00	5.870E+02	2.647E+02	5.246E-01	6.071E+02	3.772E-01	1.506E-01
323.00	6.263E+02	1.640E+02	-2.095E+00	5.588E+02	5.146E-01	1.461E-01

Table 3.7: Calculated binary interaction parameters for Methanol and Heptane

The calculated binary interaction parameters for Methanol and Heptane is displayed in table 3.7. The phase diagram predicted by the DWPM, NRTL and UNIQIAC models, using 10 sets of linearly interpolated parameters, and the original experimentally measured phase compositions are displayed in figures 3.1.19, 3.1.20 and 3.1.21 respectively.

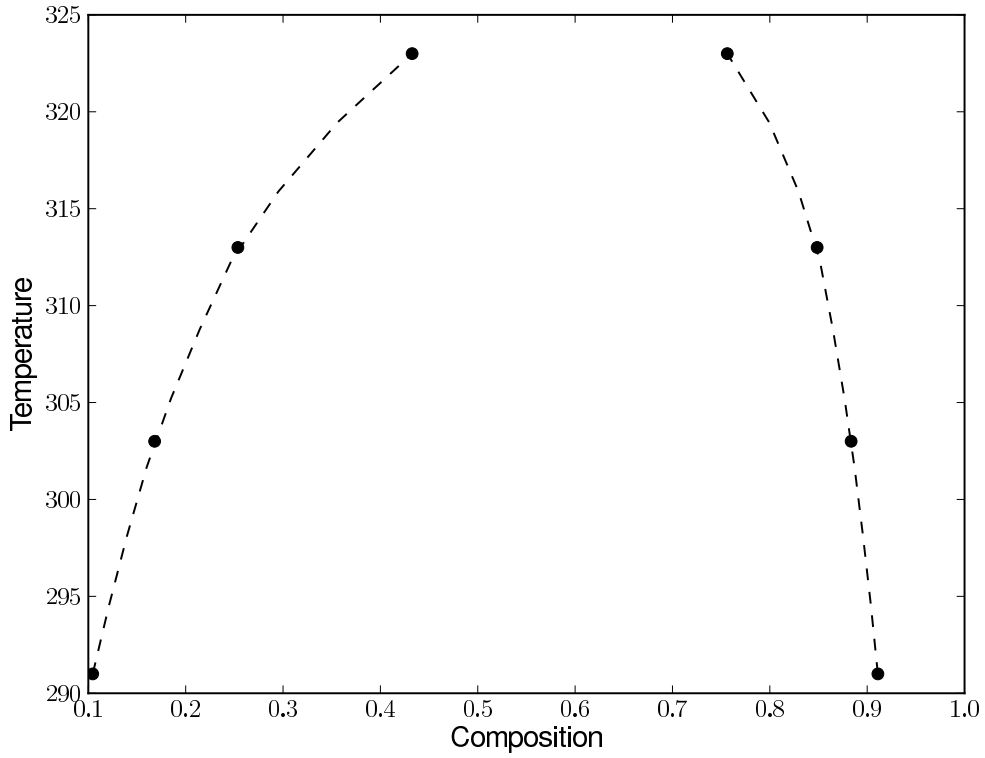

Figure 3.1.19: Calculated phase diagram for Methanol and Heptane using the DWPM model

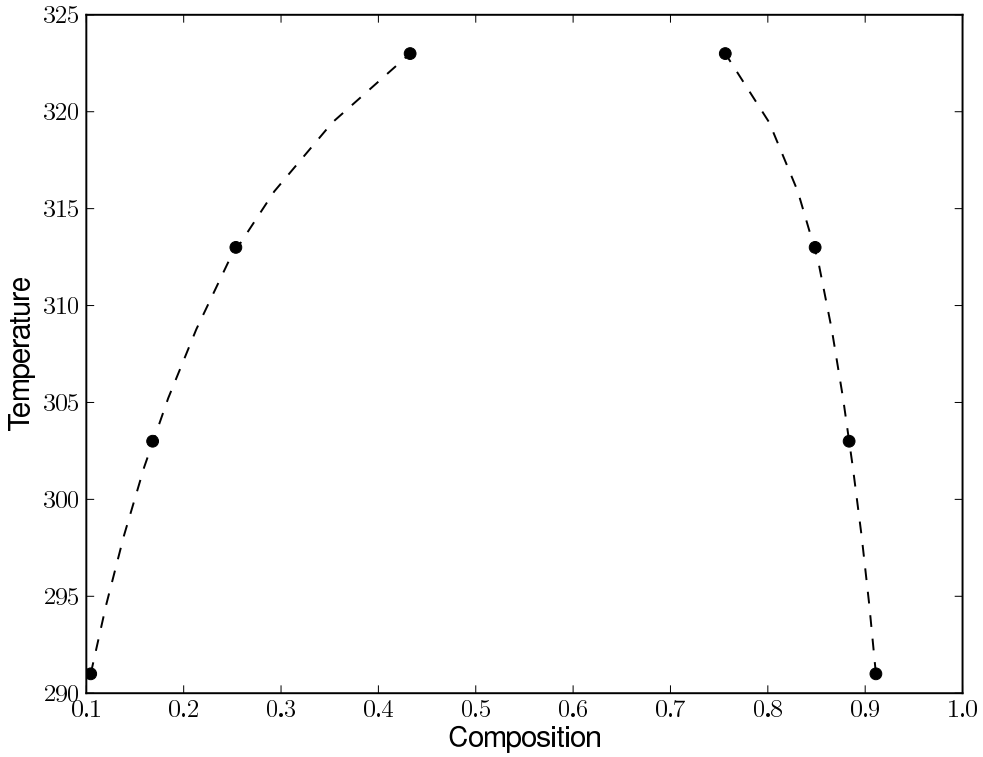

Figure 3.1.20: Calculated phase diagram for Methanol and Heptane using the NRTL model

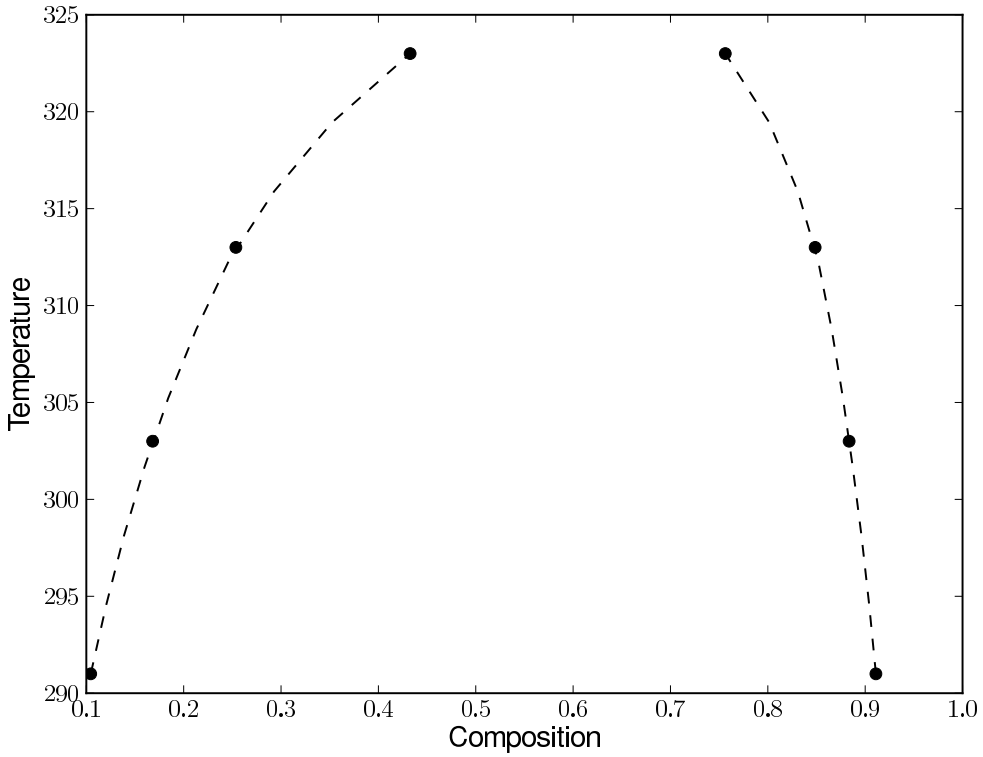

Figure 3.1.21: Calculated phase diagram for Methanol and Heptane using the UNIQUAC model

Temperature	**NRTL**		**UNIQUAC**		**DWPM**	
(K)	g_{ij}	g_{ji}	u_{ij}	u_{ji}	Λ_{ij}	Λ_{ji}
255.20	4.318E+02	5.363E+02	2.704E+01	6.656E+02	1.131E-01	1.652E-01
278.00	4.197E+02	4.631E+02	1.110E+01	6.413E+02	1.752E-01	2.019E-01
298.00	4.405E+02	3.443E+02	9.253E-02	5.877E+02	2.881E-01	2.160E-01

Table 3.8: Calculated binary interaction parameters for Methanol and Hexane

The calculated binary interaction parameters for Methanol and Hexane is displayed in table 3.8. The phase diagram predicted by the DWPM, NRTL and UNIQIAC models, using 10 sets of linearly interpolated parameters, and the original experimentally measured phase compositions are displayed in figures 3.1.22, 3.1.23 and 3.1.24 respectively.

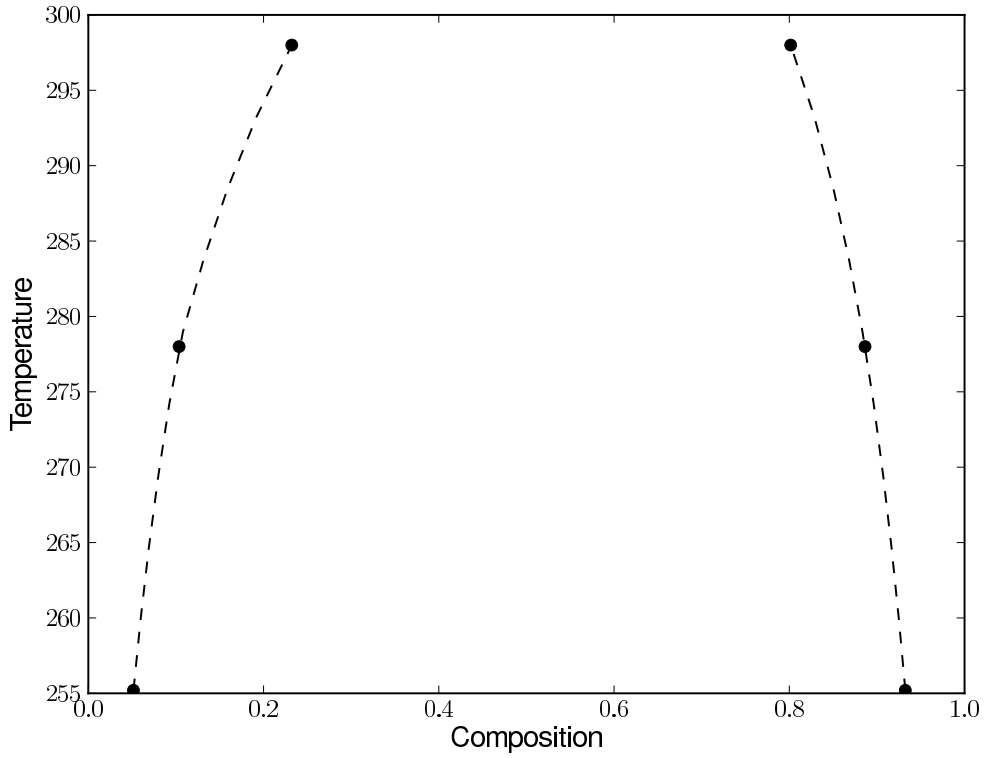

Figure 3.1.22: Calculated phase diagram for Methanol and Heptane using the DWPM model

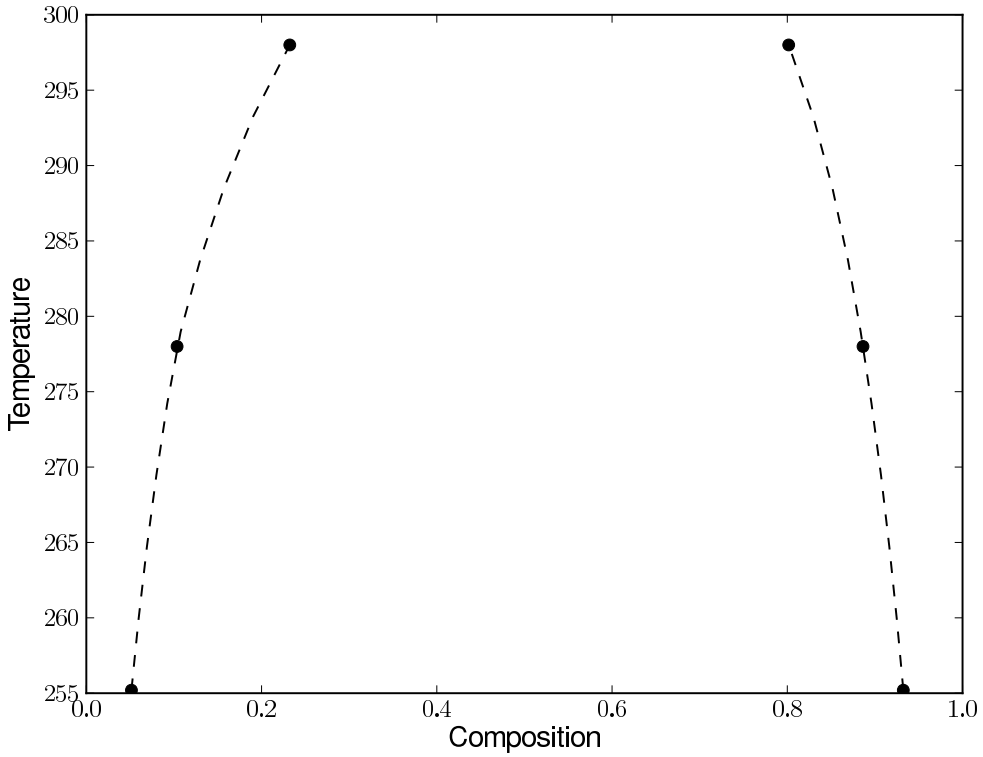

Figure 3.1.23: Calculated phase diagram for Methanol and Hexane using the NRTL model

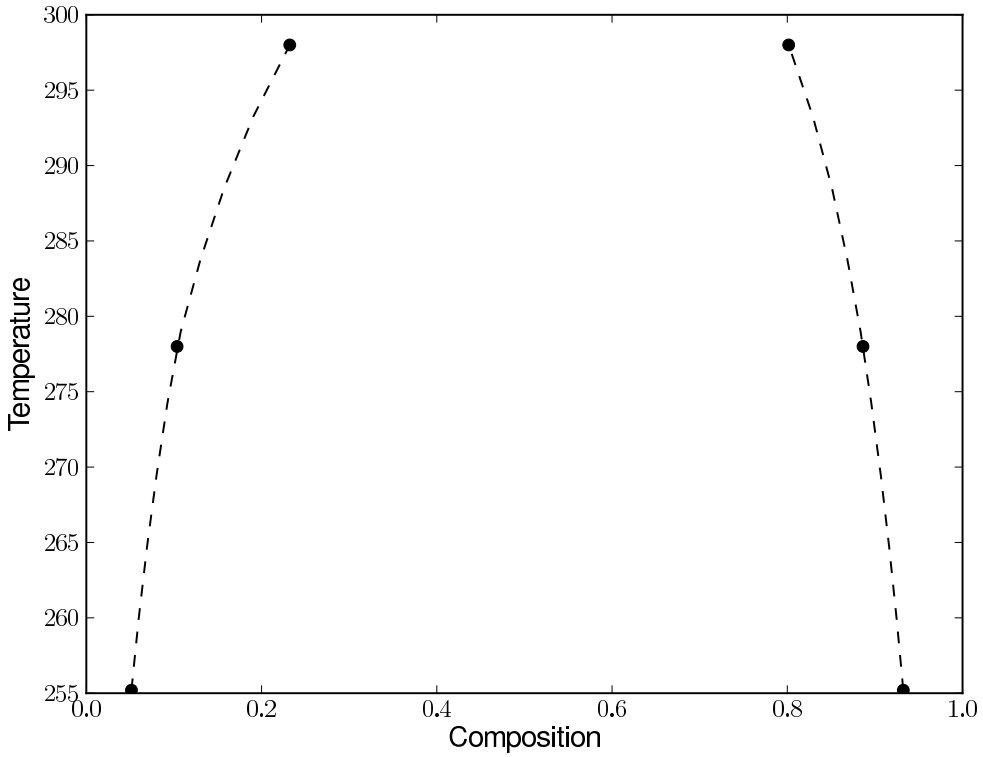

Figure 3.1.24: Calculated phase diagram for Methanol and Hexane using the UNIQUAC model

Chapter 4

Conclusions

Chapter 5

Appendices

5.1 Predicted Gibbs Energy Curves for Binary Mixtures

2-Hexanol and Water

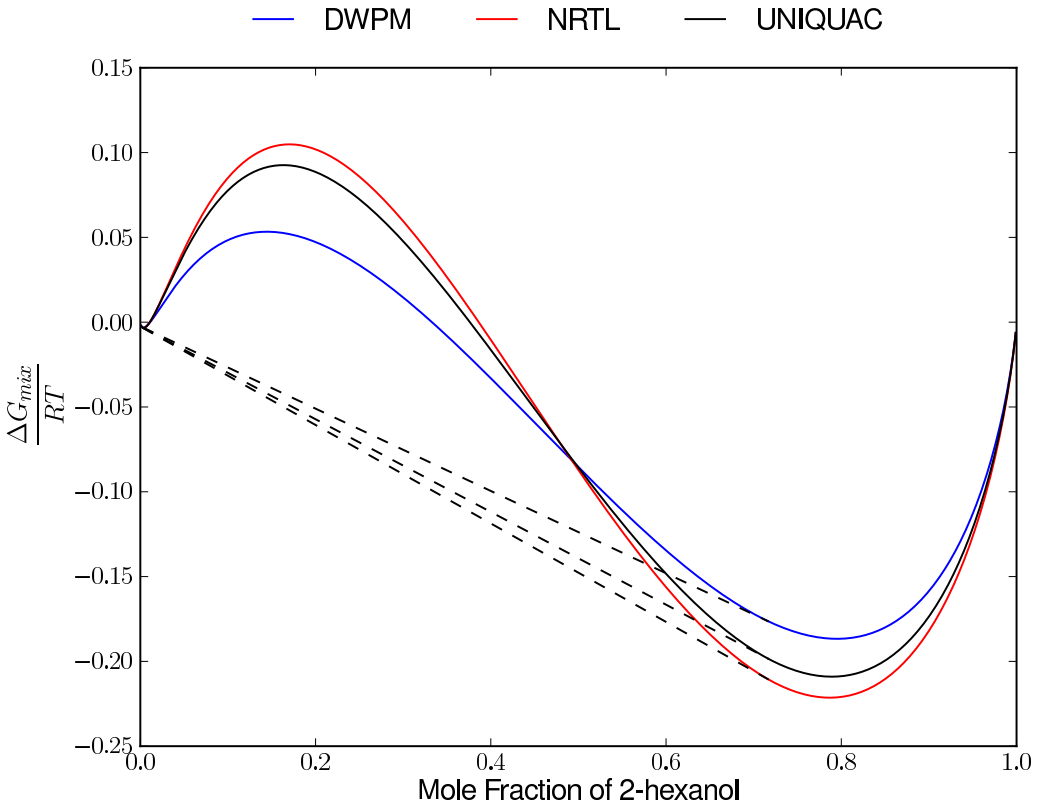

Figure 5.1.1: Calculated liquid-liquid equilibrium for 2-Hexanol and Water at 293 K

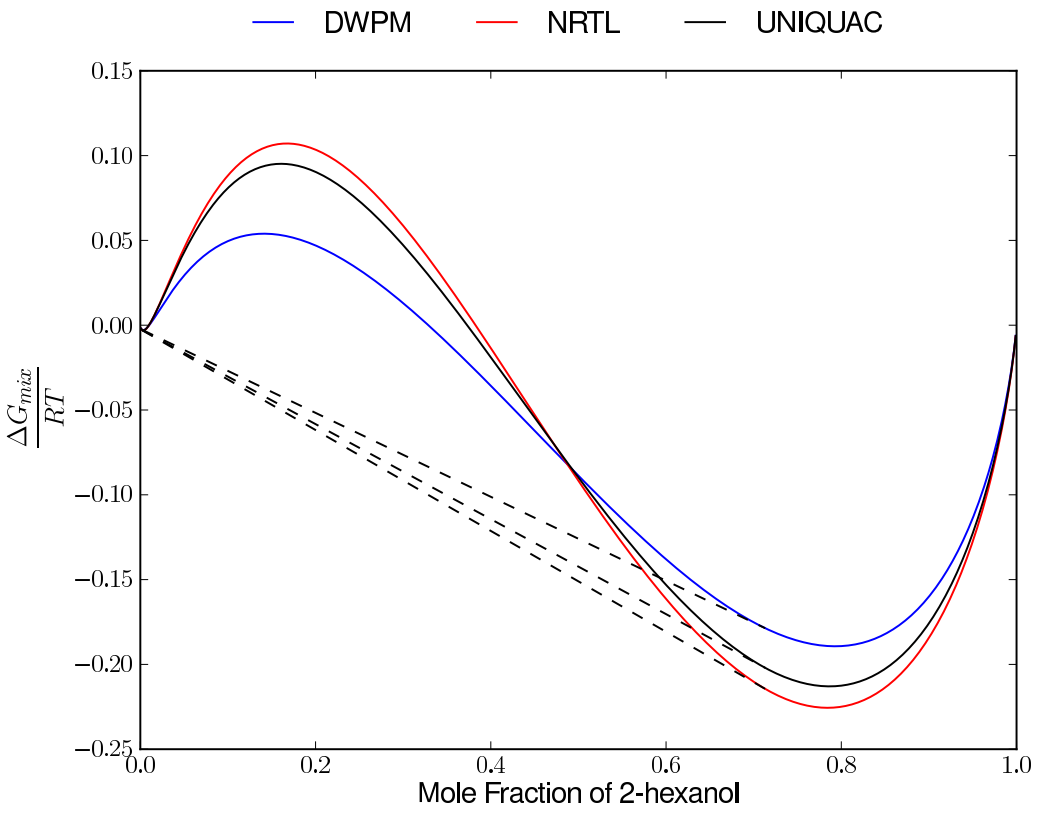

Figure 5.1.2: Calculated liquid-liquid equilibrium for 2-Hexanol and Water at 298 K

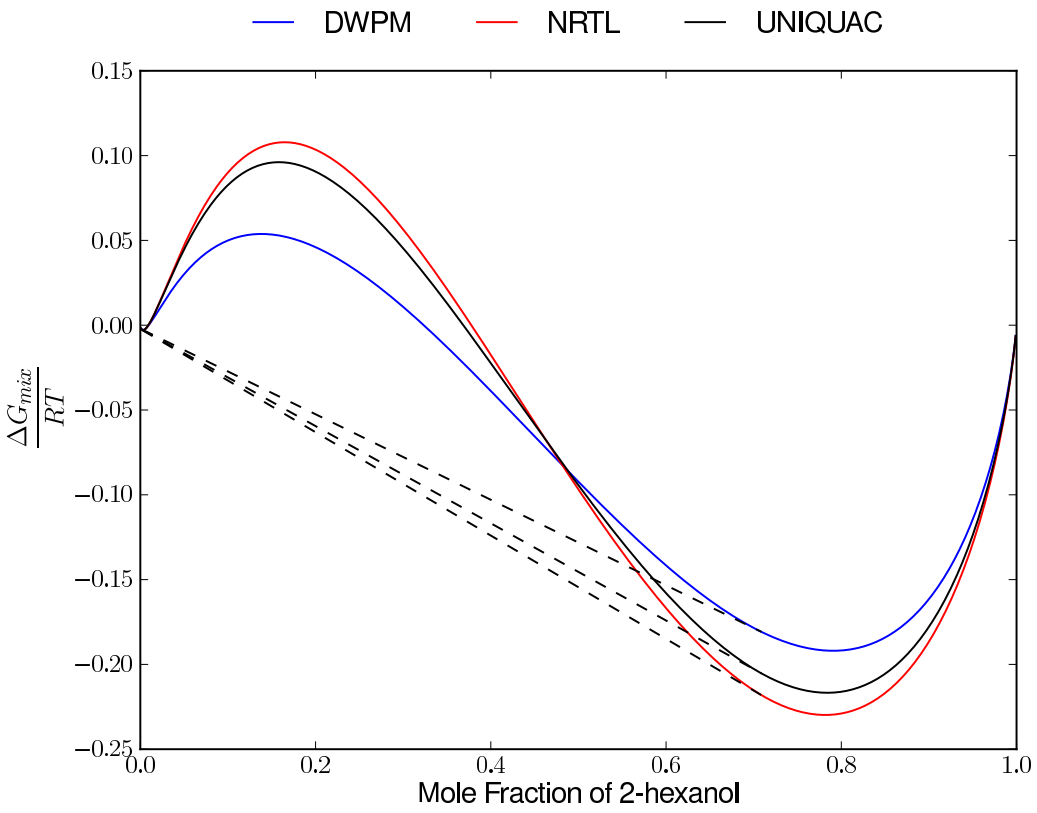

Figure 5.1.3: Calculated liquid-liquid equilibrium for 2-Hexanol and Water at 303 K

13-Dimethyl Benzene and Water

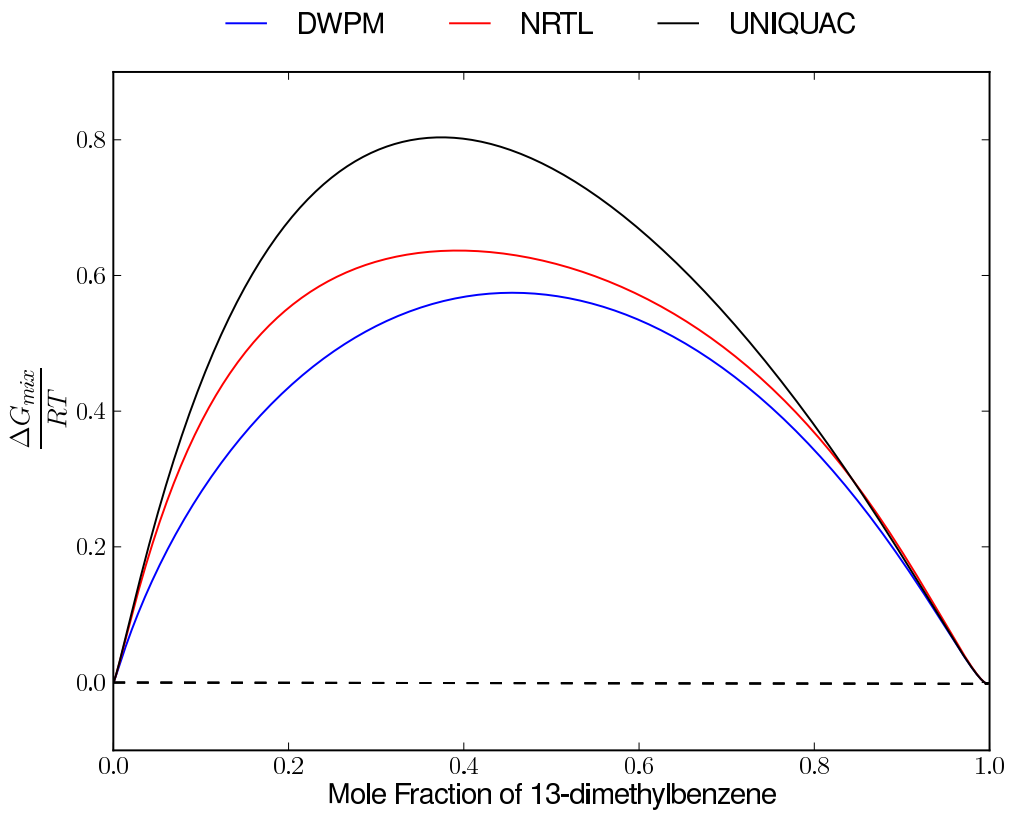

Figure 5.1.4: Calculated liquid-liquid equilibrium for 13-Dimethyl Benzene and Water at 292.85 K

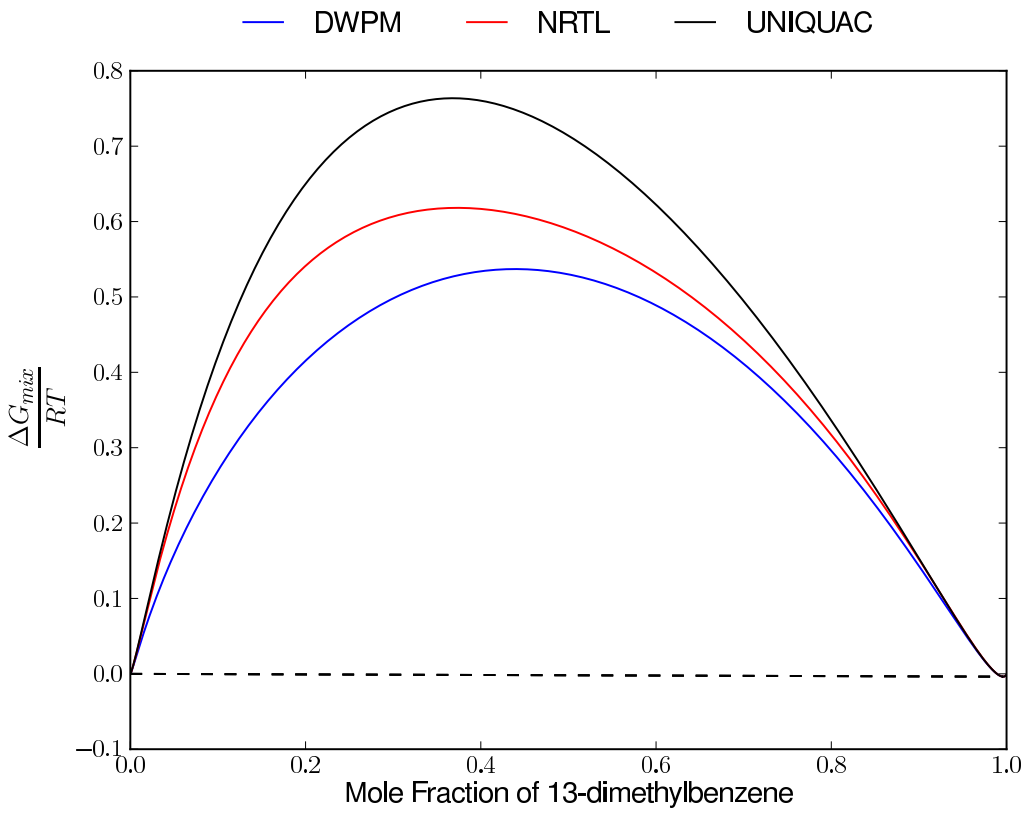

Figure 5.1.5: Calculated liquid-liquid equilibrium for 13-Dimethyl Benzene and Water at 312.85 K

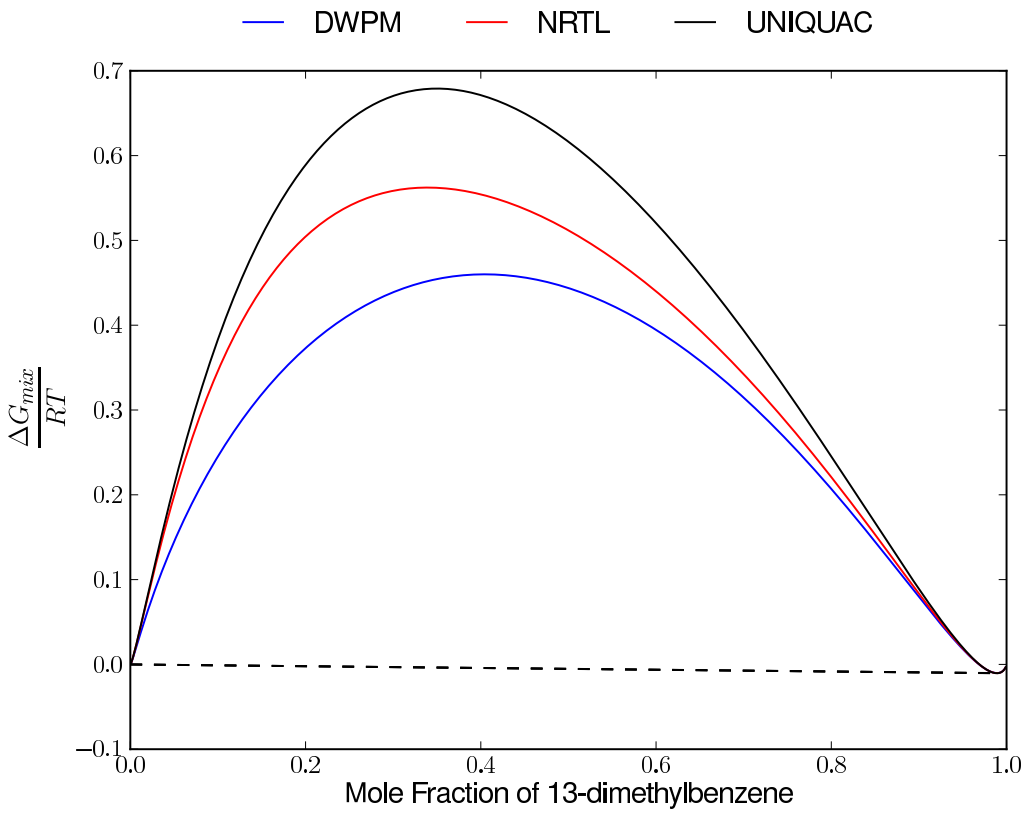

Figure 5.1.6: Calculated liquid-liquid equilibrium for 13-Dimethyl Benzene and Water at 342.85 K

Aniline and Water

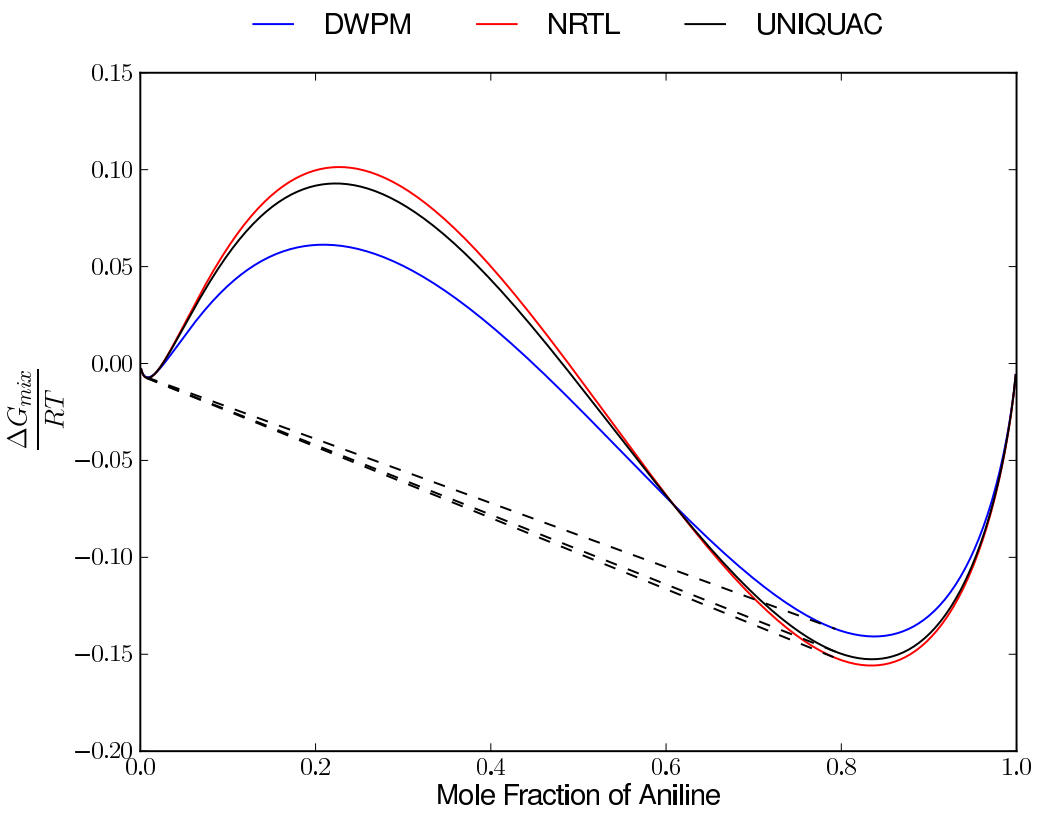

Figure 5.1.7: Calculated liquid-liquid equilibrium for Aniline and Water and Water at 281.6 K

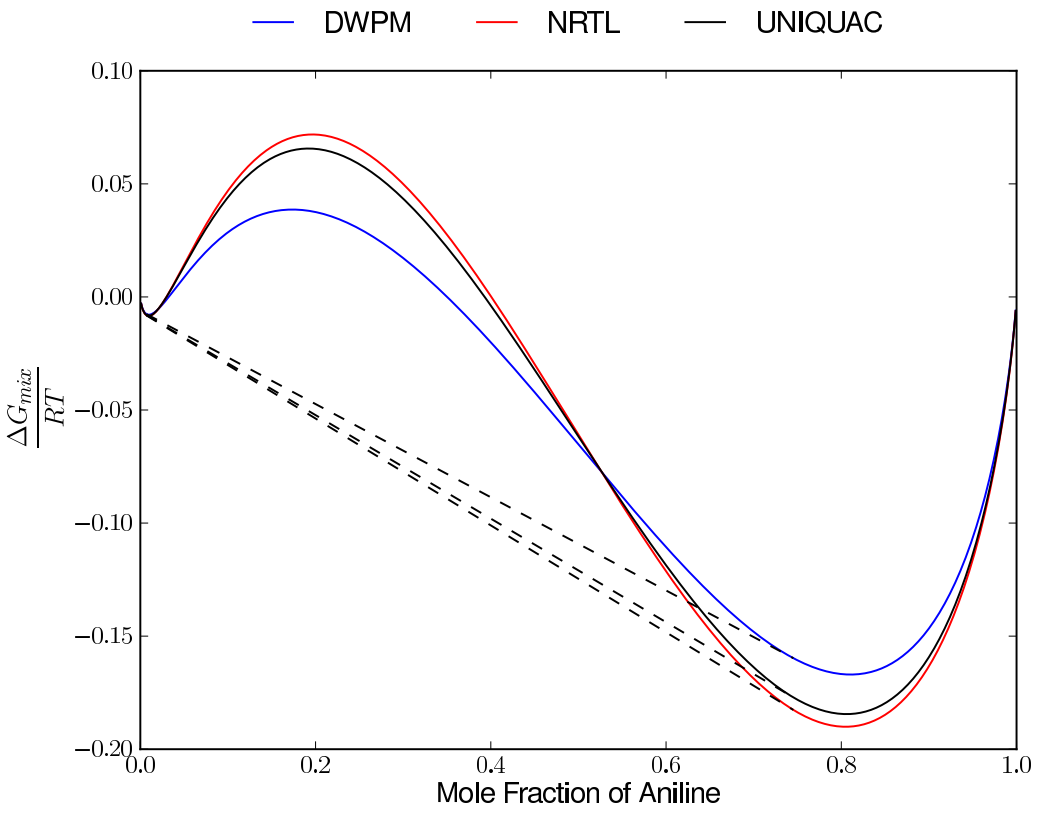

Figure 5.1.8: Calculated liquid-liquid equilibrium for Aniline and Water and Water at 298.4 K

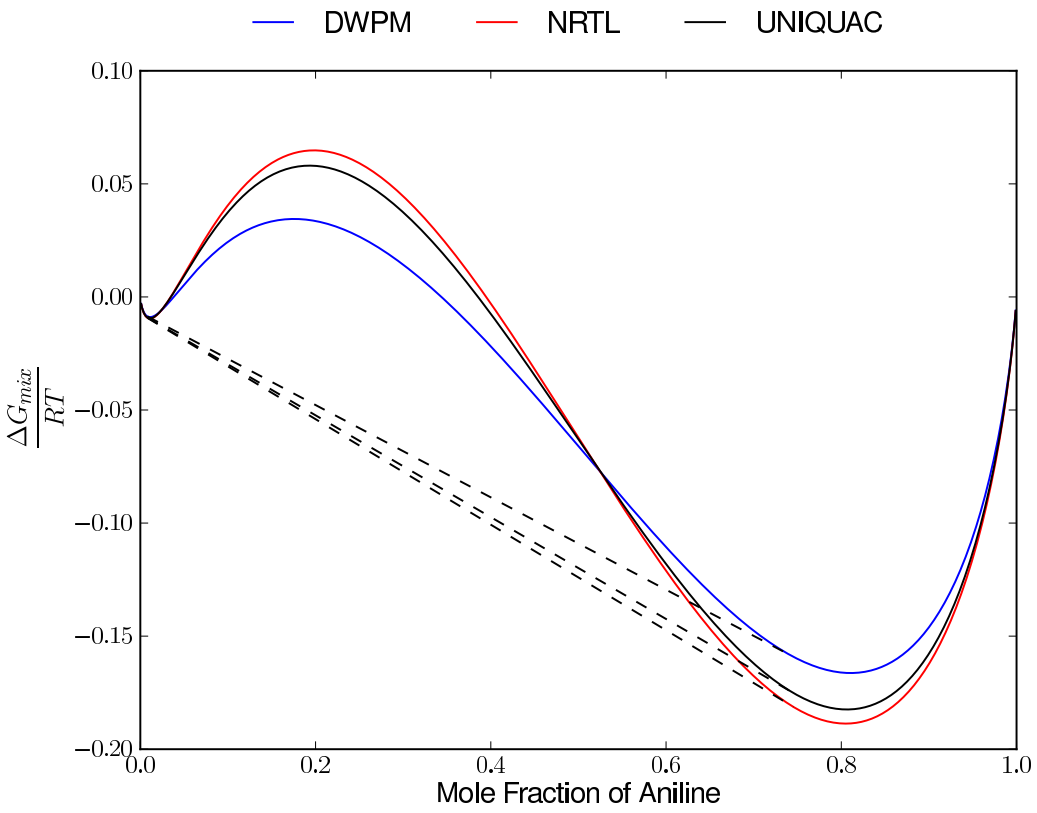

Figure 5.1.9: Calculated liquid-liquid equilibrium for Aniline and Water and Water at 321.0 K

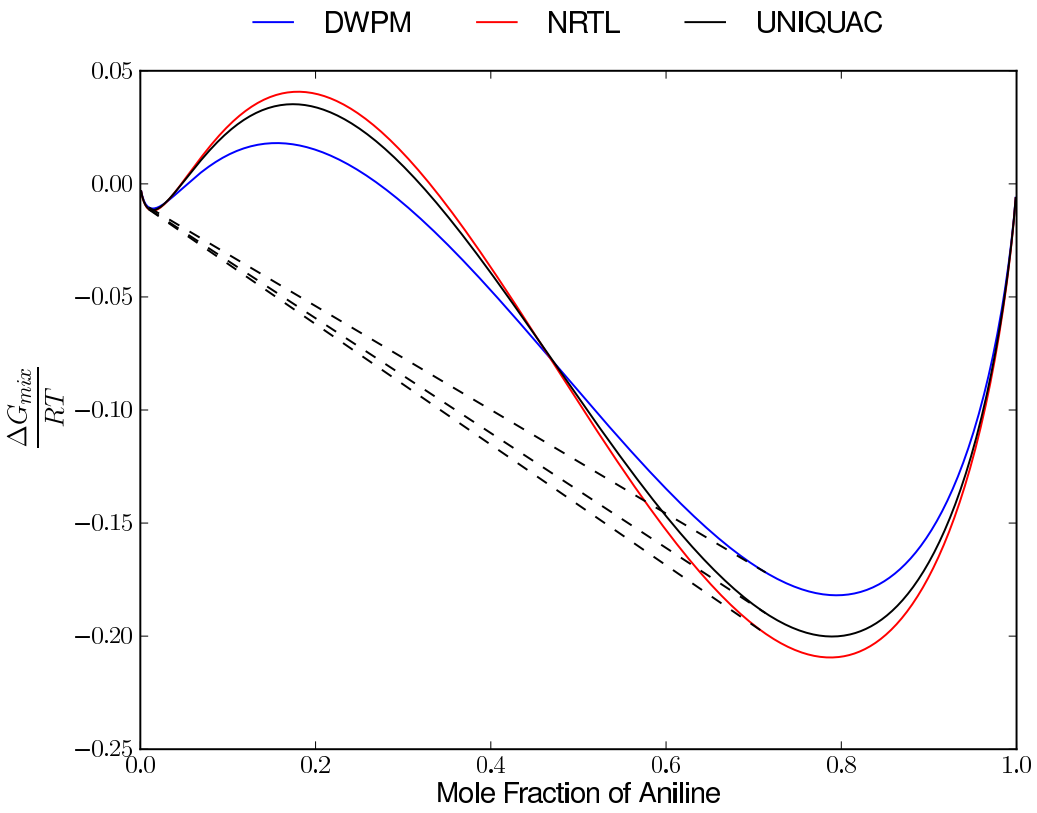

Figure 5.1.10: Calculated liquid-liquid equilibrium for Aniline and Water and Water at 339.3 K

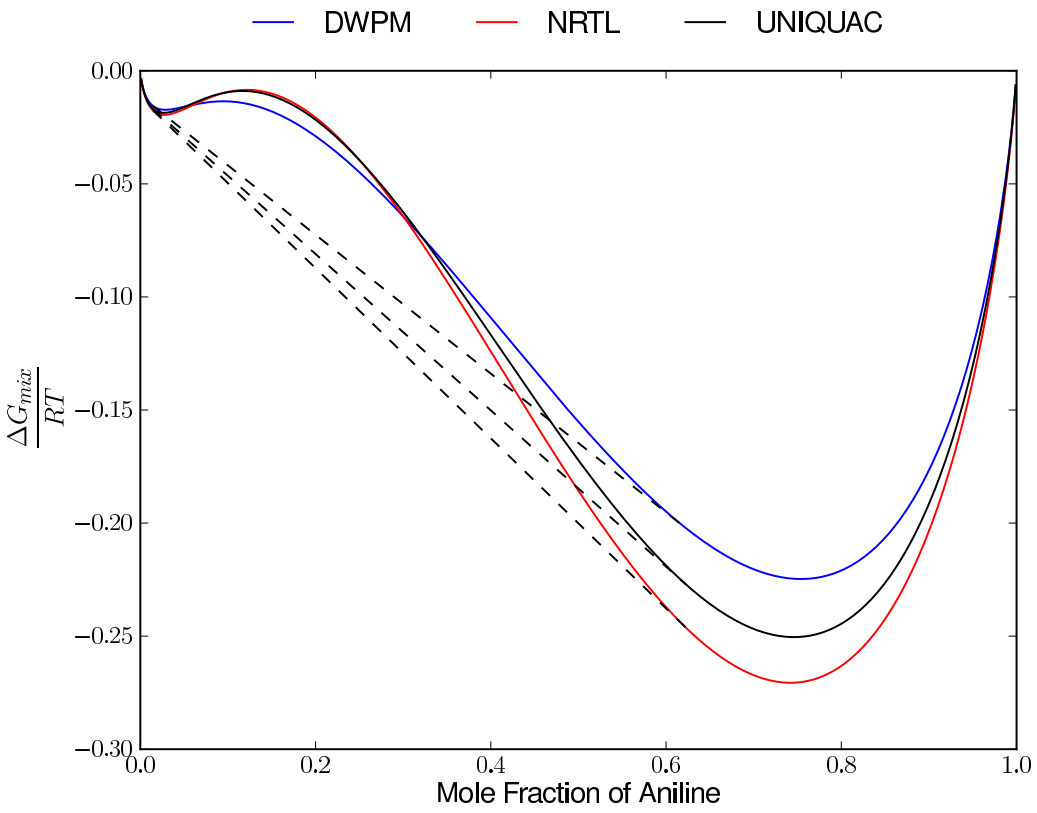

Figure 5.1.11: Calculated liquid-liquid equilibrium for Aniline and Water and Water at 369.7 K

Diethylene Glycol and 12-Dimethyl Benzene

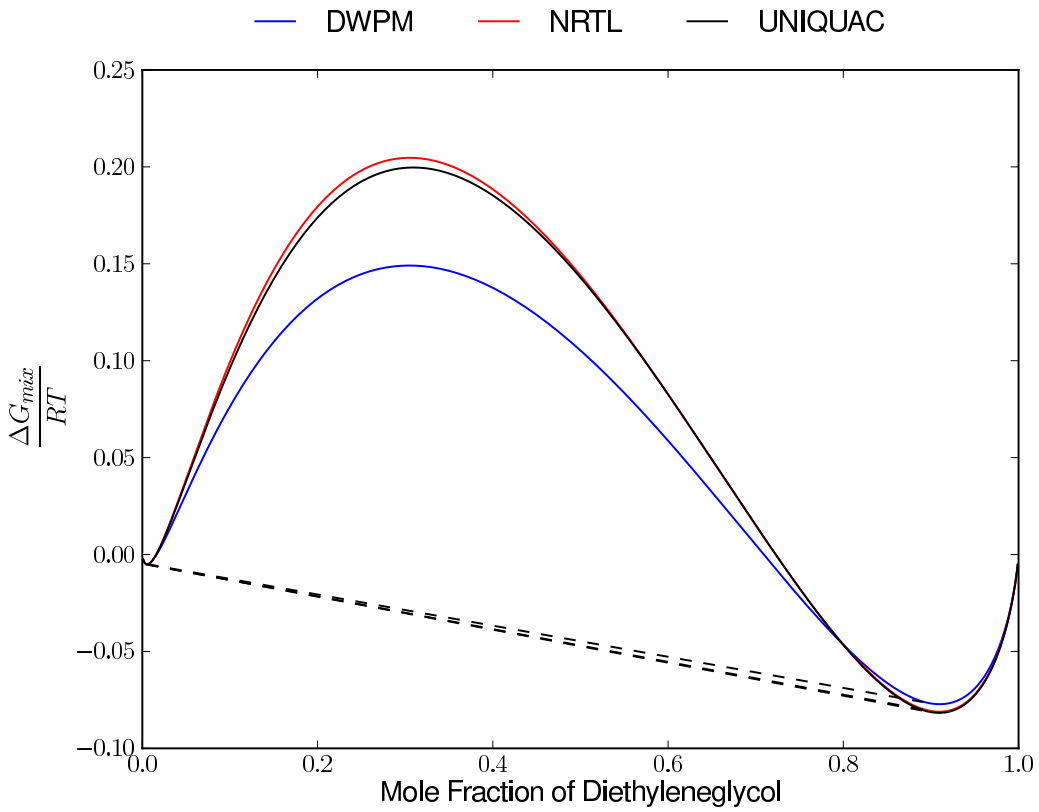

Figure 5.1.12: Calculated liquid-liquid equilibrium for Diethylene Glycol and 12-Dimethyl Benzene at 313.3 K

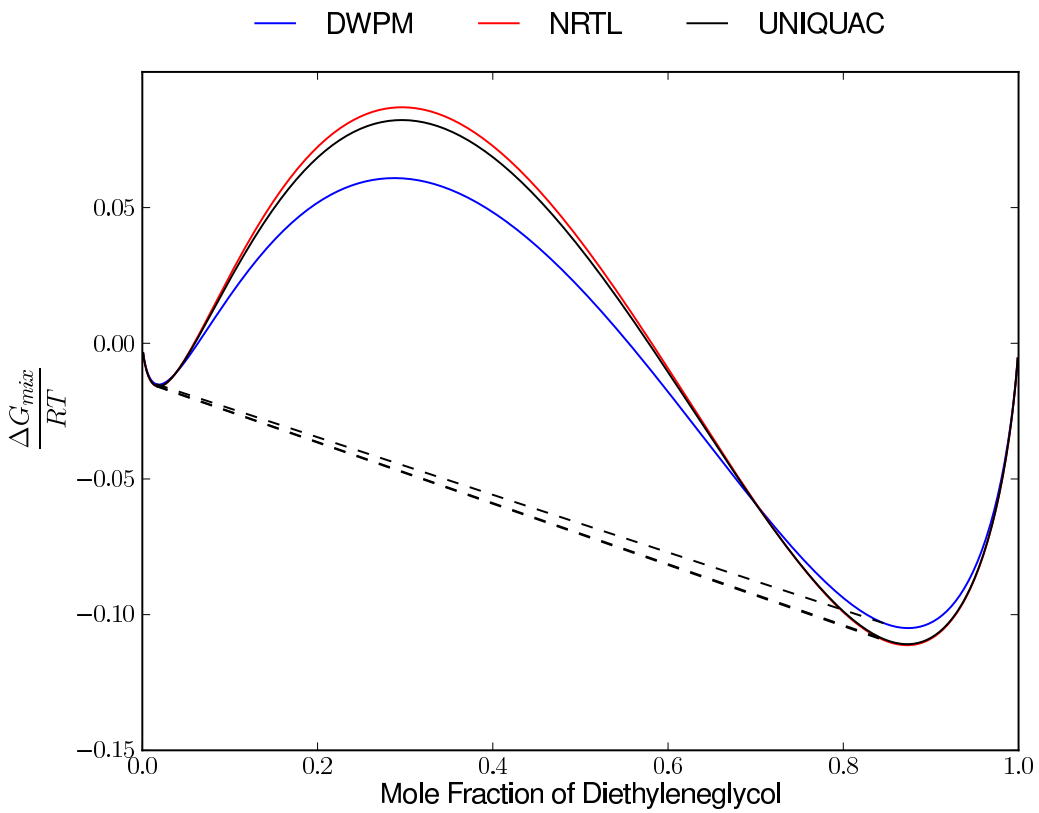

Figure 5.1.13: Calculated liquid-liquid equilibrium for Diethylene Glycol and 12-Dimethyl Benzene at 332.8 K

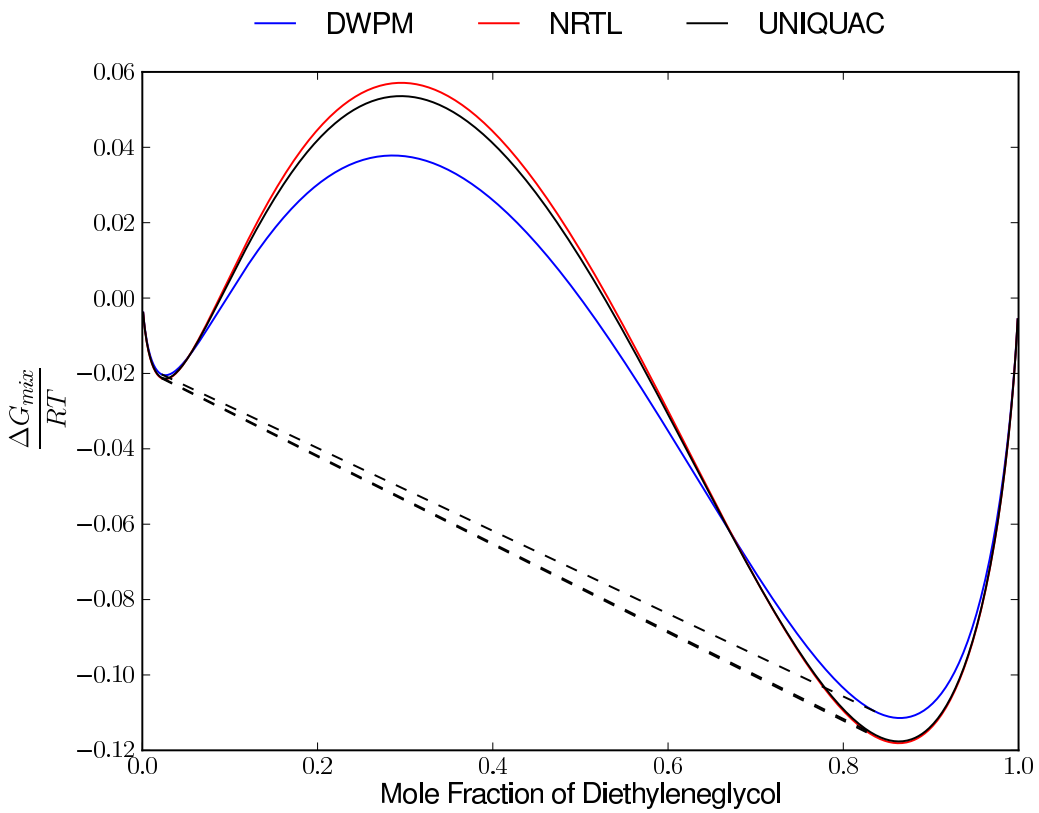

Figure 5.1.14: Calculated liquid-liquid equilibrium for Diethylene Glycol and 12-Dimethyl Benzene at 383.8 K

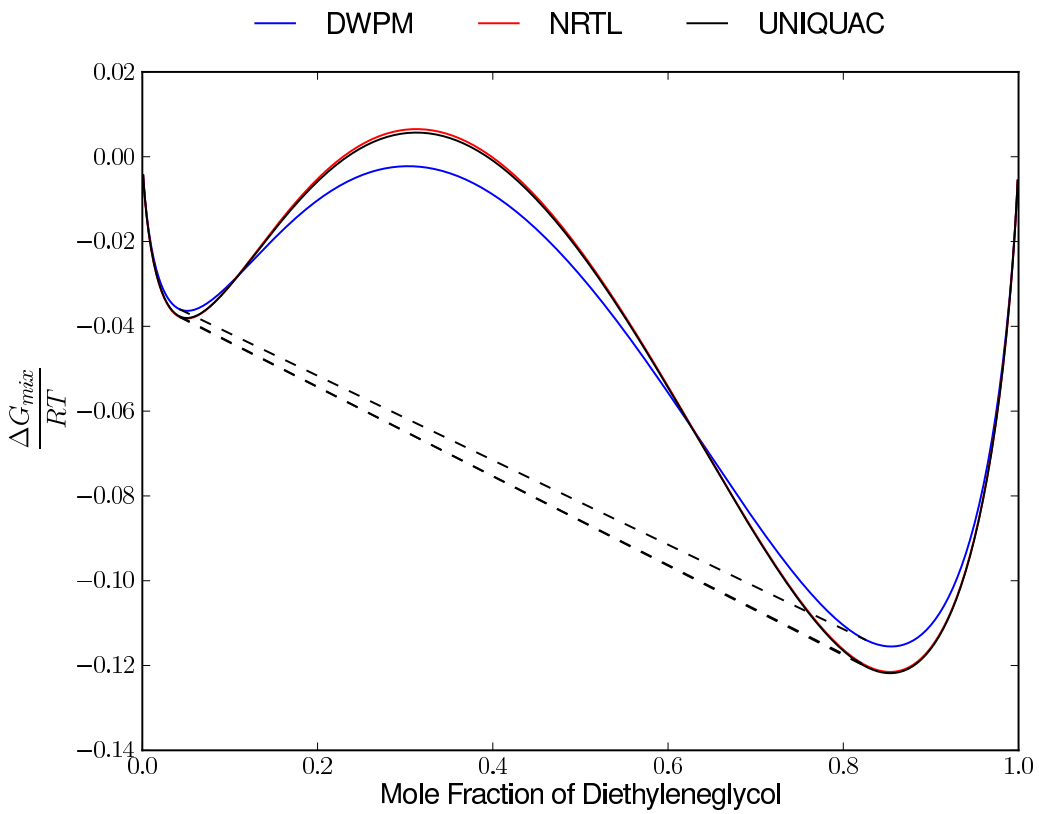

Figure 5.1.15: Calculated liquid-liquid equilibrium for Diethylene Glycol and 12-Dimethyl Benzene at 363.0 K

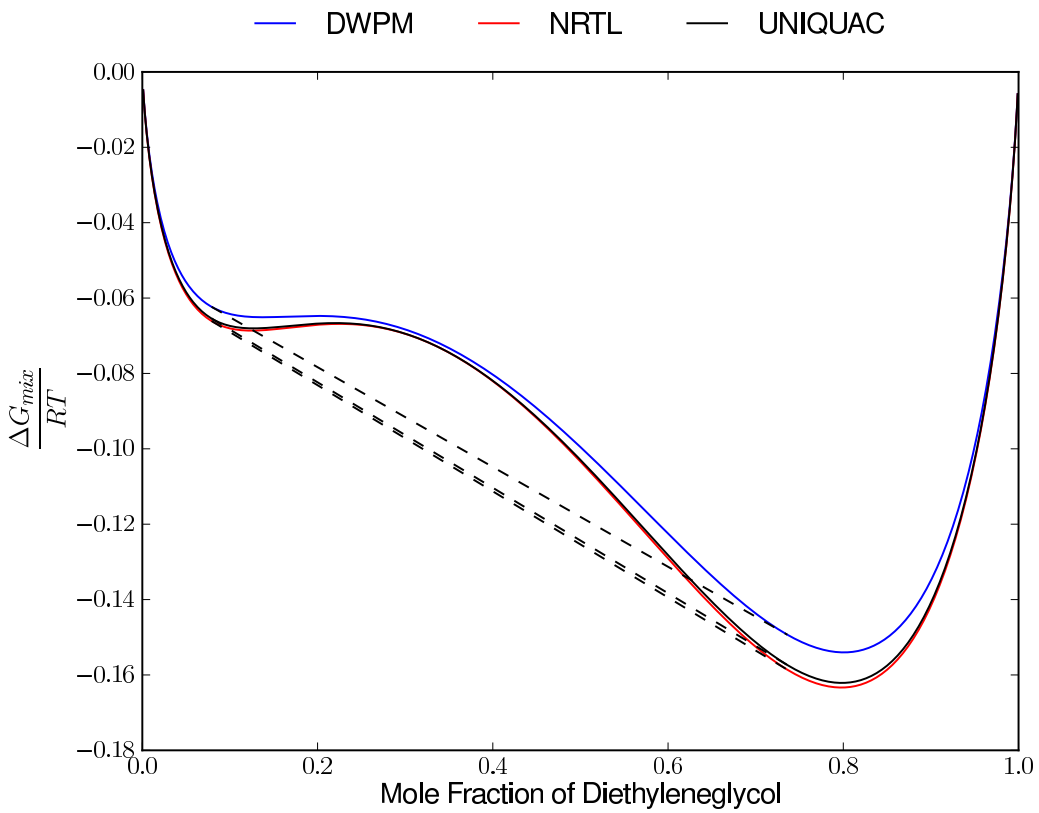

Figure 5.1.16: Calculated liquid-liquid equilibrium for Diethylene Glycol and 12-Dimethyl Benzene at 393.0 K

Dipropyl Ether and Water

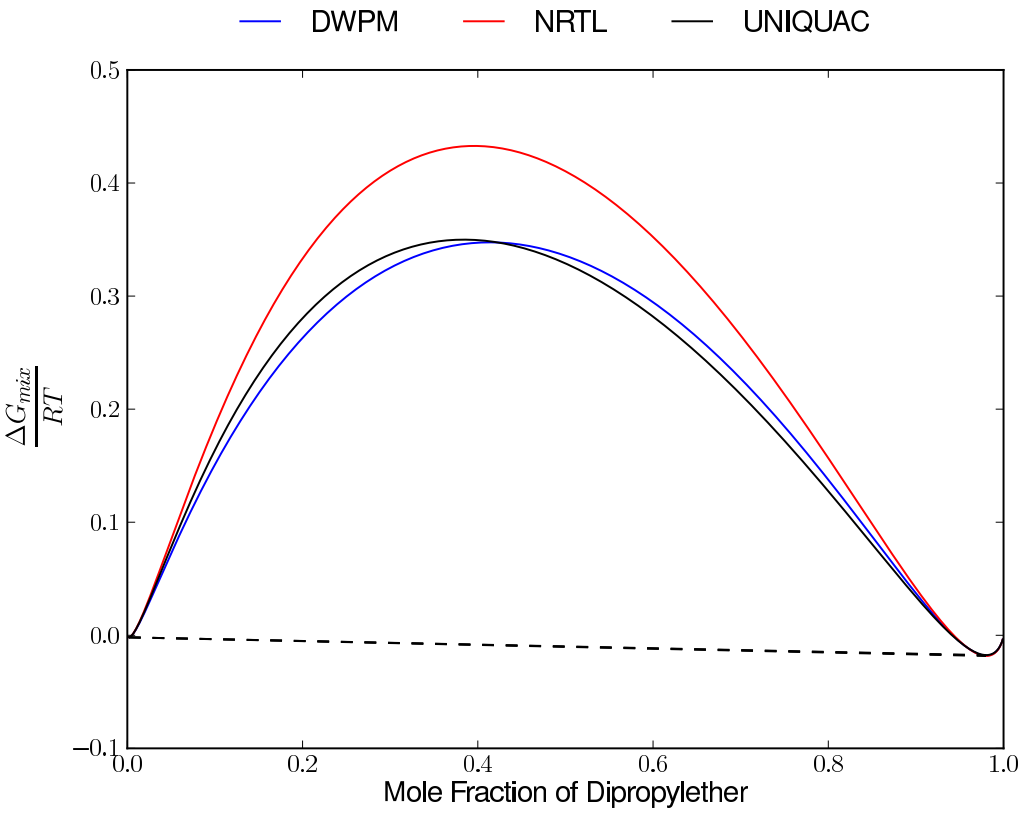

Figure 5.1.17: Calculated liquid-liquid equilibrium for Dipropyl Ether and Water at 273.0 K

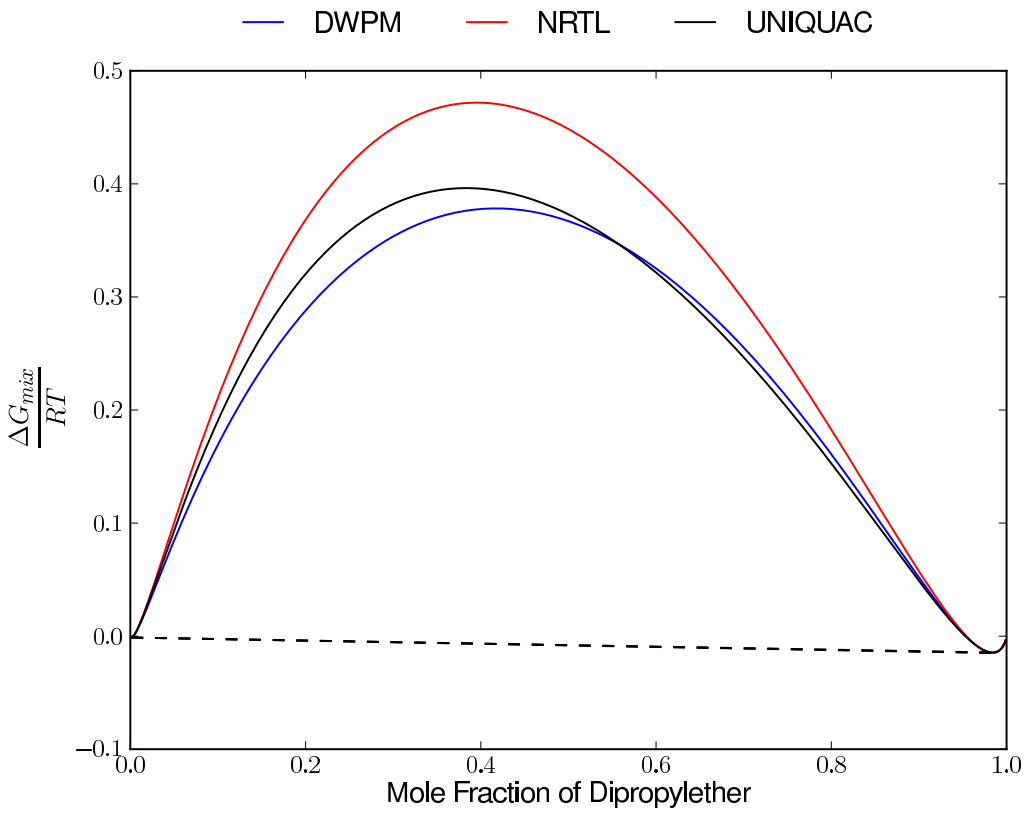

Figure 5.1.18: Calculated liquid-liquid equilibrium for Dipropyl Ether and Water at 283.0 K

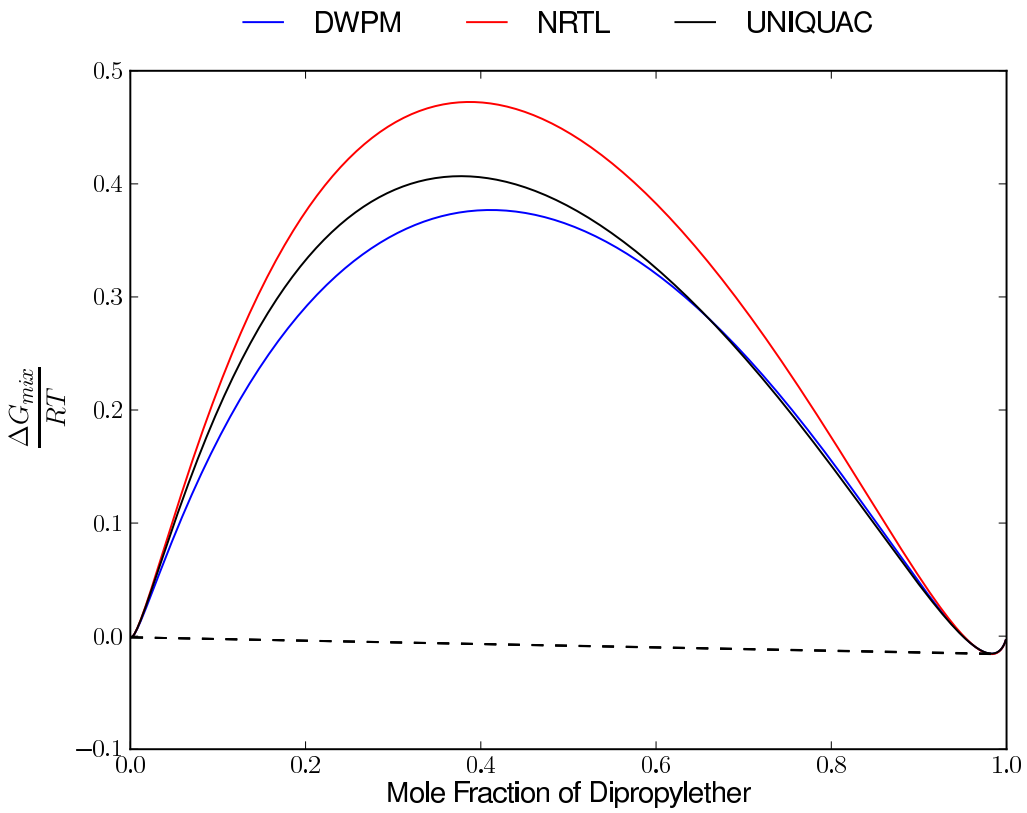

Figure 5.1.19: Calculated liquid-liquid equilibrium for Dipropyl Ether and Water at 288.0 K

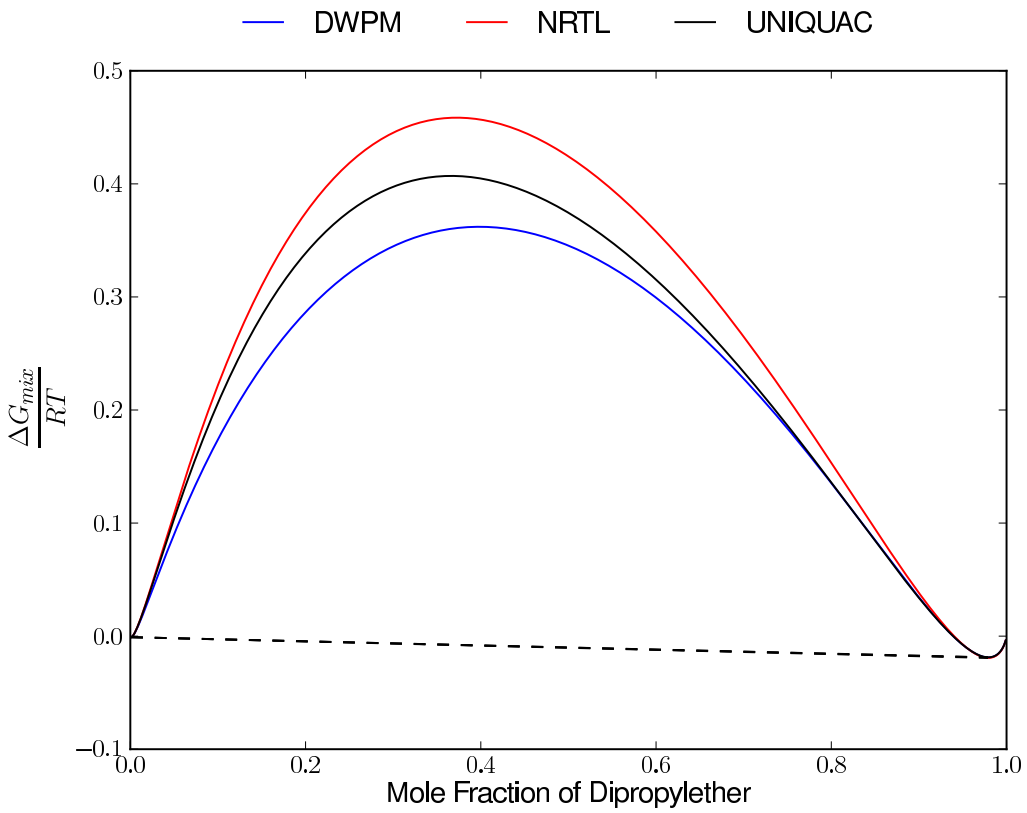

Figure 5.1.20: Calculated liquid-liquid equilibrium for Dipropyl Ether and Water at 293.0 K

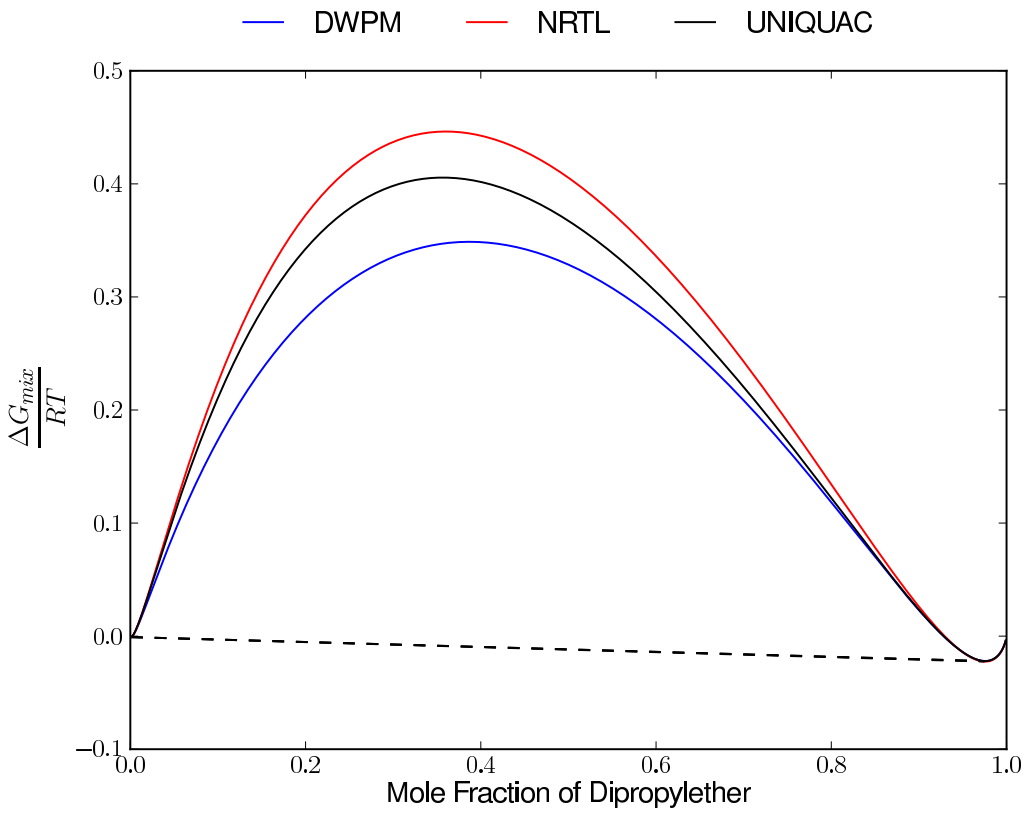

Figure 5.1.21: Calculated liquid-liquid equilibrium for Dipropyl Ether and Water at 298.0 K

Ethyl Ester Acetic Acid and Water

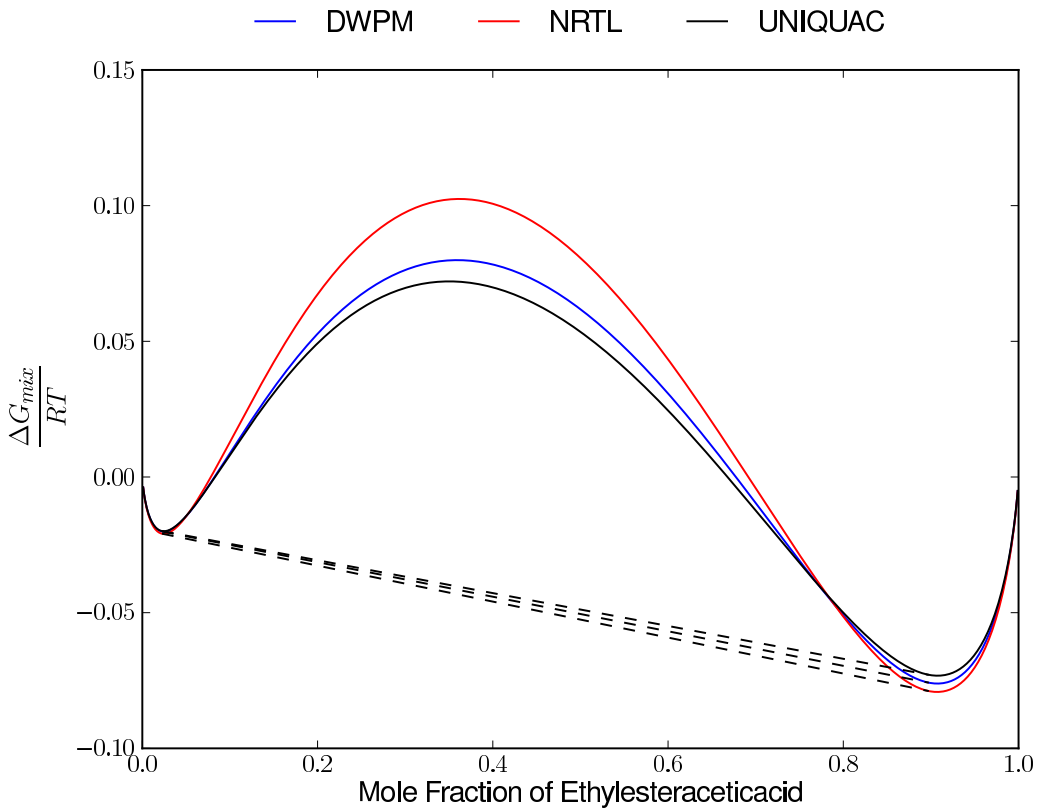

Figure 5.1.22: Calculated liquid-liquid equilibrium for Ethyl Ester Acetic Acid and Water at 273.0 K

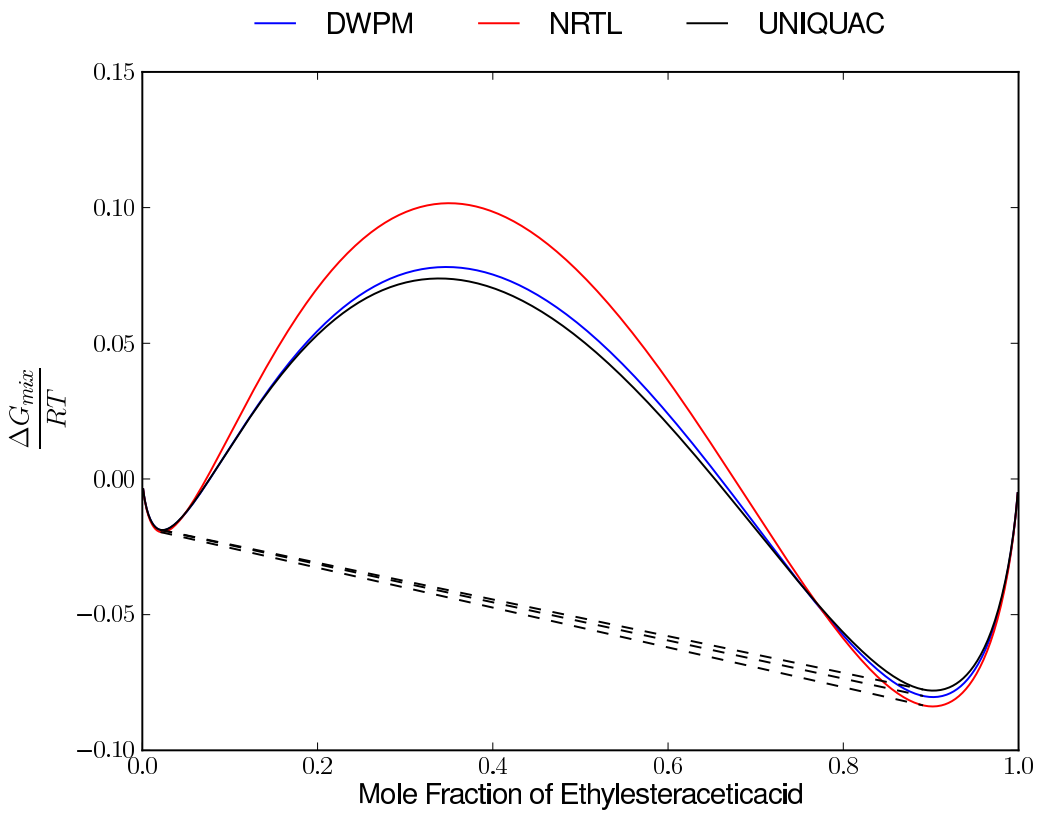

Figure 5.1.23: Calculated liquid-liquid equilibrium for Ethyl Ester Acetic Acid and Water at 278.0 K

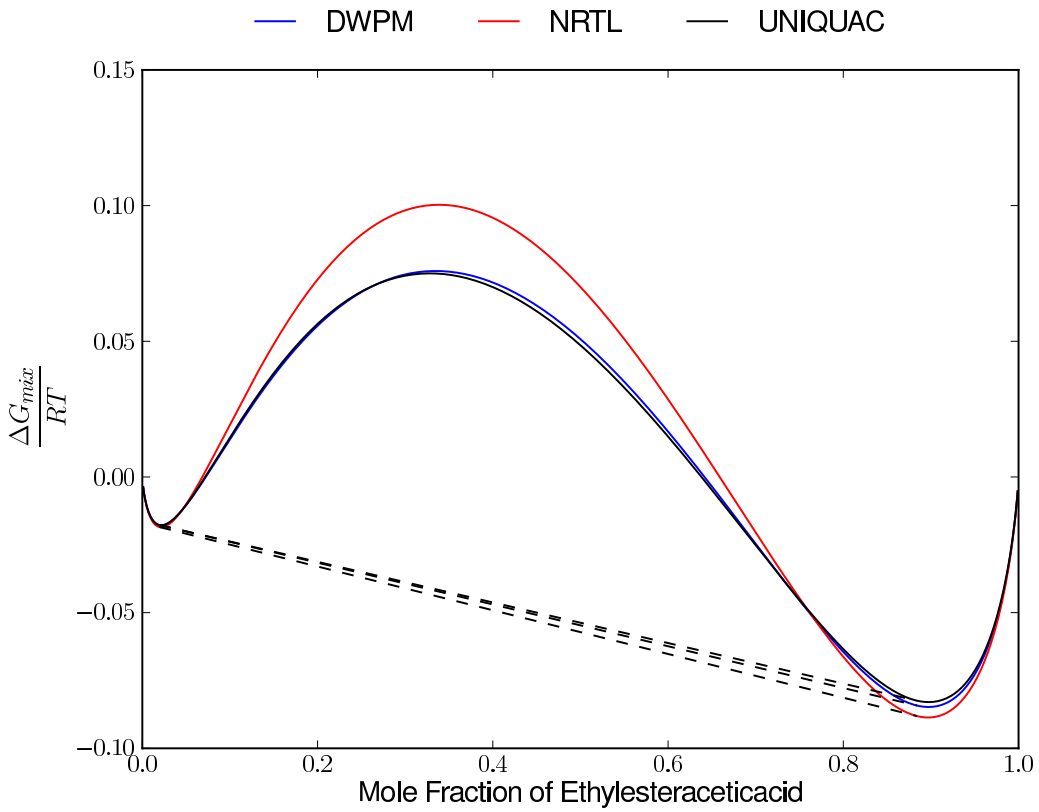

Figure 5.1.24: Calculated liquid-liquid equilibrium for Ethyl Ester Acetic Acid and Water at 283.0 K

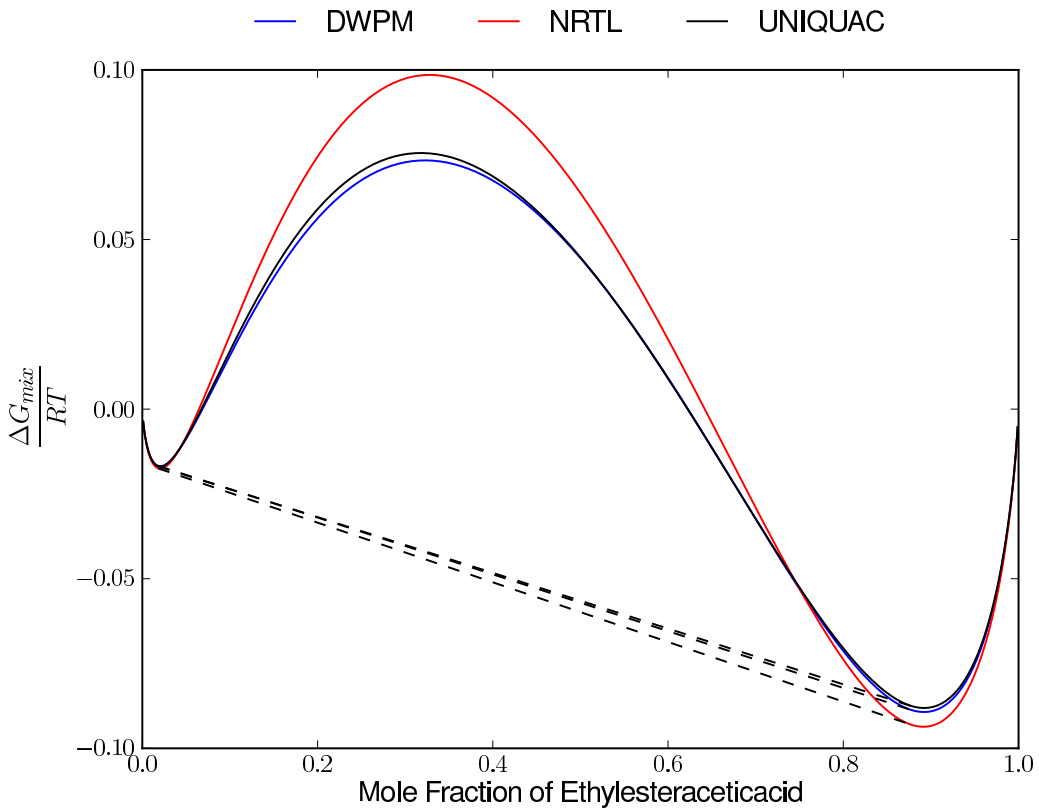

Figure 5.1.25: Calculated liquid-liquid equilibrium for Ethyl Ester Acetic Acid and Water at 288.0 K

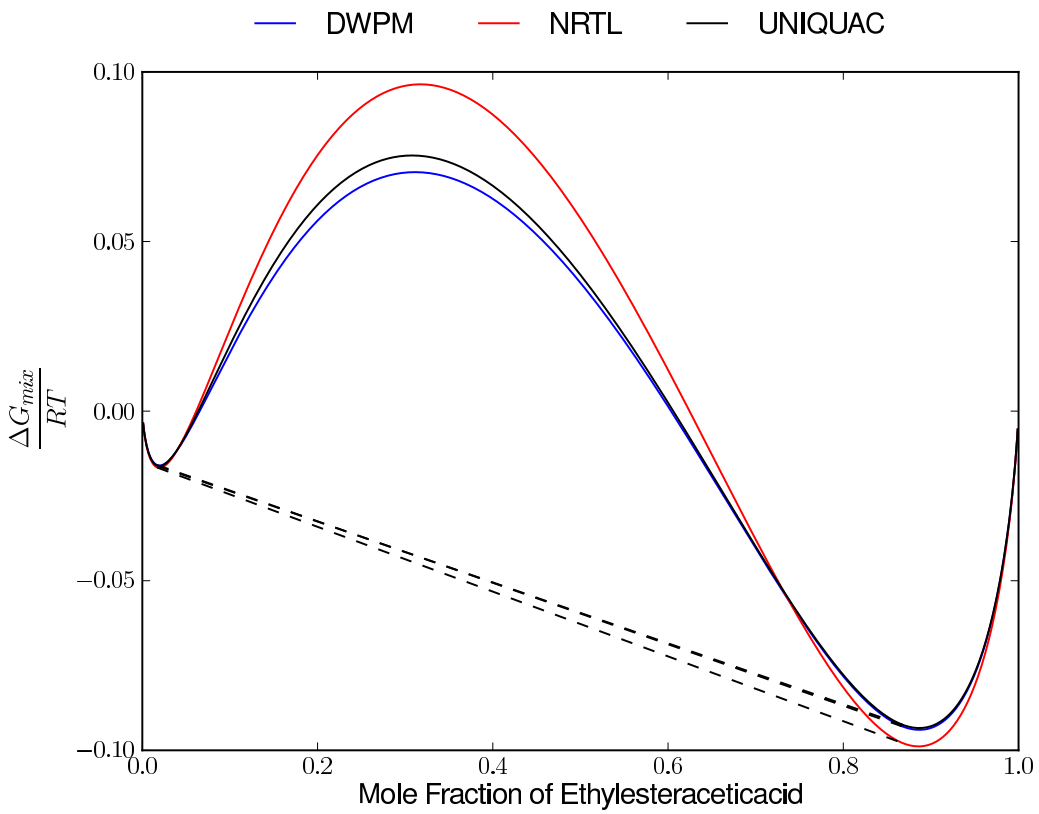

Figure 5.1.26: Calculated liquid-liquid equilibrium for Ethyl Ester Acetic Acid and Water at 293.0 K

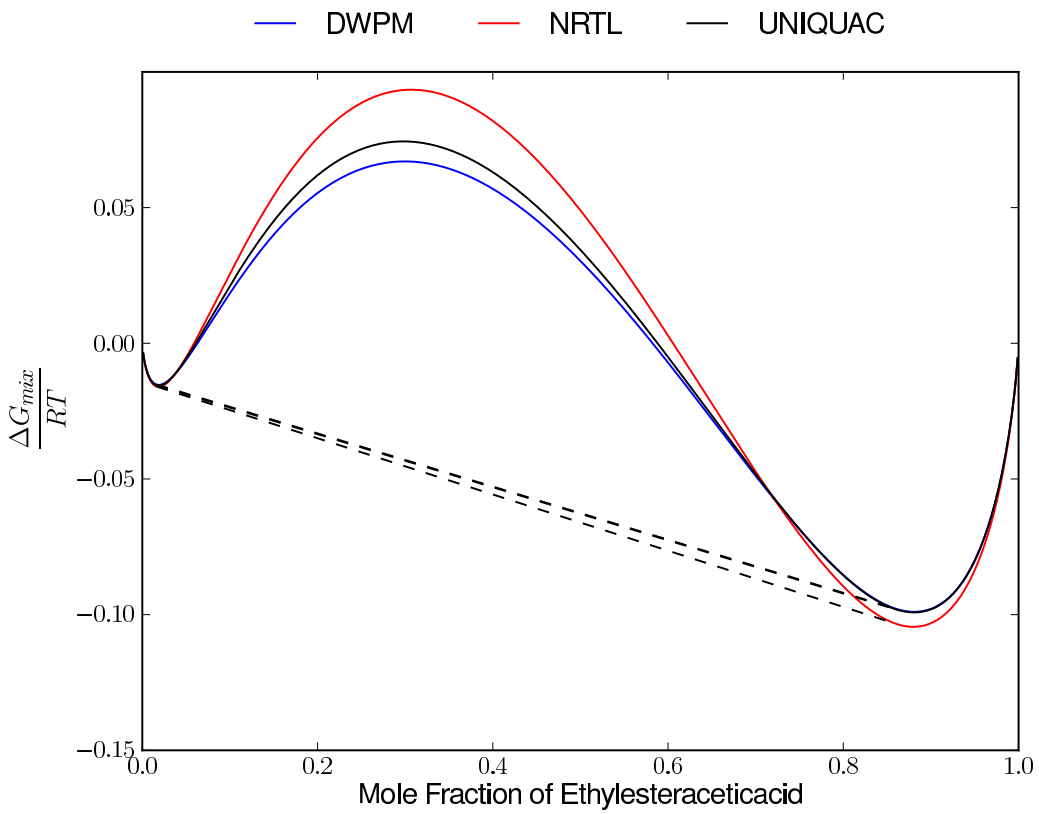

Figure 5.1.27: Calculated liquid-liquid equilibrium for Ethyl Ester Acetic Acid and Water at 298.0 K

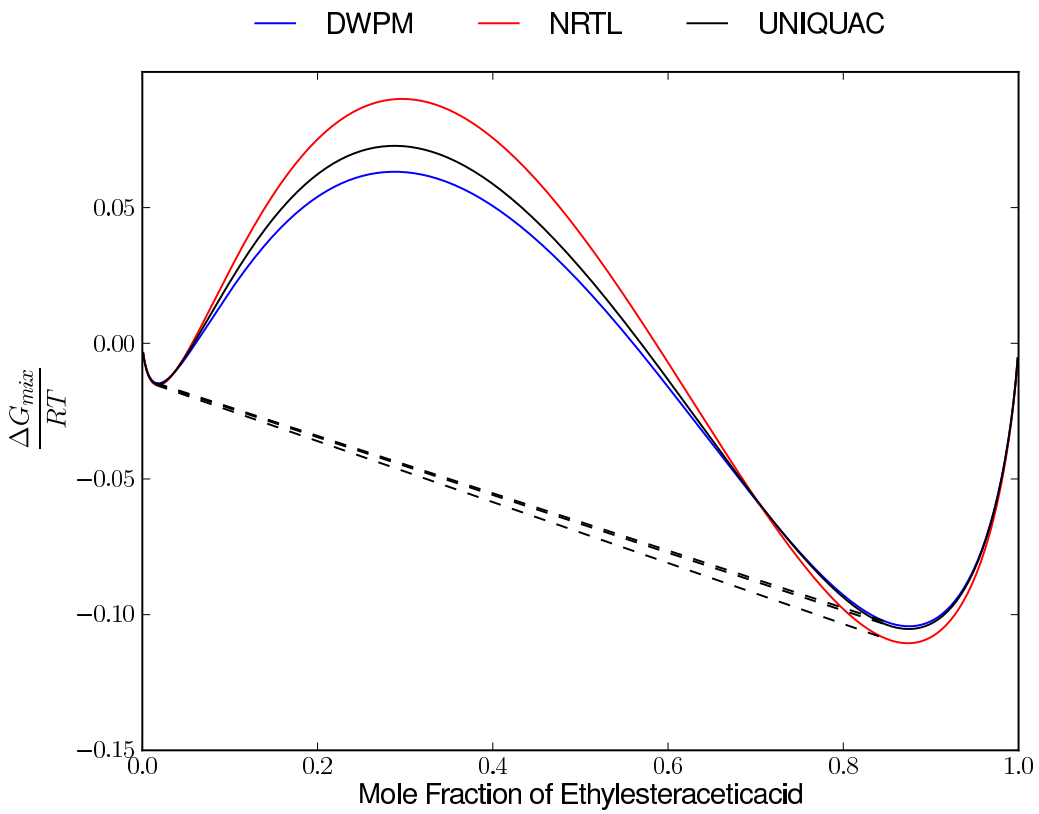

Figure 5.1.28: Calculated liquid-liquid equilibrium for Ethyl Ester Acetic Acid and Water at 303.0 K

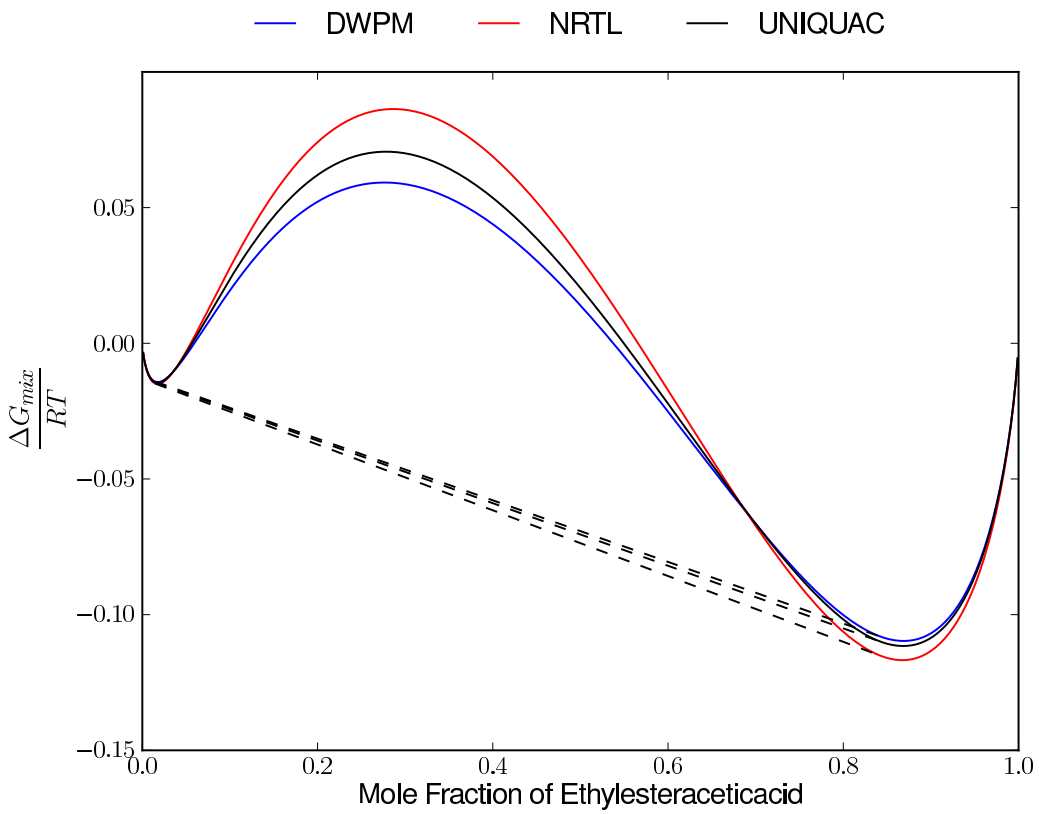

Figure 5.1.29: Calculated liquid-liquid equilibrium for Ethyl Ester Acetic Acid and Water at 308.0 K

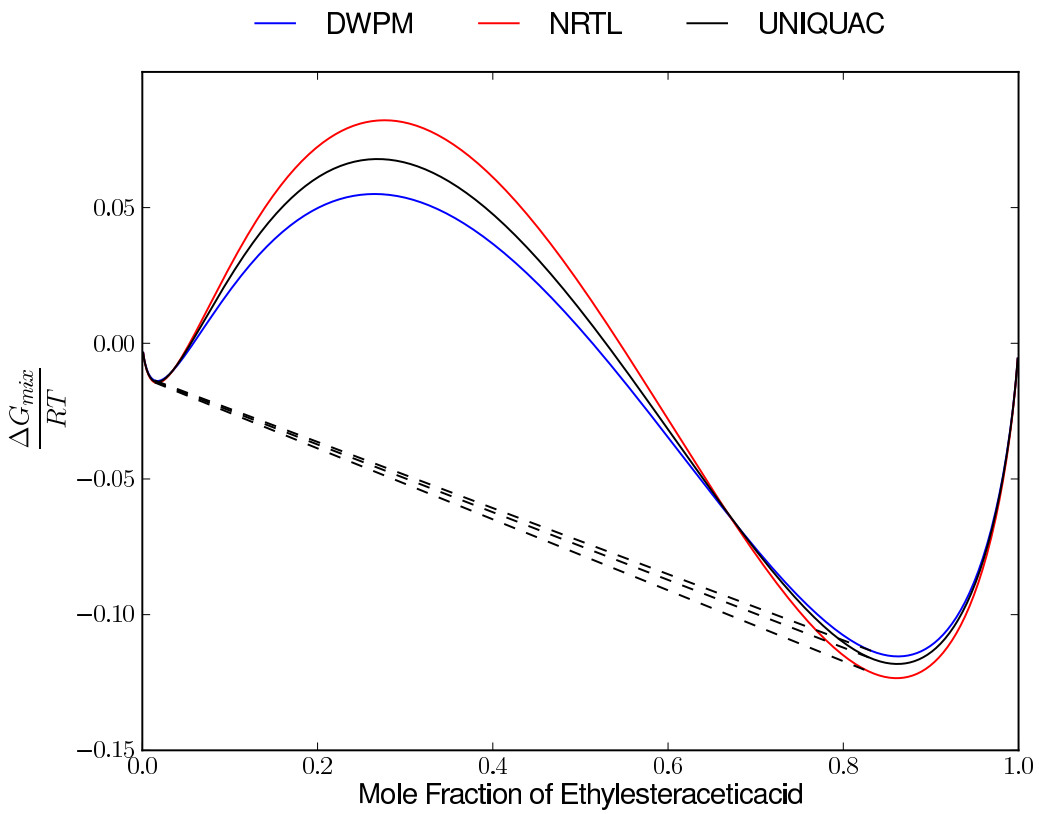

Figure 5.1.30: Calculated liquid-liquid equilibrium for Ethyl Ester Acetic Acid and Water at 313.0 K

Methanol and Heptane

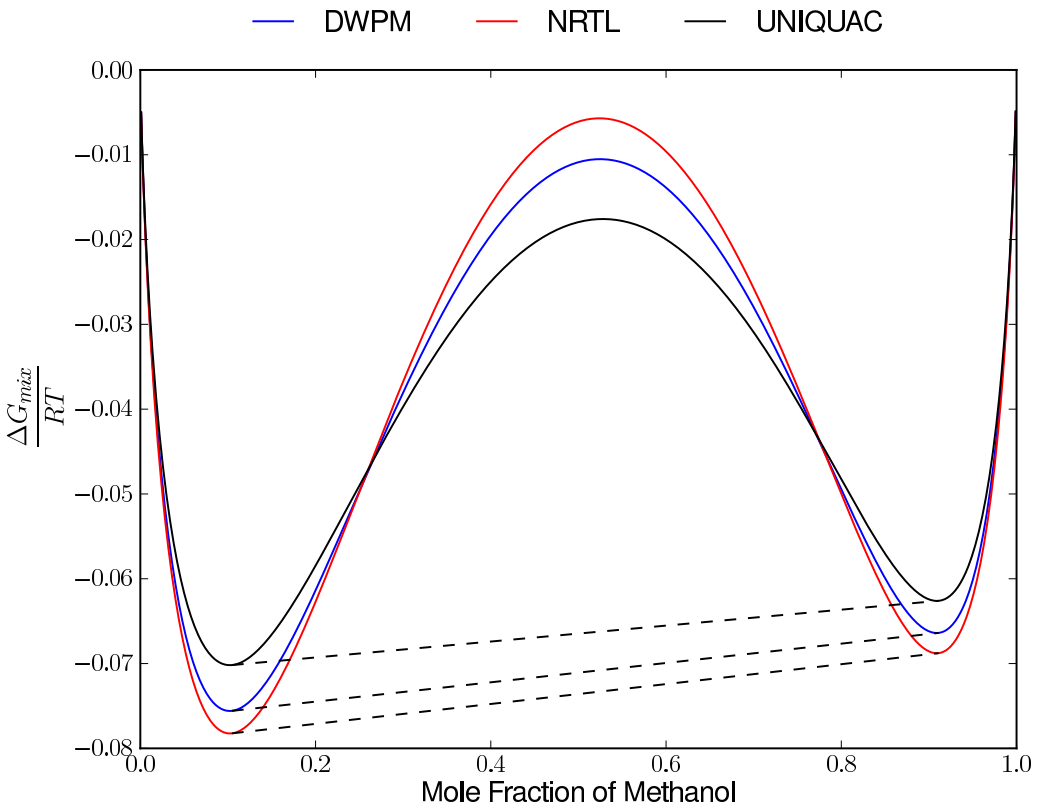

Figure 5.1.31: Calculated liquid-liquid equilibrium for Methanol and Heptane at 291.0 K

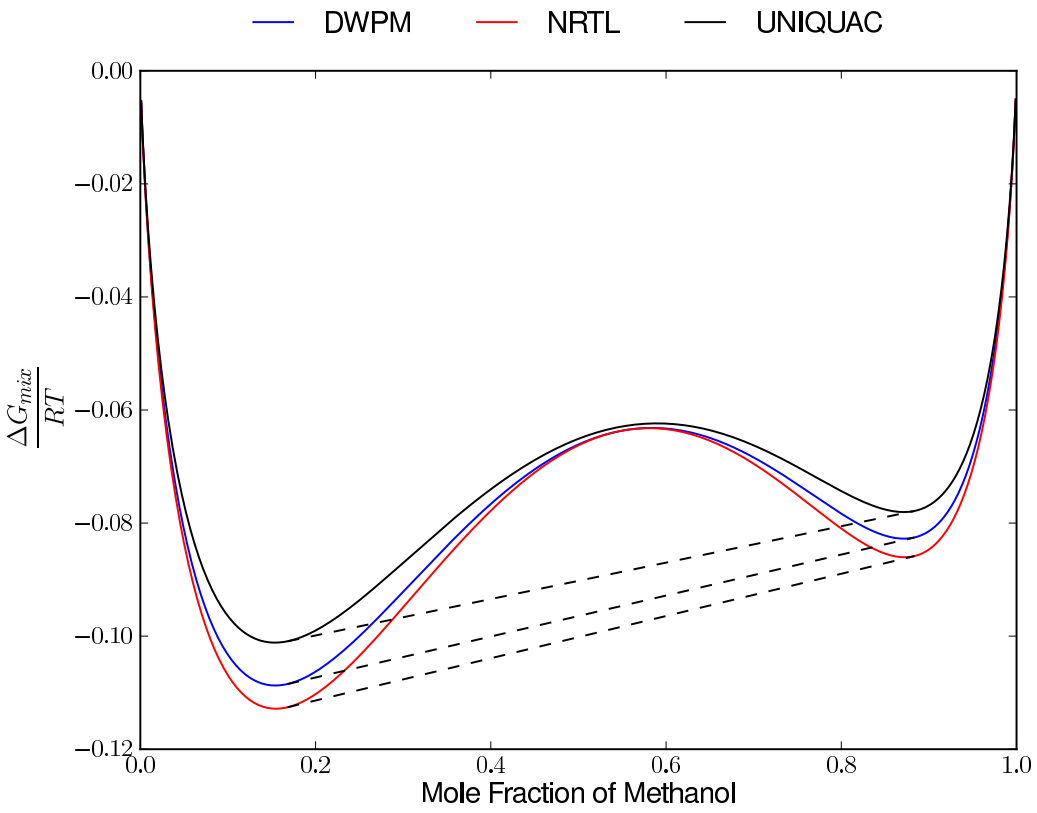

Figure 5.1.32: Calculated liquid-liquid equilibrium for Methanol and Heptane at 303.0 K

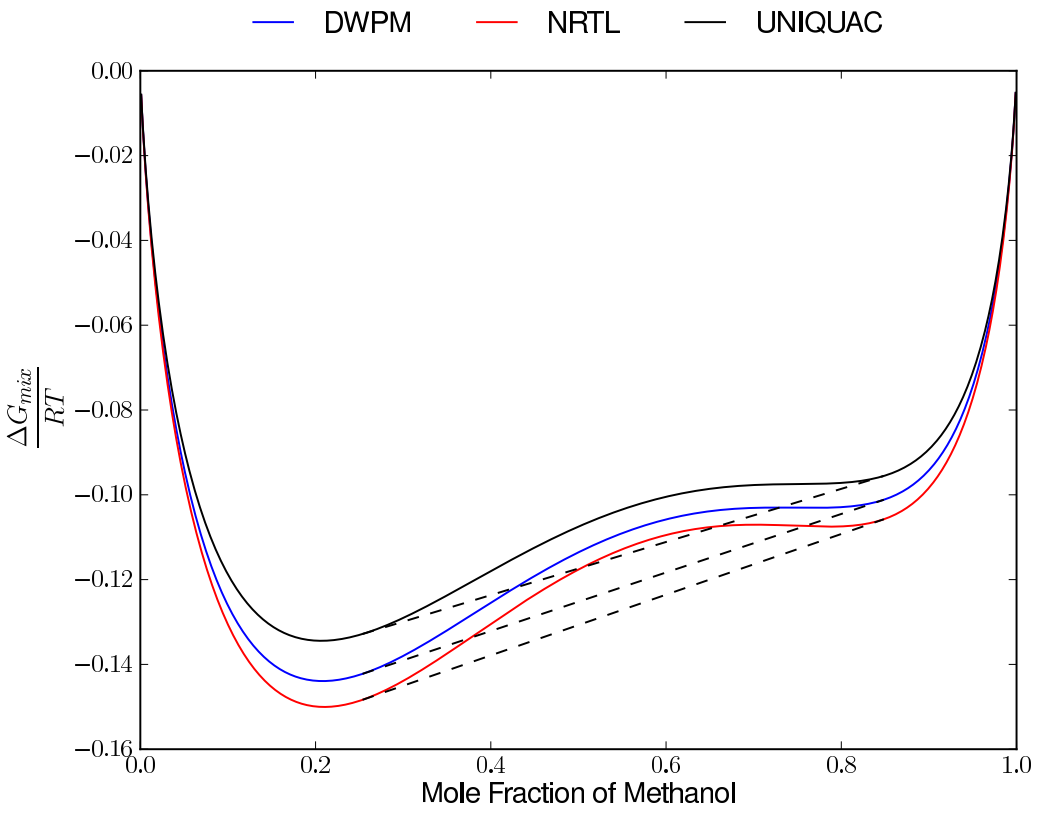

Figure 5.1.33: Calculated liquid-liquid equilibrium for Methanol and Heptane at 313.0 K

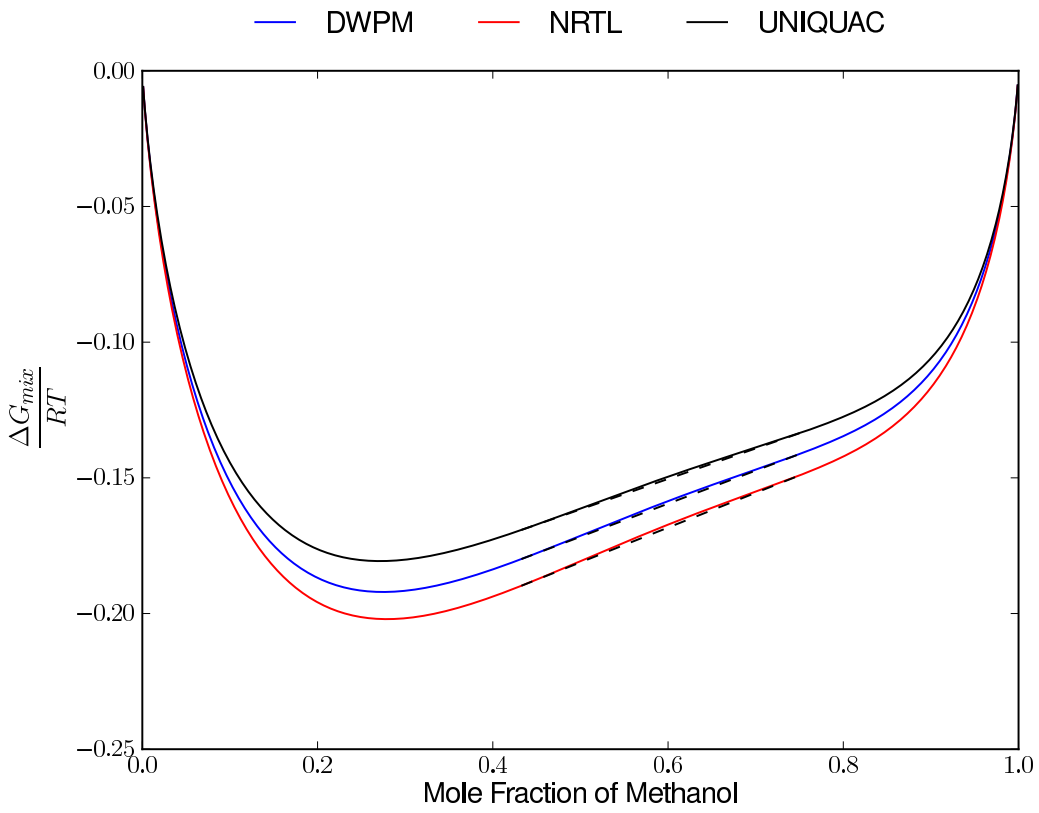

Figure 5.1.34: Calculated liquid-liquid equilibrium for Methanol and Heptane at 323.0 K

Methanol and Hexane

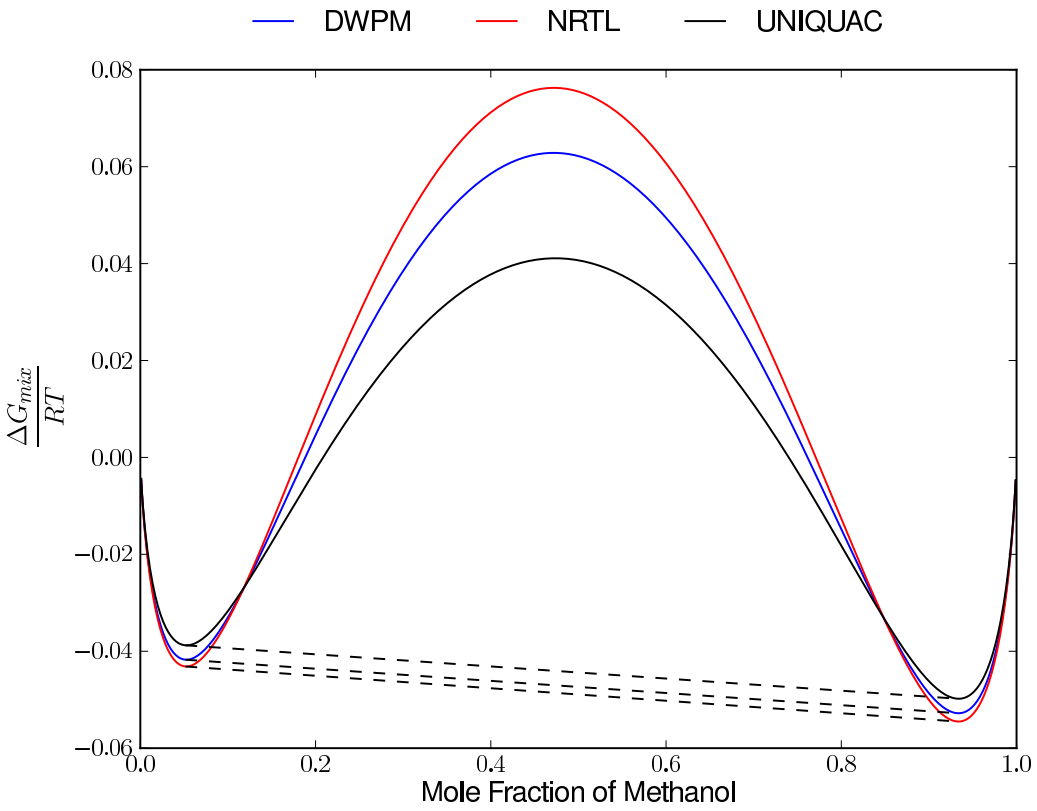

Figure 5.1.35: Calculated liquid-liquid equilibrium for Methanol and Hexane at 255.2 K

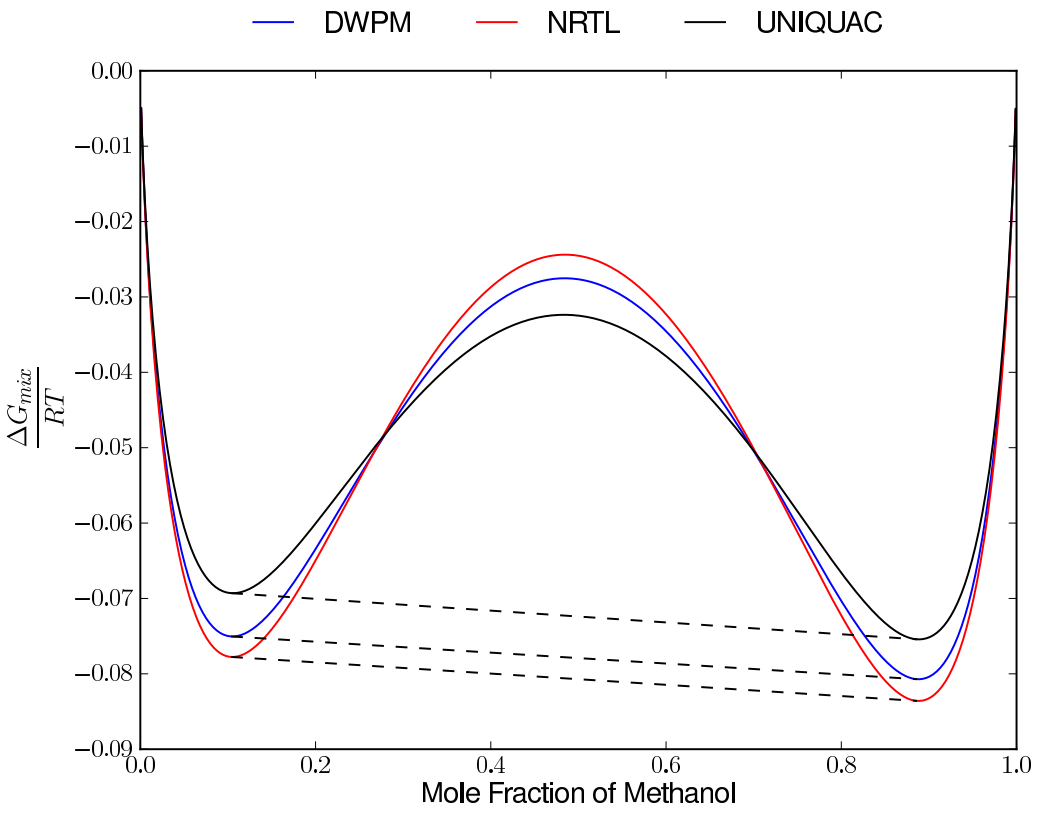

Figure 5.1.36: Calculated liquid-liquid equilibrium for Methanol and Hexane at 278.0 K

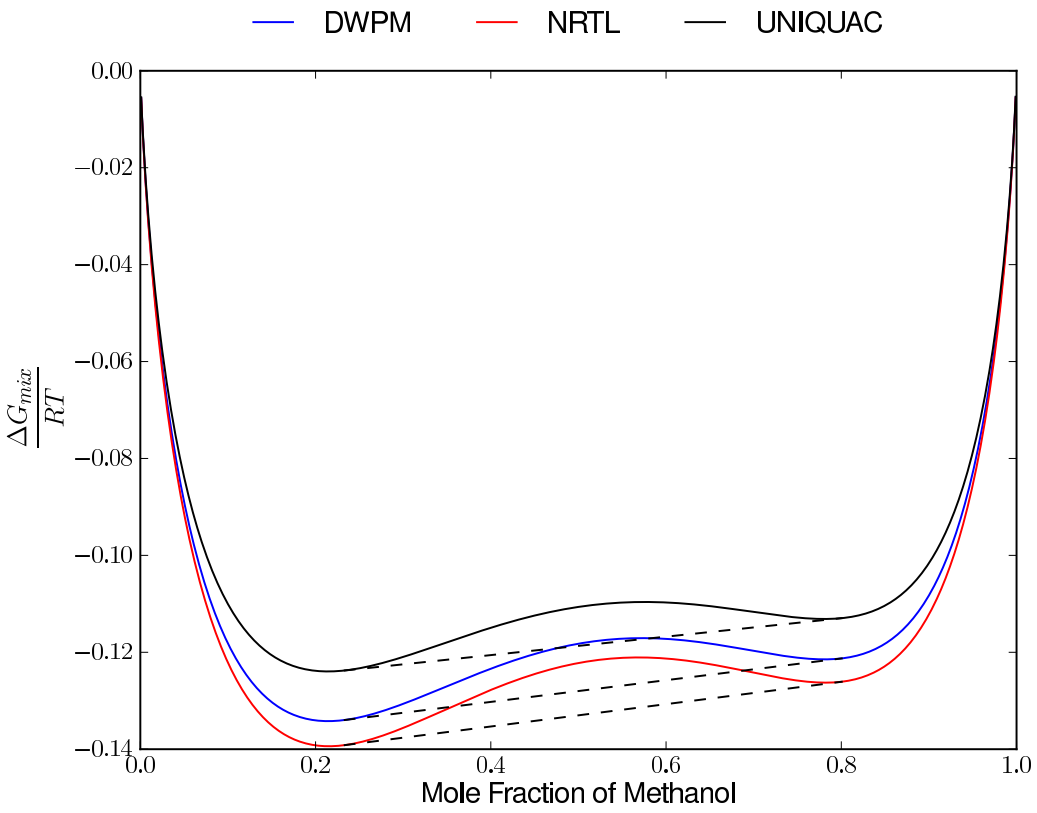

Figure 5.1.37: Calculated liquid-liquid equilibrium for Methanol and Hexane at 298.0 K

Acknowledgements

Bibliography

[1] D. S. Abrams and J. M. Prausnitz. Statistical thermodynamics of liquid mixtures: A new expression for the excess gibbs energy of partly or completely miscible systems. *AIChE*, 21 (1):116, 1975.

[2] Y. Adachi and B.C.Y. Lu. Simplest equation of state for vapour-liquid equilibrium: A modification of the van der waals equation. *AIChE*, 1984.

[3] T. F. Anderson and J. M. Prausnitz. Application of the uniquac equation to calculation of multicomponent phase equilibria 1. vapour-liquid equilibria. *Ind.Eng.Chem.Process Des.Dev.*, 17(4):552, 1978.

[4] M. J. Assael, J. P. M. Trusler, and T. F. Tsolakis. *Thermophysical Properties of Fluids: An Introduction to Their Prediction*. Imperial College Press, 1996.

[5] G.M. Bennet and W.G. Philip. The influence of structure on the solubilities of ethers. part ii. some cyclic ethers. *J.Chem.Soc*, page 1930, 1928.

[6] G. M. Bollas, P. I. Barton, and A. Mitsos. Bilevel optimization formulation for parameter estimation in vapour-liquid(-liquid) phase equilibrium problems. *Chemical Engineering Science*, 64:1768–1783, 2009.

[7] R.L. Burden and J.D. Faires. *Numerical Analysis*. Brooks/Cole Cenage Learning, 2005.

[8] A.N. Campbell. The system aniline-phenol-water. *J.Am.Chem.Soc.*, 67:981, 1945.

[9] F.S. Chernoglazova and Yu.N. Simulin. Mutual solubility in the system m-xylene-water. *Zh.Fiz.Khim.*, 50:809, 1976.

[10] Y. Demirel and H. O. Paksoy. Calculations of thermodynamic derivative properties from the nrtl and uniquac models. *Thermochimica Acta*, 303:129–136, 1997.

[11] W. W. Focke. Weighted-power-mean mixture model for the gibbs energy of fluid mixtures. *Ind.Eng.Chem.Res.*, 48:5537–5541, 2009.

[12] A.P. Foucault, P. Durand, E. Camacho Frias, and F. Le Goffic. Biphasic mixture of water, dimethyl sulfoxide, and tetrahydrofuran for use in centrifugal partition chromatography. *Anal.Chem.*, 65:2150, 1993.

[13] P.M. Ginnings and R. Webb. Aqueous solubilities of some isomeric hexanols. *J.Am.Chem.Soc.*, 60(6):1388, 1938.

[14] H. Huang and S. I. Sandler. Prediction of vapour-liquid equilibria at high pressures using activity coefficient parameters obtained from low-pressure data: A comparison of two equation of state mixing rules. *Ind.Eng.Chem.Res.*, 32:1498–1503, 1993.

[15] M.J. Huron and J Vidal. New mixing rules in simple equations of state for representing vapour-liquid equilibria if strongly non-ideal mixtures. *Fluid Phase Equilibria*, 3:255, 1979.

[16] T.M. Lesteva, G.A. Timofeev, and V.I. Chernaya. Phase equilibria in binary systems formed by diethylene glycol with hydrocarbons and water. *Zh.Prikl.Khim.*, 45:2117, 1972.

[17] T. Magnussen, J. M. Sorensen, P. Rasmussen, and A. Fredenslund. Liquid-liquid equilibrium data: Thier retrieval, correlation and prediction part iii:prediction. *Fluid Phase Equilibria*, 4: 151–163, 1980.

[18] G. C. Maitland, M. Rigby, E. B. Smith, and W. A. Wakeham. *Intermolecular Forces*. Oxford Clarendon Press, 1987.

[19] R.W. Merriman. The mutual solubilities of ethyl acetate and water and the densities of mixtures of ethyl acetate and ethyl alcohol. *J.Chem.Soc*, 103:1774, 1913.

[20] M. L. Michelsen and J. M. Mollerup. *Thermodynamic Models: Fundamentals and Computational Aspects*. Tie-Line Publications, 2nd edition, 2007.

[21] L. U. O. Mingjian, M. A. Piesheng, and X. I. A. Shunqian. A modification of α in srk equation of state and vapour-liquid equilibria prediction. *Chin.J.Chem.Eng.*, 15:102–109, 2007.

[22] A. Mitsos, G. M. Bollas, and P. I. Barton. Bilevel optimization formulation for parameter estimation in liquid-liquid phase equilibrium problems. *Chemical Engineering Science*, 64: 548–559, 2008.

[23] I. Nagata. Representation of ternary liquid-liquid equilibria by means of a modified form of the wilson equation. *Thermochimica Acta*, 249:75–87, 1995.

[24] D. V. Nichita, S. Gomez, and E. Luna. Multiphase equilibria calculation by direct minimization of gibbs free energy with a global optimization method. *Computers and Chemical Engineering*, 26:1703–1724, 2002.

[25] U. Onken, J. Gmehling, and J. R. Rarey-Nies, editors. *Liquid-liquid Data Collection*, volume 5. Frankfurt/Main: Dechema, 1996.

[26] G.A. Parsafar and C. Izanloo. Deriving analytical expressions for ideal curves and using the curves to obtain the temperature dependence of equation-of-state parameters. *International Journal of Thermodynamics*, 2006.

[27] B. E. Polling, J. M. Prausnitz, and J. .M. O'Connell. *The Properties of Gases and Liquids*. Mc Graw-Hill, 5th edition, 2004.

[28] J. M. Prausnitz, R. N. Lichtenthaler, and E. G. de Azevedo. *Molecular Thermodynamics of Fluid Phase Equilibria*. Prentice-Hall PTR, 3rd edition, 1999.

[29] F.C. Radice and H.N. Knickle. *J.Chem.Eng.Data*, 20:371, 1975.

[30] H. Renon and J. M. Prausnitz. Local compositions in thermodynamic excess functions for liquid mixtures. *AIChE*, 14(1):135, 1968.

[31] H. Renon and J. M. Prausnitz. Estimation of parameters for the nrtl equation for excess gibbs energies of strongly nonideal liquid mixtures. *I and EC Process Design and Development*, 8 (3):413, 1969.

[32] J. A. Reyes, J. A. Conesa, A. Marcilla, and M. M. Olaya. Solid-liquid equilibrium thermodynamics: Checking stability in multiphase systems using the gibbs energy function. *Ind.Eng.Chem.Res.*, 40:902–907, 2001.

[33] S.I. Sandler. *Chemical, Biochemical and Engineering Thermodynamics*. John Wiley and Sons, 4th edition, 2006.

[34] V.P. Sazonov and M.F. Chernysheva. See onken et.al. *Zh.Prikl.Khim.*, 51:1764, 1978.

[35] V.P. Sazonov, N.P. Markuzin, and V.V. Filippov. Equilibrium of vapor with two and three liquid phases in the hexyl alcohol-water-nitromethane system. *Zh.Prikl.Khim.*, 50:1524, 1977.

[36] L. D. Simoni, Y. Lin, J. F. Brennecke, and M. A. Standtherr. Reliable computation of binary parameters in activity coefficient models for liquid-liquid equilibrium. *Fluid Phase Equilibria*, 255:138–146, 2007.

[37] J. M. Smith, H. C. van Ness, and M. M. Abbott. *Introduction to Chemical Engineering Thermodynamics*. Mc Graw-Hill, 6th edition, 2001.

[38] M. A. Solokhin, A. V. Solokhin, and V. S. Timofeev. Calculation of multiphase liquid-liquid equilibria and automated synthesis of the structures of phase diagrams. *Theoretical Foundations of Chemical Engineering*, 36(6):564–569, 2002.

[39] M.A. Solokhin, A.V. Solokhin, and V.S. Timofeev. Calculation of multiphase liquid-liquid equilibria and automated synthesis of the structures of phase diagrams. *Technical Foundations of Chemical Engineering*, 36(6):564, 2002.

[40] M.A. Solokhin, A.V. Solokhin, and V.S. Timofeev. Phase-equilibrium stability criterion in terms of the eigenvalues of the hessian matrix of the gibbs potential. *Technical Foundations of Chemical Engineering*, 36(5):444, 2002.

[41] G. Tagliavini and G. Arich. The liquid-liquid equilibrium in the methanol-n-heptane-morpholine system. *Ric.Sci.*, 28:1902, 1958.

[42] Y.S. Teh and G.P. Rangaiah. A study of equation-solving and gibbs free energy minimization methods for phase equilibrium calculations. *Institution of Chemical Engineers*, 80:745 – 759, 2002.

[43] S. R. Tessier, J. F. Brennecke, and M. A. Standtherr. Reliable phase stabilty analysis for excess gibbs energy models. *Chemical Engineerning Science*, 55:1785–1796, 2000.

[44] J. Vidal. Mixing rules and excess properties in cubic equations of state. *Chem.Eng.Sci.*, 33: 787, 1977.

[45] S. M. Walas. *Phase Equilibria in Chemical Engineering*. Butterworth Publishers, 1985.

[46] H.I. Weck and H. Hunt. Vapor-liquid equilibria - in the ternary system benzene-cyclohexane-nitromethane and the three binaries. *Ind.Eng.Chem.*, 46(12):2521, 1954.

[47] T.S. Wittrig. *PhD Thesis*. PhD thesis, Uniersity of Illinois, 1977.

[48] D.H.S. Wong and S.I.A. Sandler. Theoretically correct mixing rule for cubic equations of state. *AIChE*, 38:671, 1992.

[49] C. Sandrock W.W. Focke and S. Kok. Weighted-power-mean mixture model: Application to liquid viscosity. *Ind.Eng.Chem.Res*, 46:4660, 2007.